CHEMOPREVENTIVE EFFECTS OF A NEW BENZO INDOLE DERIVATIVE AGAINST COLON CANCER

FATEMEH HAJIAGHAALIPOUR

FACULTY OF SCIENCE
UNIVERSITY OF MALAYA
KUALA LUMPUR

2018

CHEMOPREVENTIVE EFFECTS OF A NEW BENZO INDOLE DERIVATIVE AGAINST COLON CANCER

FATEMEH HAJIAGHAALIPOUR

THESIS SUBMITTED IN FULFILMENT OF THE REQUIREMENTS FOR THE DEGREE OF DOCTOR OF PHILOSOPHY

INSTITUTE OF BIOLOGICAL SCIENCES
FACULTY OF SCIENCE
UNIVERSITY OF MALAYA
KUALA LUMPUR

2018

UNIVERSITY OF MALAYA

ORIGINAL LITERARY WORK DECLARATION

Name of Candidate: Fatemeh Hajiaghaalipour

Matric No: SHC140120

Name of Degree: Doctor of Philosophy

Title of Project Paper/Research Report/Dissertation/Thesis ("this Work"):

Chemopreventive effects of a new benzo indole derivative against colon cancer

Field of Study: Medical Biotechnology

I do solemnly and sincerely declare that:

(1) I am the sole author/writer of this Work;
(2) This Work is original;
(3) Any use of any work in which copyright exists was done by way of fair dealing and for permitted purposes and any excerpt or extract from, or reference to or reproduction of any copyright work has been disclosed expressly and sufficiently and the title of the Work and its authorship have been acknowledged in this Work;
(4) I do not have any actual knowledge nor do I ought reasonably to know that the making of this work constitutes an infringement of any copyright work;
(5) I hereby assign all and every rights in the copyright to this Work to the University of Malaya ("UM"), who henceforth shall be owner of the copyright in this Work and that any reproduction or use in any form or by any means whatsoever is prohibited without the written consent of UM having been first had and obtained;
(6) I am fully aware that if in the course of making this Work I have infringed any copyright whether intentionally or otherwise, I may be subject to legal action or any other action as may be determined by UM.

Candidate's Signature Date:

Subscribed and solemnly declared before,

Witness's Signature Date:

Name:

Designation:

CHEMOPREVENTIVE EFFECTS OF A NEW BENZO INDOLE DERIVATIVE AGAINST COLON CANCER

ABSTRACT

Colorectal cancer is the third most common form of cancer in both genders in the world. A new synthetic compound, 2-(1,1-dimethyl-1H-benzo[e]indol-2-yl)-3-((2-hydroxyphenyl)amino)acrylaldehyde, abbreviated as DBID was screened its anti-proliferation effect against two colorectal cancer cell lines, and its possible mechanism of action was elucidated. In order to investigate the effect of the DBID compound on the azoxymethane-induced colonic aberrant crypt foci in rats, twenty-four adult male rats were injected subcutaneously with 15 mg/kg per body weight azoxymethane (AOM) once a week for two weeks and were then divided randomly into four groups in this experiment. The rats in cancer and treatments groups received two-month treatment with oral administration of 10% Tween 20 as the vehicle (cancer control), 20 and 40 mg/kg of DBID compound (treated groups), and intraperitoneal injection with 35 mg/kg 5-fluorouracil once a week in the reference control group. The normal control group with no AOM injections were orally administered with 10% Tween 20 for two months (non-cancer control or sham group). On the last day of the experiment, the animals were euthanized and the colon tissues were evaluated grossly and histopathologically for aberrant crypt foci (ACF). The colon tissue homogenate was also evaluated for antioxidant enzyme activities, gene and protein expression. The acute toxicity test and subacute toxicity were used to evaluate the safe usage of DBID compound. *In vitro* antioxidant activities of the compound were investigated. The DBID compound showed high antioxidant activity in ferric reducing antioxidant power (FRAP) and DPPH radical scavenging assays. It inhibited the proliferation of HCT 116 and HT-29 cells with an IC_{50} of 9.32, and 11.85 μg/ml and significantly increased the levels of caspase -8, -9 and -3/7 in the treated cells compared to untreated cells. Apoptosis features in HCT 116 and HT-

29 cells were detected in treated cells by using flow cytometric analysis of Annexin V and AO/PI staining. The apoptotic changes in expression of caspase were confirmed by gene and protein quantification using RT-PCR and western blot analysis, respectively. The acute toxicity and subacute toxicity studies showed no nephrotoxic and no hepatotoxic effects or any serum biochemical changes in rats. Colon tissue evaluation showed that DBID compound diminished azoxymethane-induced aberrant crypt foci formation and pathological changes in the colonic mucosal tissues. Following treatment with the compound, antioxidant enzyme activity was increased compared to carcinogen groups. Moreover, the downregulation of Bcl2 and upregulation of Bax protein and caspase 3 were confirmed by RT-PCR and western blot. This study has shown that the DBID compound has demonstrated chemotherapeutic activity which was evidenced by significant increases in the expression and activation of caspase and exploits the apoptotic signaling pathways to trigger cancer cell death. There was significant inhibition of azoxymethane-induced colonic aberrant crypt foci formation by a new benzo indole derivative compound in rats that might be associated with its potent antioxidant activity and effective activity against free radicals involved in the formation of colorogenic lesions followed by alteration of the expression of apoptotic genes.

Keywords: Colon cancer, Synthetic compound, AOM-induced colon cancer, HCT 116 cell line, HT-29 cell line.

KESAN PECEGAHAN-KEMO OLEH TERBITAN BENZO INDOLE BARU KE ATAS KOLON KANSER

ABSTRAK

Kanser kolorektal adalah merupakan kanser yang ketiga paling tinggi di dunia yang menyerang lelaki dan wanita. Kompaun sintetik yang baru, 2-(1,1-dimethyl-1H-benzo[e]indol-2-yl)-3-((2-hydroxyphenyl)amino)acrylaldehyde, atau nama ringkasnya DBID telah disaring untuk kemampuan anti-proliferasi terhadap dua jenis sel kanser kolorektal di mana mekanismanya diketahui. Bagi mengenalpasti kesan kompoun DBID, tikus-tikus dirangsang penyakit kanser kolorektal menggunakan azoxymethane. Sebanyak dua puluh empat ekor tikus jantan dewasa telah disuntik di bawah kulit dengan 15 mg/kg azoxymethane (AOM) sekali seminggu untuk tempoh dua minggu dan selepas itu tikus tersebut dibahagikan secara rawak kepada empat kumpulan dalam eksperimen ini. Tikus yang berada di dalam kumpulan kanser dan kumpulan rawatan masing-masing menerima dua bulan rawatan 10% Tween 20 (kanser kontrol) secara oral, 20 dan 40 mg/kg kompaun DBID (kumpulan rawatan) juga secara oral, dan suntikan pada bahagian peritoneal dengan 35 mg/kg 5-fluorouracil sekali seminggu dalam kumpulan kawalan rujukan. Kumpulan kawalan normal tidak disuntik dengan AOM tetapi 10% Tween 20 diberi secara oral untuk tempoh dua bulan. Pada hari terakhir eksperimen, tikus-tikus tersebut telah di bedah dan tisu kolon dikaji menggunakan kaedah histopatologi untuk mengenapasti kanser kolon (ACF). Tisu homogenat kanser kolon dinilai untuk paras aktiviti enzim antioksidan, gen dan ekspresi protein. Ujian toksik akut dan subakut juga dilakukan untuk mengesan kompaun kimia dan tahap keselamatan penggunaan kompaun DBID. Aktiviti *in vitro* kompaun antioksida tersebut juga dikaji. Hasil kajian adalah kompaun DBID menunjukkan tahap aktiviti antioksida yang tinggi dalam ferik pengurang kuasa antioksida (FRAP) dan pengujian skaveng radikal DPPH. DBID menghalang penyebaran sel HCT 116 dan HT-29 dengan IC_{50} of 9.32 dan 11.85 μg/ml dan juga

meningkatkan kadar caspase -8, -9 and -3/7 secara signifikan dalam sel-sel yang dirawat berbanding dengan sel-sel yang tidak dirawat. Ciri-ciri apoptosis di dalam sel HCT 116 dan HT-29 yang dirawat telah dikesan menggunakan ujian *flow cytometry* dengan menggunakan teknik pewarnaan Annexin dan AO/PI dan perubahan apoptosis dalam ekspresi caspase disahkan melalui ujian kuantifikasi gen dan protein dengan menggunakan kaedah RT-PCR dan *Western blot*. Kajian terhadap toksik akut dan subakut menunjukkan tiada sebarang kesan toksin pada ginjal dan hati serta tiada perubahan yang ketara dalam ujian darah tikus-tikut tesebut. Penilaian tisu-tisu kolon menunjukkan bahawa kompaun DBID mengurangkan kanser kolon yang dihasilkan oleh *azoxymethane* serta perubahan patologikal di dalam mukosa tisu kolon. Berikutan rawatan dengan menggunakan kompaun antioksida, aktiviti enzim meningkat berbanding dengan kumpulan karsinogenik. RT-PCR dan *Western blotting* telah mengesahkan pengurangan gen Bcl2 dan peningkatan gen protein Bax. Kajian ini juga menunjukkan bahawa kompaun DBID mendemonstrasikan akiviti kemoterapi yang dapat dibuktikan dengan peningkatan yang signifikan dalam ekspresi dan pengaktifan *caspase* serta menggunakan laluan isyarat apoptotis untuk mematikan sel-sel kanser. Selain itu, pembentukan kanser kolon yang dirangsang oleh *azoxymethane* dihalang secara signifikan oleh kompaun derivatif *benzo indole* yang terhasil dalam tikus. Ini disebabkan oleh aktiviti antioksida yang tinggi serta tindakan yang berkesan terhadap radikal bebas yang terlibat dalam pembentukan kanser kolon disusuli dengan perubahan dalam ekspresi yang ditunjukkan oleh gen-gen apoptosis.

Kata Kunci: Kanser Kolon, Sebatian Sintetik, Kolon Kanser AOM-teraruh, Titisan Sel HCT 116, Titisan Sel HT-29.

ACKNOWLEDGEMENTS

I would like to extend my deepest gratitude to my supervisors, Assoc. Prof. Dr. Nazia bt Abdul Majid from Institute of Biological Sciences, Faculty of Science and Prof. Dr. Mahmood Ameen Abdulla from Department of Biomedical Science, Faculty of Medicine.

Special thanks to my parents and my beloved husband, Mohammadreza Shams, who were beside me in any difficulty of my life and my study.

I would also like to express my heartfelt gratitude and appreciation to Dr. Haryanti Azurawali bt Hj Mohd Wali, Dr. Syahar Amir b A.Rani, Mrs Hamidah bt Hamid and Dzuzaini Mohd bt Ghazali in Laboratory Animal Centre.

Special thanks go to all staffs in Department of Molecular Medicine, Biomedical Science and Medical Biotechnology in the Faculty of Medicine and Institute of Biological Sciences in the Faculty of Science.

I wish to express my most sincere gratitude and appreciation to all my friends for their support.

This study was funded by High Impact Research grant (UM.C/625/1/HIR/MOE/MED/11/07), PG073-2015B and RP043A-15HTM provided by the University of Malaya.

TABLE OF CONTENTS

LIST OF FIGURES

LIST OF TABLES

LIST OF SYMBOLS AND ABBREVIATIONS

5-FU	:	5-Fluorouracil
ACF	:	Aberrant crypt foci
ALP	:	Alkaline phosphatase
ALT	:	Alanine aminotransferase
ANOVA	:	One-way analysis of variance
AO/PI	:	Acridine orange and propidium iodide staining
AOM	:	Azoxymethane
ATCC	:	American type culture collection
BAX	:	B-cell lymphoma 2-associated X protein
BCL2	:	B-cell lymphoma 2
CAT	:	Catalase
CH2THF	:	5, 10-methylenetetrahydrofolate
cm	:	Centimeters
CO_2	:	Carbon dioxide
DAB	:	3,3'-diaminobenzidine
DBID	:	2-(1,1-dimethyl-1H-benzo[e]indol-2-yl)-3-((2-hydroxyphenyl)amino)acrylaldehyde
DCF	:	2',7'-dichlorofluorescein
DCFH-DA	:	2',7'-dichlorofluorescin diacetate
dH2O	:	Distilled water
DMSO	:	Dimethyl sulfoxide
DPD	:	Dihydropyrimidine dehydrogenase
DPPH	:	2,2-diphenyl-1-picrylhydrazyl
dTMP	:	Deoxythymidine monophosphate
dTTP	:	Deoxythymidine triphosphate
dUMP	:	Deoxyuridine monophosphate
dUTP	:	Deoxyuridine triphosphate
EtOH	:	Ethanol
FADD	:	Fas-associated protein with death domain
FBS	:	Fetal bovine serum
FdUMP	:	Fluorodeoxyuridine monophosphate
Fe (III)-TPTZ	:	Ferric tripyridyltriazine

FeSO4	:	Ferrous sulfate
FOM-IACUC	:	Faculty of medicine-institutional animal care and use committee
FRAP	:	Ferric reducing antioxidant power
GGT	:	Gamma-glutamyl transferase
GPX	:	Glutathione peroxidase
H&E	:	Haematoxylin and eosin staining
HCL	:	Hydrochloric acid
HD	:	High dose
HDL	:	High-density lipoprotein
HRP	:	Horseradish peroxidase
IAP	:	Inhibitor of apoptosis protein
JNK	:	Jun N-terminal kinase
LD	:	Low dose
LDL	:	Low-density lipoprotein,
LFT	:	Liver Function Test
MAPK	:	Mitogen-activated protein kinase
MDA	:	Malondialdehyde
mg	:	Milligram
ml	:	Milliliter
mm	:	Millimeter
mmol	:	Millimole
MTT	:	(3-(4,5-Dimethylthiazol-2-yl)-2,5-diphenyltetrazolium bromide
nm	:	Nanometer
PBS	:	Phosphate buffer saline
PCR	:	Polymerase chain reaction
PKB	:	Protein kinase B
RFT	:	Renal function test
RIP	:	Ribosome inactive protein
ROS	:	Reactive oxygen species
SD	:	Standard deviation
SD Rat	:	Sprague-dawley rat
SDS-PAGE	:	Sodium dodecyl sulfate polyacrylamide gel
SOD	:	Superoxide dismutase
SPSS	:	Statistical package for the social sciences

TBARS	:	Thiobarbituric acid reactive substance
TG	:	Triglyceride
TPTZ	:	2,4,6-tripyridyl-s-triazine
TRADD	:	TNFR1 associated death domain
TRAF	:	TNF receptor associated factor
TRAIL	:	TNF-related apoptosis-inducing ligand
TS	:	Thymidylate synthase
UV	:	Ultraviolet
WB	:	Western blotting
µg	:	Microgram
µl	:	Microliter
µM	:	Micromolar
µm	:	Micrometer
µmol	:	Micromole

LIST OF APPENDICES

CHAPTER 1: INTRODUCTION

1.1 Cancer

Cancer is defined as a disease that results from the uncontrolled growth of abnormal cells which then other infect tissue cells in various parts of the body by spreading through the blood and lymphatics. Cancer cells begin from normal cells and many different cell types are susceptible to such occurrences.

A typical life cycle of a cell is as follows: growth, division, and subsequently death. Normally, apoptosis, which is the equilibria in regards to cell proliferation and programmed cell death, is a tightly regulated process, which in return guarantees the continued normal function of organs and tissues (Alberts et al., 2002; Beahrs & Henson, 1992).

Somatic cell mutation is generally the starting point of cancer and a complex mechanism exists to eradicate such abnormalities and prevent the spread of cancer to other cells, known as programmed cell death, which destroys mutant cells once the significant errors occur. Only once this tightly regulated sequence malfunctions or breaks down cancer begin to form. The abnormality of cancer cells lies in their failure to exhibit programmed death. They abnormally continue to grow and divide out of control leading to a mass of abnormal cells (Alberts et al., 2002; Bertram, 2000).

The metamorphosis of a normal cell into a tumorous one is not a single step process, but rather a multiple step one, starting from a pre-cancerous lesion to a malignant tumour. The entire line of processes from which a normal cell transforms into a cancerous one is called carcinogenesis (Weinberg, 1989).

Damage to the DNA which are usually repaired or used for senescence induction and the elimination of the cell, subject to the extent of the damage received by aforementioned

factors, leads to carcinogenesis (Weinberg, 2013). Weinberg (2013) states that the accumulation of multiple mutations is the most basic precondition for cancer to progress from *in situ* dysplasia to a malignant tumour. DNA mutations cause disruptions in the normal processes of cell function and the maintenance of such functions and is a causal factor in the formation of cancer (American Cancer Society, 2017; Rosen, 2013; Weinberg, 2013).

While the causal factors of many cancers that appear during the onset of childhood remain undiscovered, a list of internal and external factors, among them, tobacco product usage, an imbalanced diet based on unhealthy food choices, inherited genetic mutations, immune system conditions, hormonal imbalance, and infectious organisms may come together or in sequence to lead to the onset of cancer in individuals (Alberts et al., 2002; American Cancer Society, 2015a).

In 2012 alone, over 8 million deaths were attributed to cancer, making it the top ranked cause of death globally. Despite varying estimations, GLOBOCAN 2012 has estimated that by the year 2025, the steady growth of both the global human population and its corresponding older citizens' category will result in 19.3 million new cases of the disease (Ferlay et al., 2015).

The World Cancer Report states that within the next 20 years, an annual tally of 22 million global new cancer cases with an estimated annual death rate of between 8.2 million to 13 million is to be expected with Asia, Africa, and the Americas - excluding the US and Canada - to account for 60% of these new cases and 70% of its fatalities (American Cancer Society, 2015b; Torre et al., 2015).

Cancer is the second highest ranked cause of death in the United States, accounting for as estimated 25% of all fatalities reported. The American Cancer Society has placed an

estimate of nearly 1.7 million new diagnoses of cancer in 2017. There are various types of cancer in the body. Each cancer is called based on location of the tumour, or the place where it originates in the body. The colon, lung, breast and prostate cancer are the most common types of cancer (American Cancer Society, 2017; Torre et al., 2015).

1.2 Colon cancer

The third highest cause of death among cancers around the world is colorectal cancer (CRC), making one of the deadliest diseases worldwide, tallying in 2012 an estimated 1.4 million new cases and approximately 693,000 deaths (American Cancer Society, 2015b).

All types of cancers which originate in range from the cecum to the anus are considered colorectal cancer. They in turn are further subdivided into colon cancer and rectal cancer. Colon cancer occurs between the caecum and the sigmoid. The sigmoid is an area about 15cm above the anal verge. The second subdivision, rectal cancer, occurs between the recto-sigmoid area to the anus (Vainio & Miller, 2003). The etiology of colon cancer is multifactorial, which includes familial, environmental, and dietary agents. Similar to other cancers, colorectal cancer occurs when changes occur to several genes, which in turn alter the regulatory pathways in which cancerous cells are not subsequently able to perform their normal functions (Ebert et al., 2005).

A total of 91% of all colorectal cancer patients are diagnosed aged 50 and above leading age to be considered as one of the major risk factors for the disease along with those with a history of colorectal cancer and / or known to have polyps, some genetically-inherited manifestations, and chronic inflammatory bowel disease. Modifiable risk factors include alcohol consumption, long-term smoking, obesity, a lack of physical activity, and a diet high in red or processed meat (American Cancer Society, 2017).

There are some significant markers in development of colorectal cancer via adenoma-carcinoma as follows: the loss or mutation of APC gene changes normal epithelium into hyper proliferative epithelium; and the methylation of DNA, which is responsible for the hyper-proliferative epithelium morphing into early adenoma. APC loss and K-ras gene mutations cause early adenoma to progress to dysplastic adenoma, in which the loss of p53 function subsequently causes carcinoma. Despite the fact that the adenoma-carcinoma concept is well established, not all adenomas will transform into carcinomas because many may regress (Sillarshardebol et al., 2010). As a matter of fact, genetic alterations rather than an order of a preferred sequence is basically responsible to determine the properties of the tumour (Vogelstein et al., 1988a).

Colorectal adenocarcinomas start in the innermost layer and can develop into other layers. Most of the carcinomas arise from adenomatous polyps that are bounded masses of epithelial tissue characterised by uncontrolled cell proliferation, resulting in a progression from adenoma to carcinoma (McKinnell et al., 1998; Shih et al., 2001).

Dysplasia onset is the first event that occurs when tumours develop from normal epithelium. In particular in the colonic crypt, the normal sequence of proliferation-differentiation of the colonic cells alters. Documented to exist in both humans and animals, putative pre-neoplastic colon lesions are known as Aberrant Crypt Foci (ACF) (Cheng & Lai, 2003). Additionally, the ACF are alleged to be precursors of colon cancers and colonic carcinogenesis biomarkers (Takayama et al., 1998). The ACF plays a role of an intermediate biomarker to assess rapidly the potential of an agent to be chemopreventive against colon cancer (Corpet & Taché, 2002). The ACF are monoclonal collection of strange crypts that are always formed in reaction to carcinogen exposure in a dose-dependent manner (Bird, 1987). These hyper proliferative lesions are located in

human colon and share various similarities with colon tumours of lab animals which have been treated with carcinogen (Corpet & Taché, 2002; McKinnell et al., 1998).

Following exposure to AOM as a reaction to DNA damage, crypt progenitor cells develop apoptosis within a time period of 6 – 8 hours. Progenitor cells that have avoided apoptosis exhibit proliferative responses within a time period of 48 – 72 hours. It seems that these aberrant crypt foci are formed as monoclonals and develop through incomplete crypt fissioning (Hirose et al., 1996; Siu et al., 1999) .

Adenomatous polyps will then progressively grow and enlarge and morph from being tubular to villous. Dysplastic crypt cells then exhibit early, intermediate, and late adenoma. Malignant change ensues resulting in local invasion and distant site metastasis (Davies et al., 2005).

The following figure shows the morphological changes and major mutations that are involved in the formation of pre-cancerous lesions (or adenomas), which eventually evolve into colon adenocarcinoma.

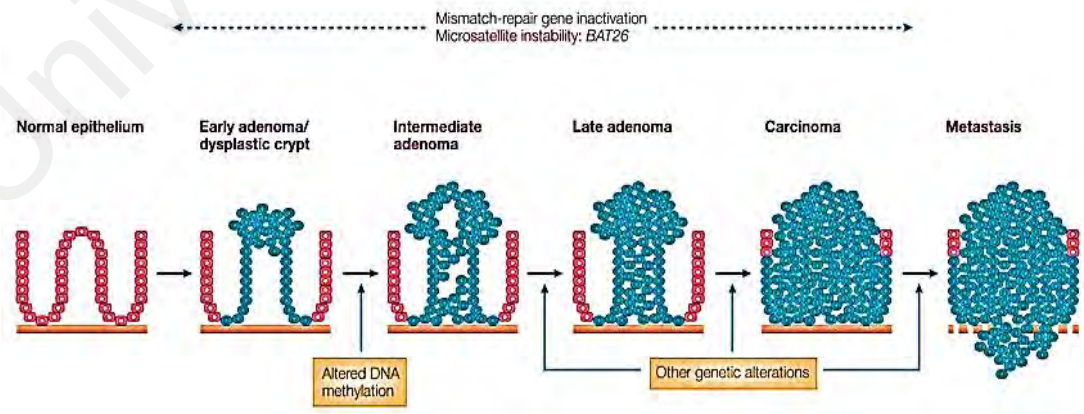

Figure 1.1: The colorectal adenoma-carcinoma sequence (Davies et al., 2005).

Occurrences of colon cancer is on the rise globally and at an alarming rate, despite significant and rapid developments in the early diagnosis and in strategies for conventional treatment. Surgical removal, followed in succession with adjuvant chemotherapy or radiotherapy, is considered the standard treatment for colon and rectal cancer. For localised cancers, surgical resection may be curative. However, many patients who have undergone therapeutic resection develop tumour recurrences. Chemotherapy, either by itself or in conjunction with either neo-adjuvant or adjuvant radiation, tend to benefit most patients whose cancer has deeply invaded, and have spread to nearby tissues or the lymph node (American Cancer Society, 2015a). Such therapies have proven, however, to only have moderate success with patients who have late stage cancer. As a result of this failure of patients inflicted with advanced colon cancer to respond to the latest treatment regiments, a new approach is needed to be developed to reduce the rate of mortality.

1.3 Indole derivatives in drug discovery

The discovery of many indole derivates with varied biological activities has attracted the organic chemistry to evolve new routes for the synthesis of novel compounds with pharmacologically active indole derivatives. Indole is one of the most significant drug discoveries in advantage scaffolds (Kaushik et al., 2013).

Indole is the main substance of many natural compounds e.g. Indole-3-carbinol, reserpine and mitomyein with significant pharmacological activity. It is also present in numerous organic compounds such as in amino acids like tryptophan and tryptophan-containing protein (Adelstein et al., 2011; Kaushik et al., 2013).

Furthermore, a large number of indole-containing drugs are being used as important drugs in the treatment of various diseases. Indole and its derivatives are considered as

potent pharmacophores which play an important role in synthetic organic chemistry (Kaushik et al., 2013).

In the medical field, large number of indole derivates such as Vincristine, Vinblastine, Vinorelbine, Vindesine, Mitraphylline, Cediranib and Apaziquone have been acknowledged to have anti-cancer medicinal properties (Faraj et al., 2014a; Faraj et al., 2014b; Kaushik et al., 2013). They have also been found to have anti-inflammatory (Gupta et al., 2012; Misra et al., 1996; Rani et al., 2004), anti-hypertensive (Rapolu et al., 2011), anti-bacterial (Panda & Tripathy, 2010), antioxidant (Panda et al., 2012), anti-viral, antifungal and antibacterial activities (Mgomha et al., 2012; Prasad et al., 2014).

Synthetic compounds, for example 2-Aroylindole, epoxides and aziridines have been recognised as preventative with regard to the development of cancer. Compelling evidence from studies has repeatedly highlighted the vital role of synthetic compounds in reducing cancer risk and in the inhibition in the development and spread of tumours in experimental animals (Ali et al., 2008; Islam et al., 2012; Jesmin et al., 2010; Kaushik et al., 2013; Shivarama Holla et al., 2003).

The objectives of this research is to study the efficacy of a new benzo indole derivative, 2-(1,1-dimethyl-1H-benzo[e]indol-2-yl)-3-((2-hydroxyphenyl)amino)acrylaldehyde, abbreviated as DBID against colon cancer and also to elucidate the *in vivo* and *in vitro* action mechanisms.

1.4 Objectives of the study

The specific objectives of this study are:

A. *In vitro* studies

i. To determine the antioxidant properties of the DBID compound

ii. To evaluate the effect of DBID on a normal and cancer colon cell lines

iii. To elucidate the possible mechanism of action underlying the growth inhibitory effects of DBID compound on colon cancer cells

B. *In vivo* studies

i. To determine the acute toxicity and subacute toxicity of DBID

ii. To investigate the chemo-preventive effects of DBID compound in azoxymethane-induced colorectal cancer in rats

iii. To reveal the possible inhibition mechanisms of action of aberrant crypt foci formation in an azoxymethane-induced rat colon

CHAPTER 2: LITERATURE REVIEW

2.1 Cancer epidemiology

Carcinomas make up the majority of all tumours. They are derived from epithelial cells which include breast, colorectal, lung, prostate, and skin cancers. Sarcoma forms from non-epithelial cells. Among them include the connective tissue or mesenchymal cells like fibroblasts and osteoblasts. Blood-forming cells called haematopoietic cells are the origin points for lymphoma and leukaemia. Germ cell tumours, on the other hand, are those which are derived from totipotent cells in the testicles and ovary. Blastic tumours or blastomas are malignant tumours. They closely resemble immature or embryonic tissues (Beahrs & Henson, 1992; Weinberg, 2013).

The American Cancer Society estimated about 589,430 cancer deaths occurred in 2015, and about 595,690 cancer deaths, a slight increase, in 2016 (American Cancer Society, 2015b, 2016). A total figure of 600,920 cancer deaths have been estimated to occur in 2017, averaging 1,650 people per day (American Cancer Society, 2017). According to the American Cancer Society, lung and bronchial cancer contribute the most toward the death statistics in both genders while the most common occurrences of cancer are colon, breast, prostate, and lung cancer (American Cancer Society, 2017).

The most common cancer among men in the United States in 2016 was prostate cancer with more than 180,890 new diagnosed cases reported, while the corresponding cancer in women was breast cancer with more than 246,660 new diagnosed cases reported (American Cancer Society, 2016).

An estimate on the number of new cases and death for each common cancer type in 2016 and 2017 as determined by the American Cancer Society is shown in the following figures:

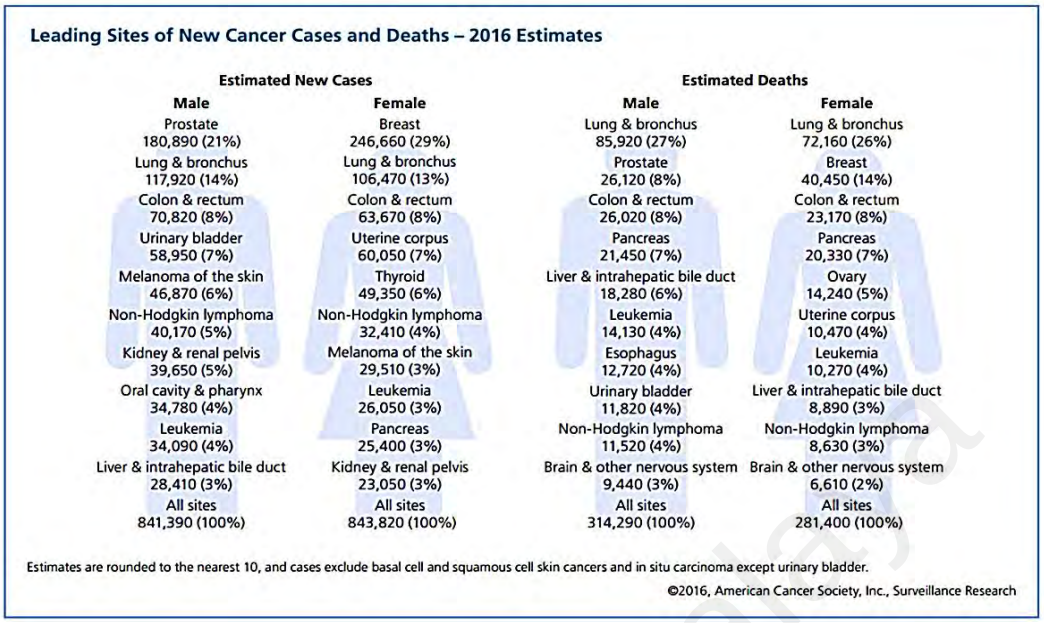

Leading Sites of New Cancer Cases and Deaths – 2016 Estimates

Estimated New Cases		Estimated Deaths	
Male	**Female**	**Male**	**Female**
Prostate 180,890 (21%)	Breast 246,660 (29%)	Lung & bronchus 85,920 (27%)	Lung & bronchus 72,160 (26%)
Lung & bronchus 117,920 (14%)	Lung & bronchus 106,470 (13%)	Prostate 26,120 (8%)	Breast 40,450 (14%)
Colon & rectum 70,820 (8%)	Colon & rectum 63,670 (8%)	Colon & rectum 26,020 (8%)	Colon & rectum 23,170 (8%)
Urinary bladder 58,950 (7%)	Uterine corpus 60,050 (7%)	Pancreas 21,450 (7%)	Pancreas 20,330 (7%)
Melanoma of the skin 46,870 (6%)	Thyroid 49,350 (6%)	Liver & intrahepatic bile duct 18,280 (6%)	Ovary 14,240 (5%)
Non-Hodgkin lymphoma 40,170 (5%)	Non-Hodgkin lymphoma 32,410 (4%)	Leukemia 14,130 (4%)	Uterine corpus 10,470 (4%)
Kidney & renal pelvis 39,650 (5%)	Melanoma of the skin 29,510 (3%)	Esophagus 12,720 (4%)	Leukemia 10,270 (4%)
Oral cavity & pharynx 34,780 (4%)	Leukemia 26,050 (3%)	Urinary bladder 11,820 (4%)	Liver & intrahepatic bile duct 8,890 (3%)
Leukemia 34,090 (4%)	Pancreas 25,400 (3%)	Non-Hodgkin lymphoma 11,520 (4%)	Non-Hodgkin lymphoma 8,630 (3%)
Liver & intrahepatic bile duct 28,410 (3%)	Kidney & renal pelvis 23,050 (3%)	Brain & other nervous system 9,440 (3%)	Brain & other nervous system 6,610 (2%)
All sites 841,390 (100%)	All sites 843,820 (100%)	All sites 314,290 (100%)	All sites 281,400 (100%)

Estimates are rounded to the nearest 10, and cases exclude basal cell and squamous cell skin cancers and in situ carcinoma except urinary bladder.

Figure 2.1: Estimated new cancer cases and deaths by sex, US, 2016.

Source: American Cancer Society. Cancer Facts & Figures 2016. Atlanta: American Cancer Society; 2016

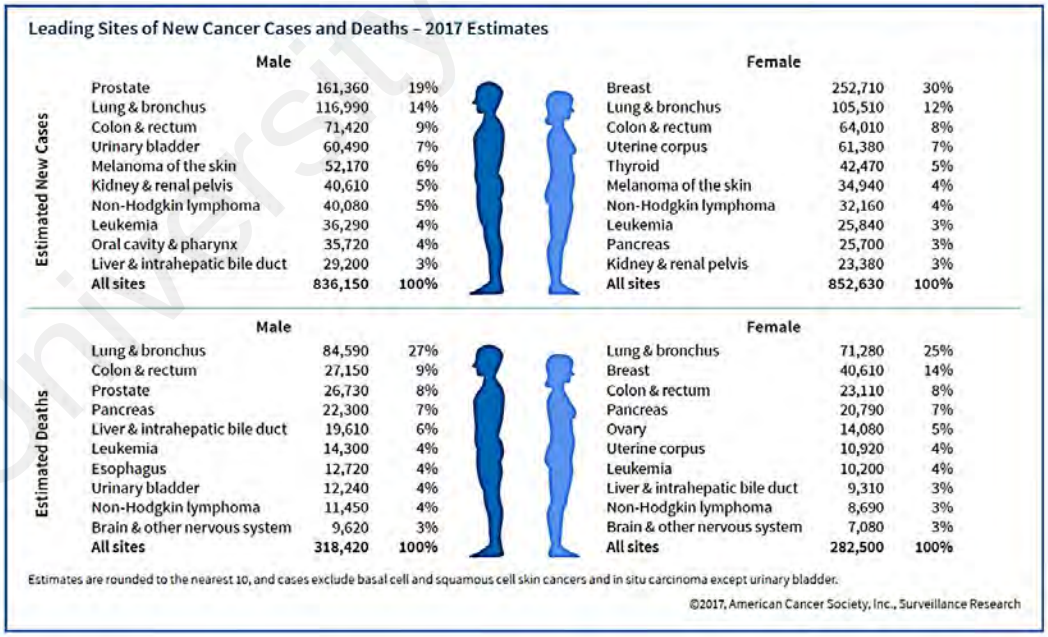

Leading Sites of New Cancer Cases and Deaths – 2017 Estimates

Estimated New Cases

Male			Female		
Prostate	161,360	19%	Breast	252,710	30%
Lung & bronchus	116,990	14%	Lung & bronchus	105,510	12%
Colon & rectum	71,420	9%	Colon & rectum	64,010	8%
Urinary bladder	60,490	7%	Uterine corpus	61,380	7%
Melanoma of the skin	52,170	6%	Thyroid	42,470	5%
Kidney & renal pelvis	40,610	5%	Melanoma of the skin	34,940	4%
Non-Hodgkin lymphoma	40,080	5%	Non-Hodgkin lymphoma	32,160	4%
Leukemia	36,290	4%	Leukemia	25,840	3%
Oral cavity & pharynx	35,720	4%	Pancreas	25,700	3%
Liver & intrahepatic bile duct	29,200	3%	Kidney & renal pelvis	23,380	3%
All sites	**836,150**	**100%**	**All sites**	**852,630**	**100%**

Estimated Deaths

Male			Female		
Lung & bronchus	84,590	27%	Lung & bronchus	71,280	25%
Colon & rectum	27,150	9%	Breast	40,610	14%
Prostate	26,730	8%	Colon & rectum	23,110	8%
Pancreas	22,300	7%	Pancreas	20,790	7%
Liver & intrahepatic bile duct	19,610	6%	Ovary	14,080	5%
Leukemia	14,300	4%	Uterine corpus	10,920	4%
Esophagus	12,720	4%	Leukemia	10,200	4%
Urinary bladder	12,240	4%	Liver & intrahepatic bile duct	9,310	3%
Non-Hodgkin lymphoma	11,450	4%	Non-Hodgkin lymphoma	8,690	3%
Brain & other nervous system	9,620	3%	Brain & other nervous system	7,080	3%
All sites	**318,420**	**100%**	**All sites**	**282,500**	**100%**

Estimates are rounded to the nearest 10, and cases exclude basal cell and squamous cell skin cancers and in situ carcinoma except urinary bladder.

Figure 2.2: Estimated New Cancer Cases and Deaths by Sex, US, 2017.

Source: American Cancer Society. Cancer Facts & Figures 2017. Atlanta: American Cancer Society; 2017

The Malaysian National Cancer Registry (NCR) reported that 21,773 Malaysians were diagnosed and registered with cancer in 2006 and 18,219 new cancer cases were reported in 2007. This total is comprised of 9,974 males and 11,799 females in 2006, and 8,123 males and 10,096 females in 2007. It also reported that cancer prevalence is more in women than men with a ratio of 1 : 1.2 men to women (National Cancer Registry, 2006, 2007). In Malaysia, lung, colorectal, nasopharyngeal, prostate cancer, and lymphoma were reported as the five most frequent cancers among males, while the five most common cancers in females were breast, colorectal, cervical, ovarian, and lung (Malaysia National Cancer Registry, 2015).

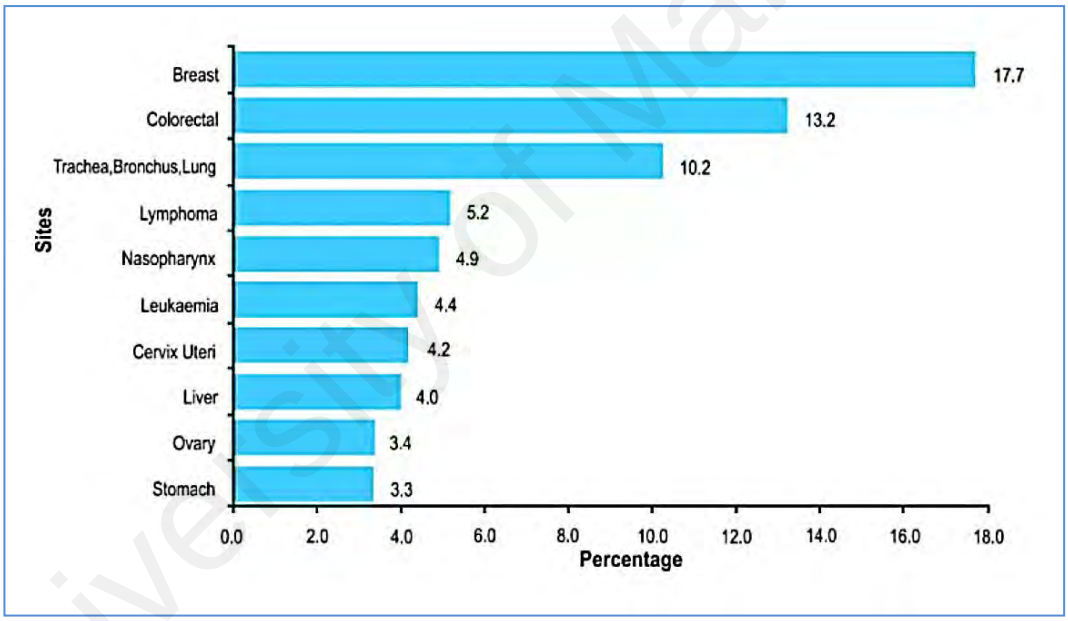

Figure 2.3: Percentage of ten most common cancers, Malaysia, 2007-2011.

Source: Malaysian National Cancer Registry Report (MNCR) 2007-2011

Table 2.1: The ten most common cancers in Malaysia by sex, 2007-2011.

Sites	Number	%	Sites	Number	%
MALE			FEMALE		
Colorectal	7,646	16.3	Breast	18,206	32.1
Trachea, Bronchus, Lung	7,415	15.8	Colorectal	6,047	10.7
Nasopharynx	3,785	8.1	Cervix Uteri	4,352	7.7
Lymphoma	3,171	6.8	Ovary	3,472	6.1
Prostate	3,132	6.7	Trachea, Bronchus, Lung	3,193	5.6
Liver	3,054	6.5	Lymphoma	2,203	3.9
Leukaemia	2,549	5.4	Corpus Uteri	2,181	3.8
Stomach	2,014	4.3	Leukaemia	2,024	3.6
Bladder	1,477	3.2	Thyroid	1,723	3.0
Other Skin	1,384	3.0	Stomach	1,447	2.6
Others	11,167	23.9	Others	11,865	20.9
Total	46,749	100	Total	56,713	100

Source: Malaysian National Cancer Registry Report (MNCR) 2007-2011

2.2 Epidemiology of colorectal cancer

According to the American Cancer Society, colorectal cancer ranks as the third most commonly occurring cancer in both genders worldwide and they have further indicated in their reports that it will be the third-ranked cause of cancer deaths in women and second-ranked correspondingly for men in 2017. The American Cancer Society estimates about 50,260 deaths from colorectal cancer. Furthermore, a surge in the number of reported colon cancer cases has occurred recently. This surge has highlighted this cancer as a health issue of serious concern, with 135,430 cases of colorectal cancer being estimated and expected to take place in 2017 (American Cancer Society, 2017).

Between 2008 and 2013, it has been reported by the National Cancer Registry of Colorectal Cancer that for Malaysia, the incidence of colorectal cancer was 21.3 cases per 100,000 people with a mortality rate of 9.8 cases per 100,000 people. Malaysian men suffered a mortality rate from colorectal cancer which has been calculated at roughly 1.42 that of Malaysian women (National Cancer Patient Registry-Colorectal Cancer, 2014).

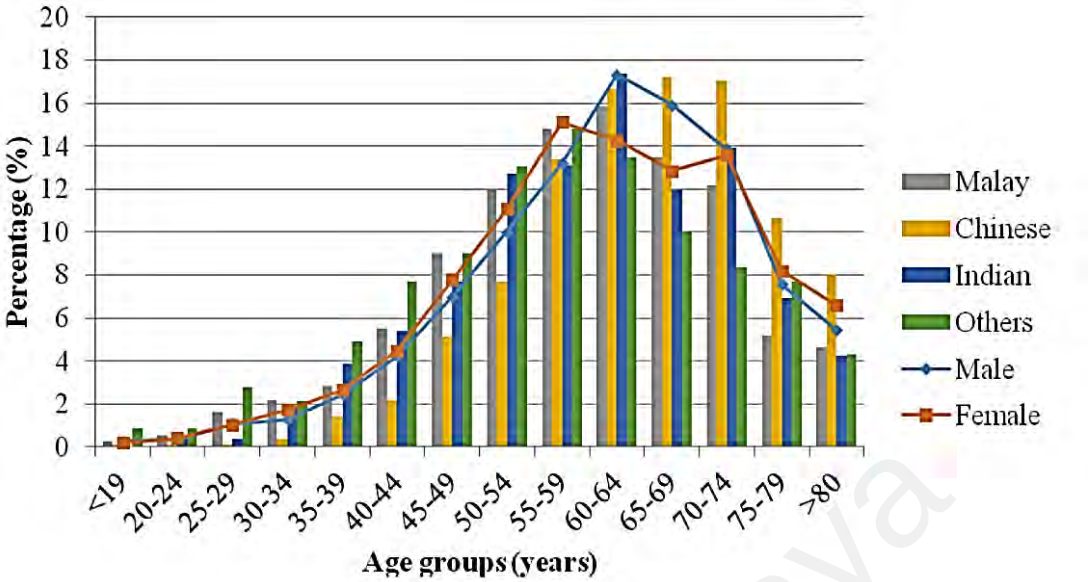

Figure 2.4: Colorectal cancer patients, Malaysia, 2008-2013.

Age groups by gender and ethnicity of patients enrolled in the NCPR-Colorectal Cancer
Source: National Cancer Patient Registry-Colorectal Cancer, Malaysia, 2008-2013

2.3 Etiology of colorectal cancer

Most colorectal cancer cases occur due to lifestyles and age factors and only in a few cases are they associated with generic disorders. Statistics show that in 20% - 30% of colon and rectal cancer cases, the patient's family had a history of chronic inflammatory bowel disease, colorectal cancer and/or polyps, hereditary disposition as there is an enhanced incidence in families or cancer appears at a young age and less than 5% of the cases have a specific genetic cause (American Cancer Society, 2017; Bardhan & Liu, 2013).

Lynch Syndrome, also known as hereditary nonpolyposis colorectal cancer (HNPCC), along with Familial adenomatous polyposis (FAP) are the most common forms of colon cancer syndromes that are inherited. Colorectal cancer generally begins in the bowel lining. Untreated, however, it can spread into the muscle layer underneath and subsequently grow through the bowel wall. Inflammatory bowel disease (IBD) is known to be an important risk factor for colon cancer development, particularly colitis-associated

cancer (CAC). Crohn's disease, along with ulcerative colitis, are referred to as inflammatory bowel diseases and have been proven to increase the risk of contracting colon cancer (Bardhan & Liu, 2013; Jawad et al., 2011; Kim & Chang, 2014).

As age increases, so does the risk of developing colon and rectal cancer with 91% of those diagnosed being 50 years or older. In order to reduce the death rate caused by colorectal cancer, screening programs are effective and recommended from the age of 50 and continued till the age of 75 (American Cancer Society, 2017; Bardhan & Liu, 2013).

Modifiable risk for colon cancer include a low fibre intake, smoking, lack of physical exercise, obesity, and a high fat, alcohol, or red meat intake. People with little to no genetic risks make up 75% - 90% of those diagnosed with colon cancer (Watson & Collins, 2011) with about 10% of the cases being related to insufficient activity (Lee et al., 2012). An alcohol intake of more than one drink daily also appears to be a disease risk factor (Fedirko et al., 2011).

2.4 The anatomy and physiology of the large intestine

The large intestine functions as the gastrointestinal track's terminal component and functions to observe vitamins and water, convert digested food into faeces and eliminate faeces from the body. Its four major sections are as follows: The colon, the cecum, the anus, and the rectum. Figure 2.5 depicts the anatomy of the large intestine. The first section of the large intestine is the cecum. It is roughly 6cm long and receives undigested food from the small intestine. The appendix, which is a winding tube, attaches to the cecum and it has a function within the body's immune system (Hall, 2015; Leung, 2014; Rizzo, 2015; Sherwood, 2015).

The colon extends from the cecum to the rectum and is approximately 150cm in length and 6-7cm in diameter, divided into a few sections. The cecum blends seamlessly with

the colon. There are four sections to the colon: On the abdomen's right side is the ascending colon, which is the start of the colon itself and it continues in an upwards direction and to a bend in the colon known as the hepatic flexure. The transverse colon parallels the ascending colon and the hepatic flexure which is located on the abdomen's upper part. The transverse colon comes to an end with a bend in the colon known as the splenic flexure. On the left side of the abdomen is the descending colon which parallels both the transverse colon and the splenic flexure. The final section of the colon is the sigmoid colon. This is the section of the colon that adjoins the rectum (Rizzo, 2015; Sherwood, 2015). Collectively, the ascending and transverse colon sections are referred to as the proximal colon, while the descending and signal colon sections as the distal colon. At the end of this is the anus. This is the opening located at the rectum's lower end and functions to pass faeces out of the body(Rizzo, 2015).

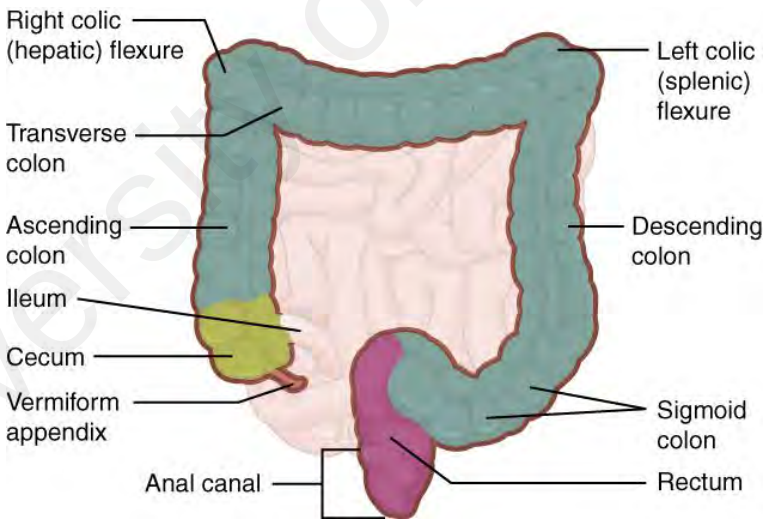

Figure 2.5: The anatomy of the large intestine.

Source: Boundless. "Digestive System: Small and Large Intestines." Boundless Biology Boundless, 27 May. 2016. Retrieved 25 May 2017 from: https://www.boundless.com/biology/textbooks/boundless-biology-textbook/animal-nutrition-and-the-digestive-system-34/digestive-systems-195/digestive-system-small-and-large-intestines-750-11983/

2.4.1 The layers of the colon

Different tissue layers make up the colon. Figure 2.6 shows a section of the colon and figure 2.7 presents the histology of a normal colon. The inner lining of the colon, closest to the lumen, is the mucosa layer. Columnar absorptive cells or enterocytes, along with goblet, endocrine and basal stem cells make up the columnar epithelium of the mucosa of the colon. The next layer is the submucosa. The submucosa is a connective tissue layer that contains nerve, blood vessels, and lymphatics. The muscularis is a thick layer of muscle that lies outside the submucosa. It consists of circular muscles and longitudinal muscles. Finally, there is the serosa which forms the outermost layer. Also, there are three longitudinal fibres along the colon called taeniae coli (Hall, 2015; Rizzo, 2015).

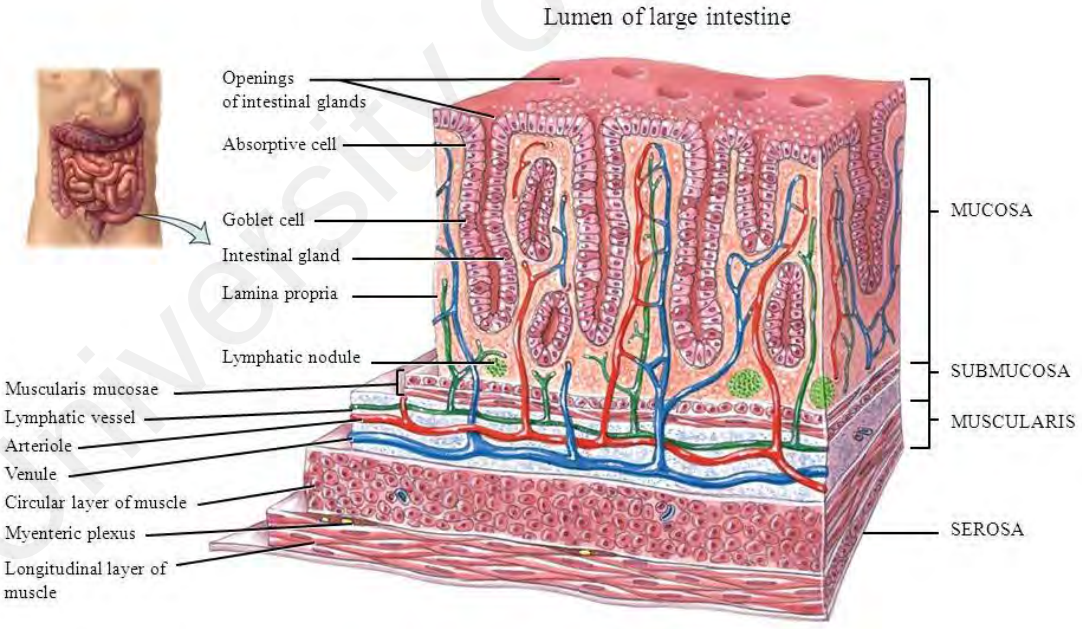

Figure 2.6: Three-dimensional view of the layers of colon (Mescher, 2013).

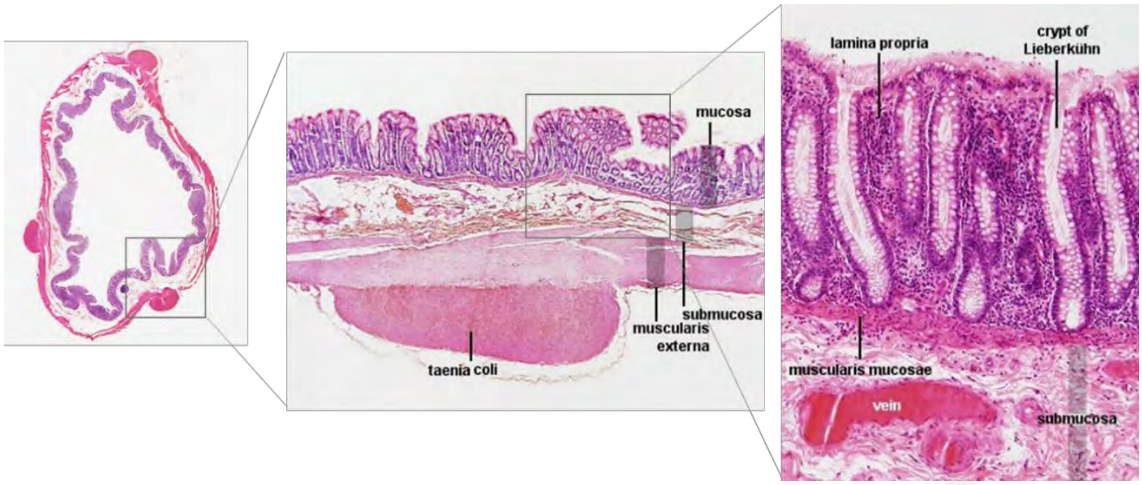

Figure 2.7: Normal colon histology overview, H & E staining.

Source: Hill, M.A. 2017 Embryology Gastrointestinal Tract - Colon Histology. Retrieved May 24, 2017, from: https://embryology.med.unsw.edu.au/embryology/index.php/Gastrointestinal_Tract_-_Colon_Histology

2.5 Pathology of colorectal cancer

Colorectal cancer generally starts off as a polyp located on the colon's inner lining which is known the mucosa layer. It can then grow outward, breaching some or even all of the other colon layers. While polyps can morph into cancer after several years, not all do so. The polyp size (generally speaking, larger than 1cm), its type and quantity detected all determine the risk of developing colorectal cancer (De Leon & Di Gregorio, 2001; Treanor & Quirke, 2007).

Colon tissue analysis by way of a biopsy or surgery helps to determine the pathology of the colorectal tumour. The type and grade of the colorectal cells are described in a pathology report. There are three types of cells involved in colorectal cancer. Adenocarcinoma is the most common, accounting for 95% of all colon cancer cases. The remaining 5% is split between the lymphoma and squamous cell carcinoma cell types (McMahon et al., 2001; Yoshida & Nappi, 2001).

The appearance of colorectal cancer is different in the two sides of the colon. On the right side (which comprises the ascending colon and the cecum), colorectal cancer tends to exophytic with the tumour extending outwards from a single location in the bowel wall. Except in rare cases, the faeces is not obstructed with any symptoms such as anaemia. When the tumour is on the left, however, it is circumferential and the possibility of bowel obstruction (like a napkin ring) can occur (Hidalgo et al., 1989; Williams et al., 1982).

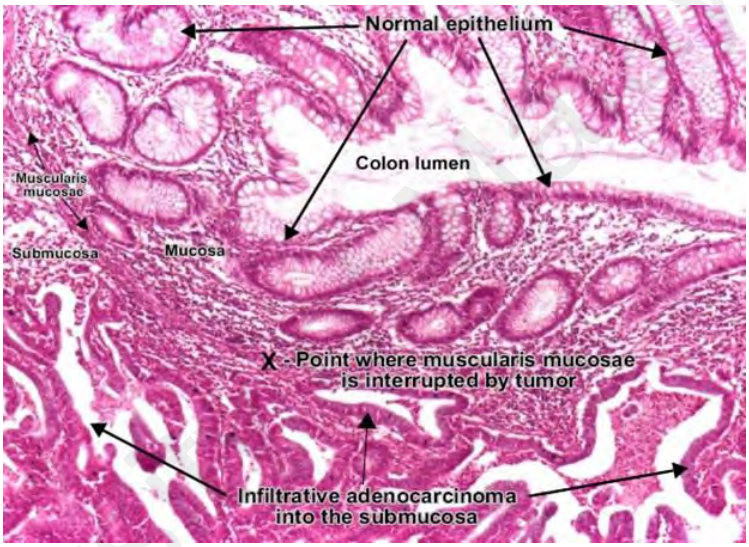

Figure 2.8: Histology of colon adenocarcinoma tissue stained with H&E.

Source: Atlas of Pathology, 3rd Edition, Retrieved 25 May, 2017, from: http://www.pathologyatlas.ro/moderatelly-differentiated-adenocarcinoma-colon gastrointestinal-pathology.php

Adenocarcinoma, which is a malignant epithelial tumour, begins from the colorectal mucosa's glandular epithelium and then spreads to the wall. Infiltration of the muscularis mucosae, the submucosa, and the muscularis propria then occurs. Tumour cells exist in irregular tubular structures, having pluristratified with multiple lumens and reduced stroma ("back to back" aspect). Occasionally dis-cohesive and mucus secreting, they attack the interstitium, resulting in the production in a large quantity of mucous/colloid

(optically “empty” spaces). Mucus (colloid) is very poorly differentiated. In a situation where the mucus exists on the inside of a tumour cell, the nucleus is pushed to the periphery, causing the cell to warp into a signet-ring shape. Three degree of differentiation exist for adenocarcinoma, which are well, moderately, or poorly differentiated. The difference is dependent on the glandular architecture, predominant polyp (three or more) pattern mucoscretion (Figure 2.8) and cellular pleomorphism (De Leon & Di Gregorio, 2001; Jass & Sobin, 2012; Treanor & Quirke, 2007).

2.6 Signs and symptoms of colorectal cancer

The site of the tumour in the bowel determines the signs, symptoms, and level of spreading (metastasis) of colorectal cancer in the body. There are typical warning signs for colorectal cancer in people over 50 years old as follows: increasingly bad constipation issues, stools with blood in them, appetite loss, fever, vomiting, or nausea. Among these symptoms, rectal bleeding or anaemia are classified as high-risk symptoms in people aged 50 years and above (Astin et al., 2011) while other common symptoms such as weight loss and change in bowel function have to be noticed if associated with blood (Adelstein et al., 2011).

It is often possible to cure those cancers that are restricted within the colon wall with surgery. However, those that widely spread around the body cannot be surgically repaired and require medical management focused on chemotherapy and to improve the patient's quality of life.

2.7 Pathogenesis of colorectal cancer

Three gene classes, including oncogenes, tumour suppressor genes, and metastasis suppressor genes, have been identified as playing a role in cancer development. Oncogenes are a group of impaired genes. They can induce cancer development when present in certain forms and/or overexpression by the expression of proteins that eventually cause uncontrolled cell growth and division. Examples of such genes include K-ras, N-ras, H-ras, myc, and L-myc and they are involved in the transduction of signals and serve as transcription factors. The functional absence of tumour suppressor genes can lead to the development of cancer with transcription regulators such as WTI, p53, and p73 being examples of them being involved in functions such as regulating transcription, DNA repair, and apoptosis-induction. Tumour progression and metastasis is not a single step, but a series of complex and multiple step events (Fearon & Vogelstein, 1990; Vogelstein et al., 1988b; Vogelstein & Kinzler, 2004).

Colorectal cancer develops from normal colonic mucosa to adenocarcinoma in an ordered process consisting of three main phases. The first phase is the initiation, followed by promotion, and lastly, progression. Several different molecular alterations play a role in the initiation and progression of colon polyps. A chain reaction sequence of genetic changes bring about irreversible progressive loss of normal control over the normal rate of cell growth and differentiation. This ultimately leads to colorectal cancer. Alterations in the DNA structure/sequence, also known as mutations, mark the initiation of a series of events that will be followed up by uncontrolled neoplastic clone growth. This characterises tumoural progression (Fearon & Vogelstein, 1990; Grady & Markowitz, 2015; Vogelstein et al., 1988b).

Colorectal cancer development is a result of the accumulation of genetic and epigenetic alterations in a progressive manner. They are the mutations in adenomatous polyposis

coli (APC) in the initial stages and rat sarcoma viral oncogene homolog (RAS) mutations and tumour protein 53 (TP53) at the later stages (Grady & Markowitz, 2015; Ponzdeleon & Percesepe, 2000; Yamagishi et al., 2016).

2.8 The molecular pathogenesis of colorectal cancer

Over the past 30 years, research has greatly increased our knowledge of the molecular pathways that are tied to the initiation and development of colorectal cancer. Numerous activation pathways have been found to be connected with the colon carcinogenesis mechanism (Figure 2.9). They are namely RAS, Wnt/ß-catenin, p53, TGFß, and inflammation. However, there is no consensus in the explanation of this model's mechanisms (Yamagishi et al., 2016).

The K-ras gene, a small G-protein which regulates both MAPKs and the P13K/Akt intracellular signal pathways, determines the adenoma to carcinoma transition at the very beginning. The K-ras gene regulates glucose metabolism, along with cell growth and proliferation, and has a major role in colon cancer carcinogenesis. The MAPKs and P13K/Akt intracellular signal pathways play an important part in the carcinogenesis of many cancer types with human colon cancer being an example. Levels of pEGFR, pMAPK, and pAkt have been discovered to be elevated in colon tumours when compared to normal colon tissue (Grady & Markowitz, 2015; Messersmith et al., 2005; Yamagishi et al., 2016).

The activated Ras initiates the stimulation of the Raf kinase, more specifically known as the serine/threonine-selective protein kinase, an oncogene. The encoded protein contains both regulatory and kinase domains. Ras attaches to CR1 in gulatory region and phosphorylates CR2, which has serine/threonine in the structure. As a result, the CR3 in the kinase region is activated, which activates in turn MAPK and ERK kinase (MEK) which regulates activity of several transcription factors. These transcription factors are

responsible for inducing the expressions of various genes that are needed for survival and also proliferation. Erk, JNK, p38 and ERK5 kinases are the terminal MAPKs. Carcinogenesis is initiated by MAPK and ERK via target proteins. They include the following: c-myc, RSK, CREB, p16, Mcl1, and cyclins. It has been reported that the inhibition of the above-mentioned pathways result in cancer cell death (Messersmith et al., 2005).

An important pathway in colon cancer is the P13K/Akt pathway. One in five patients exhibit PIK3CA mutations. P13K/Akt activation can result in cell survival pathways increasing through downstream target phosphorylation which include Bcl-xl, and NfκB. Akt halts the forkhead/Fas-ligand and also p53, reducing apoptosis (Messersmith et al., 2005). The p53 tumour suppressor gene has been established to have a large hand in cell cycle arrest and apoptosis and its loss of function often happens during the colorectal tumorigenesis' later stages, and this leads to stimulate high proliferative activity through cell cycle control loss and apoptosis. P53 is also known to interact with Cyclooxygenase-2 (COX-2), which is an independent prognostic factor that has a role promoting inflammation along with cell proliferation in colon cancer (Fearon & Vogelstein, 1990).

Glycogen synthase kinase 3 (GSK3) is deactivated by P13K/Akt. P13K/Akt also activates cyc D1 and c-myc. The activation increases cell proliferation in the cell cycle pathways. The activation of mammalian target of rapamycin (mTOR), which is a conserved Ser/Thr kinase by P13K/Akt, elevates cell size (Luo et al., 2003).

The activation of the Wnt/b-catenin pathway has been linked with both malignant potentials and metastasis. ß-catenin is an oncogenic protein connected to cell adhesion. It also associates with cadherin or a-catenin resulting in interactions with the actin cytoskeleton. The free form of ß-catenin is a gene co-transcriptional activator. This takes place in the Wnt signal pathway, associating with scaffolding proteins like axin and Apc.

GSK-3ß then phosphorylates it, causing it to degrade by the proteasome (Messersmith et al., 2005). ß-catenin's N-terminus is occasionally mutated, rendering it unable to form the complex and resulting in degradation. Free ß-catenin levels increase, and they form a complex by binding to the T-cell factor/lymphoid enhancer factor TCF/LEF, subsequently activating both gene transcription and cell proliferation by targeting the c-myc and cyclinD1 genes, which are well-known carcinogens. Carcinogens can cause mutations at codons 33 and 41 of ß-catenin, which codes for residues of serine and threonine targeting for the phosphorylation of GSK-3ß. The mutation causes ß-catenin accumulation for the carcinogenesis (Bienz & Clevers, 2000; Chen & Huang, 2009).

Inhibition of cell growth, cell cycle progression, and proliferation by the transforming growth factor-ß (TGFß) isoforms 1.2, and 3 indicate an anti-tumour capability. Defects in TGFß signalling has been shown in up to 30% of colon cancer patients. The TGF-ß induces apoptosis via many signalling pathways. Dimers are first formed by transforming growth factor ß (TGFß). It then binds to type 2 receptors, which then phosphorylates the type 1 receptor. This then induces apoptosis by phosphorylating receptor-regulated SMAD (R-SMAD). In the second method, the activated type-2 receptor binds itself to protein 6 (which is associated with death), resulting in apoptosis. Third, phosphorylation of p85 subunit of P13L/Akt activated by GM-CSF is inhibited by TGFß. This takes place in many myeloid leukaemia cell lines like TF-1, TF-1a, and MV4-11 (Chen & Huang, 2009; Vogelstein & Kinzler, 2004; Yamagishi et al., 2016).

A critical factor of colon cancer initiation and progression is chronic inflammation. Cell proliferation, differentiation, and the promotion of metastasis is stimulated via the pro-inflammatory cytokine tumour necrosis factor (TNF)-α, the transcription factor Signal Transducer and Activator of Transcription 3 (STAT3) protein and Interleukin (IL)-6. This happens by inducing the expression of different gene targets. Targets include:

VEGFR2 (vascular endothelial growth factor receptor Bcl-2, CyclinD1, MMP2-9, ICAM-1, and COX-2 (Coussens & Werb, 2002; Grivennikov et al., 2009; Karin & Greten, 2005).

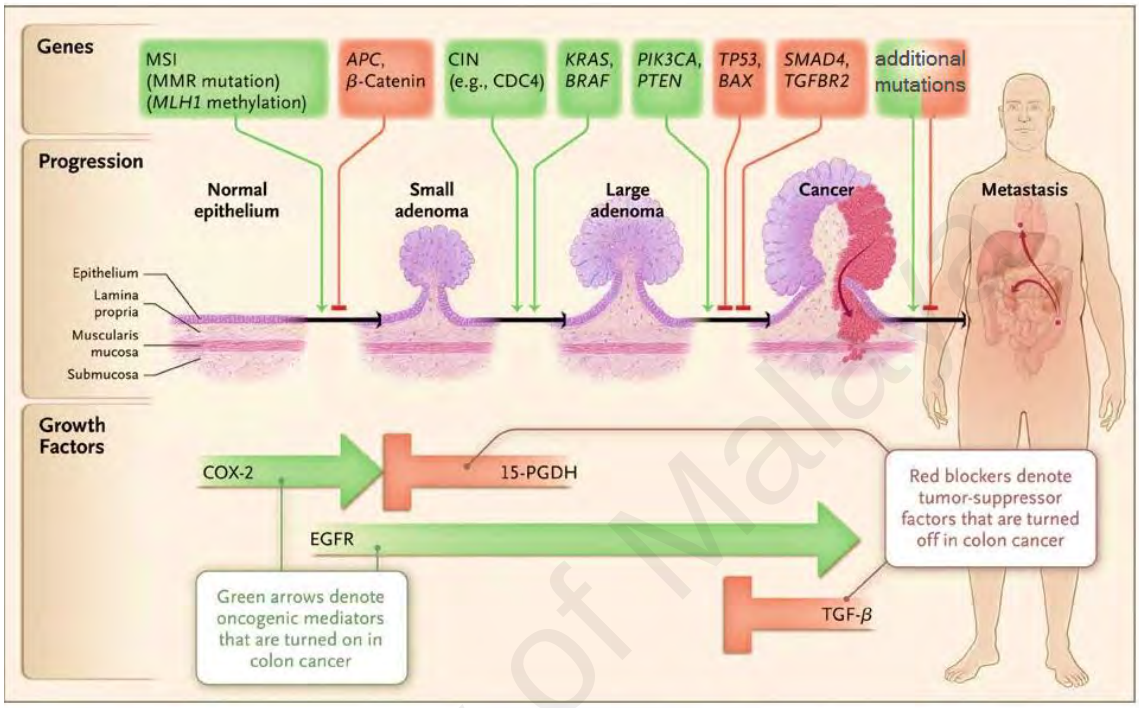

Figure 2.9: Colon carcinogenesis mechanism (Markowitz & Bertagnolli, 2009).

2.9 Diagnosis of colorectal cancer

Mortality rate and malignant neoplasm incidence can be decreased with early diagnosis of colorectal cancer (Pignone et al., 2002). The screening of faecal occult blood test (FOBT), colonoscopy, and sigmoidoscopy can also decrease mortality rates (Walsh & Terdiman, 2003).

Colonoscopy and sigmoidoscopy are usually used to diagnose localised colorectal cancer, while histopathology for tumour biopsy is another way of diagnosis. The severity of the disease from the chest, pelvis, and abdomen is determined using a computerised tomography (CT) scan. Alternately, other methods such as magnetic resonance imaging

(MRI) and positron emission tomography (PET) can be utilised in some cases. Colon cancer staging is performed using classification of malignant tumour systems to determine the level of tumour spread, lymph node involvement, and the determination of the number of metastasis (Kaushik et al., 2013; Labianca et al., 2013; Wargovich et al., 2010).

Early detection is important to improve the chances of survival for the colon, rectal, or other cancers in the long-term. For instance, a 5-year survival rate of > 90% was reported for colorectal cancer patients who were treated at an early stage but drops to 64% in the event the cancer spreads to adjacent organs. It further reduces to < 10% if the cancer moves to distant organs, such as the liver and lungs (Wargovich et al., 2010).

Screening tests and early detection considerably improves the survival rates and it provides an "early warning system" for individuals with no symptoms or one or more symptoms. Previous studies have shown that identification of intermediate biomarkers help to recognise very early stages of cancer development before an obvious tumour is formed. Progression of cancer lesions can be reversed or significantly slowed down with proper intervention. A promising colon cancer intermediate biomarker is Aberrant crypt foci (ACF) (Wargovich et al., 2010).

Many countries have prepared guidelines in which to add the screening of colorectal cancer to their respective health system's screening programmes (Power et al., 2009). However, even in developed countries, such screening programmes are still slow. Screening for colorectal cancer in Asian countries for those aged 50 and up has been suggested by The Asia Pacific Consensus (Sung et al., 2008).

2.10 Colon cancer stages

To treat cancer, information about its stage, location, if and or spreading has occurred, and whether other body parts have also been affected is crucial. Unlike solid tumour spread such as breast, bowel, or lung cancers which can described in stages, blood cancers are unable to described in such terms as they behave and are staged in a different manner. The cancer stage determines the type of surgery to be conducted and the necessity of chemotherapy or radiation therapy for treatment. Although different types of cancers have different staging systems, Generally Numbered cancer stage systems and TNM systems are utilised as staging systems (Edge & Compton, 2010).

Stage number between 0 to 4 are used in the numbered system to identify the level of cancer spread. The TMN system, on the other hand, codes the tumour extent (T), lymph nodes (N), and metastases (N). Each category is then scored which determines the level of cancer spread. Using the numbered system, Stage 0 is the point where the cancer cells are in their starting positions and have not spread in any direction. Small amounts of cancer cells with a slight spread into nearby tissues in considered Stage 1. The presence of a larger amount of cancer cells or its spread into nearby tissues or lymph nodes are Stages 2 and 3. Stage 4, or metastatic or advanced cancer, is the spread of cancer to other parts of the body (Edge & Compton, 2010; Labianca et al., 2013).

The following table presents the explanation of the TNM classification for staging of colorectal cancer.

Table 2.2: Colorectal cancer stages.

tage	Stage grouping	Stage description
0	Tis N0 M0	The cancer is in its earliest stage. This stage is also known as carcinoma in situ or intramucosal carcinoma (Tis). It has not grown beyond the inner layer (mucosa) of the colon or rectum.
I	T1 or T2 N0 M0	The cancer has grown through the muscularis mucosa into the submucosa (T1), and it may also have grown into the muscularis propria (T2). It has not spread to nearby lymph nodes (N0) or to distant sites (M0).
IIA	T3 N0 M0	The cancer has grown into the outermost layers of the colon or rectum but has not gone through them (T3). It has not reached nearby organs. It has not spread to nearby lymph nodes (N0) or to distant sites (M0).
IIB	T4a N0 M0	The cancer has grown through the wall of the colon or rectum but has not grown into other nearby tissues or organs (T4a). It has not yet spread to nearby lymph nodes (N0) or to distant sites (M0).
IIC	T4b N0 M0	The cancer has grown through the wall of the colon or rectum and is attached to or has grown into other nearby tissues or organs (T4b). It has not yet spread to nearby lymph nodes (N0) or to distant sites (M0).

Source: American Cancer Society, Colorectal Cancer Stages, Retrieved 25 May, 2017, from: https://www.cancer.org/cancer/colon-rectal-cancer/detection-diagnosis-staging/staged.html

Table 2.2, continued.

Stage	Stage grouping	Stage description
IIIA	T1 or T2 N1/N1c M0	The cancer has grown through the mucosa into the submucosa (T1), and it may also have grown into the muscularis propria (T2). It has spread to 1 to 3 nearby lymph nodes (N1) or into areas of fat near the lymph nodes but not the nodes themselves (N1c). It has not spread to distant sites (M0).
	OR	
	T1 N2a M0	The cancer has grown through the mucosa into the submucosa (T1). It has spread to 4 to 6 nearby lymph nodes (N2a). It has not spread to distant sites (M0)
IIIB	T3 or T4a N1/N1c M0	The cancer has grown into the outermost layers of the colon or rectum (T3) or through the visceral peritoneum (T4a) but has not reached nearby organs. It has spread to 1 to 3 nearby lymph nodes (N1a or N1b) or into areas of fat near the lymph nodes but not the nodes themselves (N1c). It has not spread to distant sites (M0).
	OR	
	T2 or T3 N2a M0	The cancer has grown into the muscularis propria (T2) or into the outermost layers of the colon or rectum (T3). It has spread to 4 to 6 nearby lymph nodes (N2a). It has not spread to distant sites (M0).
	OR	
	T1 or T2 N2b M0	The cancer has grown through the mucosa into the submucosa (T1), and it may also have grown into the muscularis propria (T2). It has spread to 7 or more nearby lymph nodes (N2b). It has not spread to distant sites (M0).
IIIC	T4a N2a M0	The cancer has grown through the wall of the colon or rectum (including the visceral peritoneum) but has not reached nearby organs (T4a). It has spread to 4 to 6 nearby lymph nodes (N2a). It has not spread to distant sites (M0).
	OR	
	T3 or T4a N2b M0	The cancer has grown into the outermost layers of the colon or rectum (T3) or through the visceral peritoneum (T4a) but has not reached nearby organs. It has spread to 7 or more nearby lymph nodes (N2b). It has not spread to distant sites (M0).
	OR	
	T4b N1 or N2 M0	The cancer has grown through the wall of the colon or rectum and is attached to or has grown into other nearby tissues or organs (T4b). It has spread to at least one nearby lymph node or into areas of fat near the lymph nodes (N1 or N2). It has not spread to distant sites (M0).

Table 2.2, continued.

Stage	Stage grouping	Stage description
IVA	Any T Any N M1a	The cancer may or may not have grown through the wall of the colon or rectum (Any T). It might or might not have spread to nearby lymph nodes. (Any N). It has spread to 1 distant organ (such as the liver or lung) or distant set of lymph nodes, but not to distant parts of the peritoneum (the lining of the abdominal cavity) (M1a).
IVB	Any T Any N M1b	The cancer might or might not have grown through the wall of the colon or rectum (Any T). It might or might not have spread to nearby lymph nodes (Any N). It has spread to more than 1 distant organ (such as the liver or lung) or distant set of lymph nodes, but not to distant parts of the peritoneum (the lining of the abdominal cavity) (M1b).
IVC	Any T Any N M1c	The cancer might or might not have grown through the wall of the colon or rectum (Any T). It might or might not have spread to nearby lymph nodes (Any N). It has spread to distant parts of the peritoneum (the lining of the abdominal cavity) and may or may not have spread to distant organs or lymph nodes (M1c).

2.11 Colon cancer treatment

Surgical resection, followed by adjuvant i.e., radiation therapy, chemotherapy, and specific targeted treatments are the most used methods of treatment for colon cancer and rectal cancer. The stage of colon cancer at the time of treatment determines whether one or several different types of treatment are utilised at the same time or in sequence (American Cancer Society, 2017).

Chemotherapy or chemo is a form of treatment with anti-cancer drugs. It can be used at different points of time during the treatment for colorectal cancer. For instance, it can be given post-surgery as an adjuvant chemo that helps lower the chances of cancer returning. Chemo can be given before surgery as Neoadjuvant chemo, often used in treating rectal cancer to shrink the tumour for easier surgery. In advanced stage cancers which have spread to other organs such as the liver, chemo is utilised to relieve symptoms and despite being unlikely to be able to cure the cancer itself, often enables the patient to

survive for a longer time period. The Food and Drug Administration (FDA) has approved some common drugs to be used to treat colorectal cancer. The list includes 5-Fluorourancil (5-FU), Irinotecan (Camptosar), Capecitabine (Xeloda), Trifluridine, Tipiracil (Lonsurf), and Oxaliplatin (Eloxatin). These drugs are often used in various combinations to increase their effectiveness (André et al., 2004; Cunningham et al., 1998; De Gramont et al., 2000; Twelves et al., 2005; Van Cutsem et al., 2001).

Surgical removal of cancers that have not spread may be curative. For the majority of patients whose cancer has spread deeply into the bowel or wall or even lymph nodes, chemotherapy, either as a standalone treatment or in combination with radiation, is given before or after surgery.

The following are the most common drugs used in the treatment for colorectal cancer and they are used in a combination of two or more with an increased rate of effectiveness: Irinotecan, 5-Fluorouracil (5-FU), capecitabine, and oxaliplatin.

General combinations include FOLFOX (5-FU, oxaliplatin, and leucovorin), FOLFIRI (Irinotecan, 5-FU, and leucovorin), CapeOx (Capecitabine and oxaliplatin), and lastly 5-FU and leucovorin (Andre et al., 1999; Cheeseman et al., 2002; De Gramont et al., 2000; Haller et al., 2005; Jäger et al., 1996; Loupakis et al., 2013; Van Cutsem et al., 2001).

Targeted therapies utilise drugs either along with chemotherapy or by themselves which specifically target genes or proteins that are involved in cancer development. The FDA has approved three targeted monoclonal antibody therapies to fight metastatic colorectal cancer. Bevacizumab (Avastin) hinders blood vessel growth that lead to the tumour. Panitumumab (Vectibix) and cetuximab (Erbitux) curb the hormone-like factor effects which promote growth of cancer (American Cancer Society, 2013).

Chemotherapy medications are occasionally administered with a targeted therapy drug, but both intrinsic and acquired drug resistance are major limiting factors in chemotherapy's effectiveness in colon cancer treatment.

2.11.1 Mechanism of actions of anticancer drugs

The available anticancer drugs have distinctly different mechanisms of action. Many anticancer drugs act by interfering with the structure of DNA (alkylating agents, procarbazine) or its function (dactinomycin) disorganizes and disrupts the cell (Kanamaru & Wakui, 1988; Karnofsky, 1968; Singhal, 2015). Figure 2.10 shows the information on mechanisms of action of various anticancer drugs.

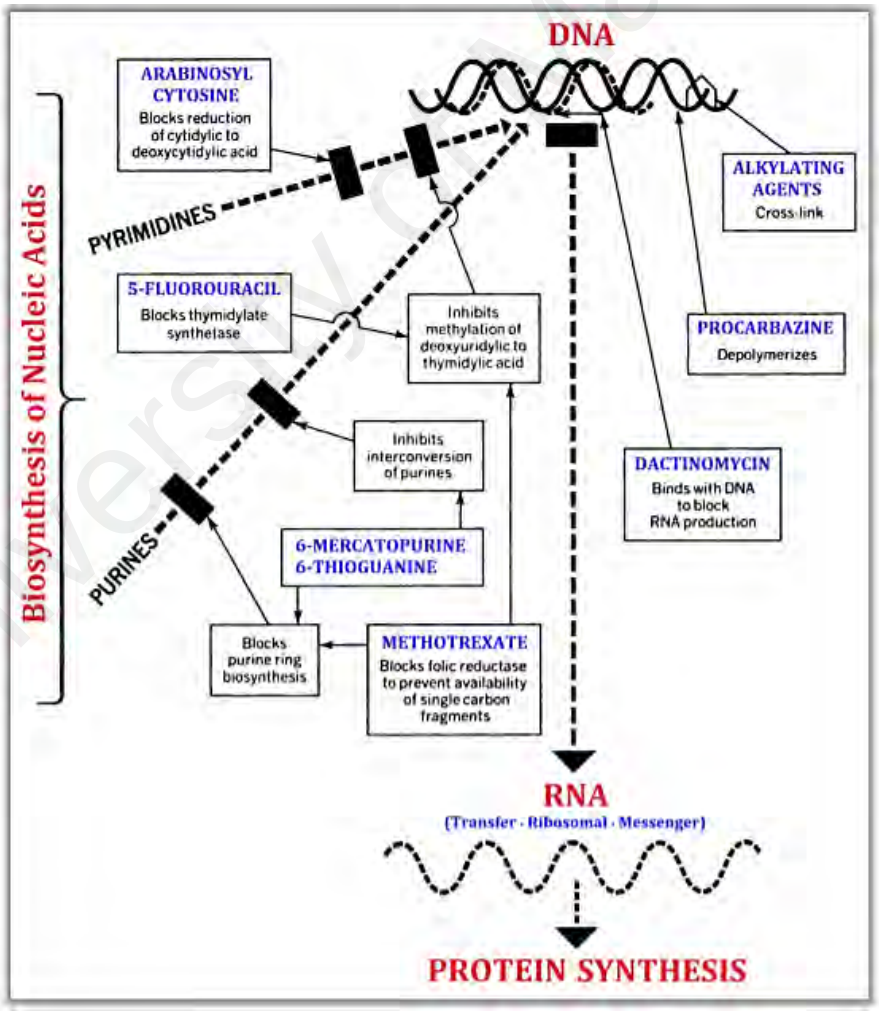

Figure 2.10: Mechanism of actions of anticancer drugs (Singhal, 2015).

Alkylating agents are reactive to DNA and cellular proteins and the primary mode of action is mostly through cross-linking of DNA strands, inhibiting replication of DNA and transcription of RNA. Some antimetabolites are structural analogs of normal molecular essentials for cell growth. The analogues change to substances to interfere with DNA or RNA synthesis after intaking into the cells. 5-Fluorouracil (5-FU), an antimetabolite drug, is widely used in the treatment of cancer (Kanamaru & Wakui, 1988; Karnofsky, 1968; Longley et al., 2003a; Singhal, 2015) .

The 5-FU is converted to fluorodeoxyuridine monophosphate (FdUMP) in mammalian cells forming a stable complex with thymidylate synthase (TS) and thus inhibiting deoxythymidine monophosphate (dTMP) production. The dTMP is required for DNA replication and repair and therefore lack of dTMP causes cytotoxicity (Longley et al., 2003b). In normal and tumor cells, dihydropyrimidine dehydrogenase (DPD)-mediated conversion of 5-FU to dihydrofluorouracil (DHFU) is the rate-limiting step of 5-FU catabolism. DPD breaks down up to 80% of administered 5-FU in the liver (He et al., 2008). TS is an essential enzyme to catalyze thymidylate biosynthesis and plays a role in theregulation of protein synthesis and apoptotic process (Chernyshev et al., 2007). TS catalyzes the methylation of deoxyuridine monophosphate (dUMP) to dTMP, where 5, 10-methylenetetrahydrofolate (CH2THF) is the methyl donor and provides thymidylate for the reaction in DNA replicationand repair (Roberts et al., 2006). There is a seriatim binding sequence in the reaction and dUMP binds at the active site before CH2THF. The reaction is then started by the nucleophilic addition of Cys 146 in the active site (numbering of amino acid residues is based on the sequence of EcTS) to the pyrimidine C (6) atom of dUMP. At the startpoint of catalysis, the binding position and substrate orientation specifically provide an efficient binding of the cofactor, and subsequently permit the formation of the ternary TS–dUMP–CH2THF complex, and the reaction (Newby et al., 2006). Previous researches have shown that 5-FU presents the anticancer

effects by inhibiting TS, but the pathways are not well understood. Previous researchers have highlighted that formation of ternary TS–FdUMP–CH2THF complex depends on time and when the fluorine substituent cannot dissociate from the pyrimidine ring, the reaction stops, which inactivate the enzyme in a slowly reversible manner (Sotelomundo et al., 2006). Reduction of dTMP causes depletion of deoxythymidine triphosphate (dTTP) in the downstream reactions, inducing perturbations in other deoxynucleotides' level (dATP, dGTP and dCTP). The imbalances of ATP/dTTP ratio specifically alter DNA synthesis and repair and cause lethal DNA damage (Danenberg, 1977). When dUMP is accumulated, it subsequently increases the levels of deoxyuridine triphosphate (dUTP), which can be misincorporated (Longley et al., 2003a).

2.12 Indole schiff bases compound

Medicinal chemistry links many scientific disciplines such as chemistry (especially synthetic organic chemistry), biology, and pharmacology in searching and developing new drugs. Pharmaceutical effects and biological activity of many synthetic compounds have been accepted (Franzén, 2000; Kaushik et al., 2013).

For a long period in pharmaceutical and medicinal chemistry, an area that has garnered a lot of interest is the chemistry and biological study of heterocyclic compounds. The history of heterocyclic chemistry began in the 1800s, in step with the development of organic chemistry. A list of various heterocyclic derivatives containing nitrogen atoms have served as unique and versatile scaffolds in the design of experimental drugs (Arora et al., 2012; Ngan et al., 2011; Patel et al., 2017).

Cyclic compounds wherein one or more of the ring carbon atoms have been replaced with another atom are known as heterocyclic compounds. Indoles, an aromatic

heterocyclic organic compound with a six-membered benzene ring attached to a five-membered pyrrole ring containing nitrogen with a bicyclic structure, are bicyclic heterocyclic compounds that contain a pyrrole ring with a benzene ring fused to an α,β-position. They are one of the most important sources to create new compounds with a huge variety of biological applications. Fused heterocyclic structures can be modelled in various ways, resulting in the creation of novel polycyclic frameworks with a great number of different physical, chemical, and biological properties (Kaushik et al., 2013).

Indole scaffold is one of the most promising structural subunits in the effort to discover new types of drugs and plays a key role in the functions of biologically important molecules. The indole derivatives unique characteristics of mimicking peptide structures and binding themselves reversibly to enzymes opens up exciting opportunities in the discovery of various new drugs with a wide range of actions. Substantial research interest has been shown toward indole derivatives and it is one of heterocyclic chemistry's most active areas. This is due to their natural occurrence and their pharmacological activities. Various indole and indole derivates have been known to possess a broad spectrum of biological properties (Salman et al., 2015).

2.12.1 Pharmacological properties for indole derivatives

An indole is an aromatic heterocyclic organic compound that provides great opportunities to discover novel drugs with various pharmacological properties. Many indole derivatives that occur in nature or synthesized in the laboratory have been reported for the treatment of various disease conditions. The importance of indole nucleus led to the development of various bioactive compounds by changing the substituents at different positions in the indole ring (Kaushik et al., 2013).

Numerous compounds possessing indole nuclei have been reported for various biological activities such as anti-cancer (Brancale & Silvestri, 2007; Huang et al., 2012),

antimicrobial and antifungal activity (Sivaprasad et al., 2006), antiviral (Villalain, 2010; Zhang et al., 2015) anti-inflammatory (Bhati & Kumar, 2008; Lee et al., 2015; Rani et al., 2004; Singh et al., 2015), anti-depressant (Baird-Lambert et al., 1982; Diers et al., 2008), anti-hypertensive (Atterhög et al., 1976; London et al., 2004), antioxidant (Estevão et al., 2010; Mohamed et al., 2014; Panda et al., 2012), antidiabetic activities (Li et al., 2007; Mohler et al., 2009).

Indole forms the main component in a great number of naturally occurring compounds such as tryptophan, indole-3-acetic acid (IAA), an essential amino acid, melatonin, and serotonin (Diss et al., 2013; Won et al., 2011; Young, 2007; Zhang et al., 2013).

Indole is the most potent pharmacodynamic nucleus found in various natural products e.g. i reserpine, bufotenine, and psilocybin. Some naturally occurring indole alkaloids such as vincristine, vinblastine, vinorelbine, and vindesine have gained FDA (Food and Drug Administration) approval for anti-tumour activity.

During the past two decades, numerous indole derivatives have been developed that are found to have wide clinical and pharmacological applications. Pharmacologically active indole derivatives in some drug molecules are listed in Table 2.3. A list of drugs in the market containing indole which have been approved by the FDA are available on the market. They include delavirdine, a drug utilized in human immunodeficiency type-1 (HIV-1) treatment in adults (Xu & Lv, 2009).

Several anticancer compounds have been reported to act via varying mechanisms. Indole-based molecules have been implicated in the treatment of several cancerous conditions. Sunitinib and osimertinib, two drugs that are available on the market, have been implicated in renal cell, carcinoma, gastrointestinal stromal tumour, and non-small cell lung cancer (NSCLC) treatments.

Table 2.3: Indole ring containing drug molecules (Kaushik et al., 2013).

Drug	*Application*	*Drug*	*Application*	*Drug*	*Application*
Vincristine	Anticancer	**Vincamine**	Vasodilator	**Roxindole**	Schizophrenia
Vinblastine	Anticancer	**Reserpine**	Antihypertensive	**Delavirdine**	Anti-HIV
Vinorelbine	Anticancer	**Peridopril**	Antihypertensive	**Atevirdine**	Anti-HIV
Vindesine	Anticancer	**Pindolol**	Antihypertensive	**Arbidol**	Antiviral
Mitraphylline	Anticancer	**Binedaline**	Antidepressant	**Zafirlukast**	Anti-Asthmatic
Cediranib	Anticancer	**Amedalin**	Antidepressant	**Bucindolol**	β-Blockers
Panobinostat	Anti-leukamic	**Oxypertine**	Antipsychotic	**Pericine**	Opioid agonist
Apaziquone	Anticancer	**Siramesine**	Antidepressant	**Mitragynine**	Opioid agonist
Tropisetron	Antiemetic	**Indalpine**	Antidepressant	**Pravadoline**	Analgesic
Doleasetron	Antiemetic	**Yohimbine**	Sexual Disorder	**Bufotenidine**	Toxin
Oglufanide	Immunomodulatory	**Indomethacin**	Anti-inflammatory	**Proamanullin**	Toxin

2.13 Discovery of anticancer activity

Indole nucleus has attracted the attention of medicinal chemists in the field of anti-cancer drug development and many substituted indole derivatives have recently earned great interest in chemotherapy as antitumor drugs (Patel et al., 2017).

A series of novel 2-phenylindole-3-carbaldehydes with lipophilic substituents exhibited significant antimitotic activities against MDA-MB 231 and MCF-7 breast cancer cells through the cell cycle arrest in G2/M phase due to the inhibition of tubulin polymerization (Kaufmann et al., 2007). Moreover, in a study conducted by Zhang et al. (2011) anti-tumor activity a number of novel 2-amino-3-cyano-6-(1H-indol-3-yl)-4-phenylpyridine derivatives were synthesized and the strong anti-tumor activity against A549, H460, HT-29 and SMMC-7721 cell lines was observed.

Aldol condensation reaction between 3-indolaldehyde and 4-methoxyacetophenone gave a chalcone compound from which some pyrazoline, pyridine, and pyrimidine derivatives linked to indole moiety were obtained and found to have promising antitumor activity against a human breast carcinoma cell line (MCF7) and a liver carcinoma cell line (HEPG2) (Nassar, 2010).

The new 3,5-bis(2-indolyl)pyridine and 3-[(2-indolyl)-5-phenyl]pyridine were act as potential CDK inhibitors. These compounds showed *in vitro* cytotoxicity against CEM human leukemia (Jacquemard et al., 2008). In addition, a novel series of indole α-methylene-γ-lactones reveled remarkable inhibition ability on phosphorylation of AKT, mTOR, p70S6 kinase, and 4E-BP1(Ding et al., 2005).

Many other indole derivatives i.e. 3, 3-diindolyl oxyindoles, 3-Aroylindoles and indolylchalcones and their pyrazoline analogs showed enhanced anti-cancer activity (Kamal et al., 2010; Wu et al., 2009; Zahran et al., 2010).

These types of derivatives of indole can serve as future therapeutic leads for the discovery of anti-cancer drugs with great promise towards good active leads in medicinal chemistry. Recently, a comprehensive review paper have been published and announced the most potential anticancer indole-based agents (Patel et al., 2017).

2.14 Programmed cell death (Apoptosis)

Potentially anticancer substances may exert their anti-proliferative effects through a number of mechanisms. For instance, the role of anticancer compounds in the modulation of apoptosis in the colorectal mucosa has been reviewed (Kim et al., 2002; Lowe et al., 1993).

Programmed cell death, or apoptosis, plays a crucial role in cancer treatment, which can be induced in many different treatment forms such as ultraviolet (UV) irradiation, cytotoxic chemotherapy, and Fas/APO-1 ligand (Borges et al., 2008; Elmore, 2007; Hassan et al., 2014) .

Extrinsic and intrinsic factors determine whether cells undergo apoptosis, necrosis, or unorganized cell death. The activation of cysteinyl aspartate proteases known as caspases are usually linked to the apoptotic pathway. Co-ordinated action by a cascade of caspases

are required for apoptotic signal transduction and execution (Ashe & Berry, 2003). Generally, apoptotic pathways are split into mitochondrial apoptosomes, mediated apoptosis intrinsic pathways and the death receptor induced extrinsic pathways. The binding of the ligand-receptors, for example TNF alpha (tumour necrosis factor) and TRAIL (TNF-related apoptosis inducing ligand), and also the Fas ligand, to their receptors causes the death receptor pathway (extrinsic) to occur, initiating protein-protein interaction in all of the cell membranes. This leads to initiate caspases-8 -10 activation. This activation results in the executioner caspases-3, -6, and -7 activation and this eventually leads up to DNA fragmentation, DNA budding, and chromatin condensation, all of which are characteristics of cells undergoing apoptosis (Elmore, 2007; Sidotide Fraisse et al., 1998).

The alteration of the pro-apoptotic (Bax) and the anti-apoptotic (Bcl2) radio mediates the intrinsic or mitochondrial pathway, with a higher Bax/Bcl2 ratio resulting in mitochondrial membrane potential loss, causing cytochrome c to be released into the cell cytosol, which then forms the apoptosome complex upon interaction with ATP, Apaf-1, and pro-caspase 9. Pro-caspase 9 is cleaved by the apoptosome into its active version, causing apoptosis by stimulating the effector caspase-induced DNA breakdown (Fan et al., 2005; Youle & Strasser, 2008).

Caspase cascade activation is an important event in the apoptotic pathway. Caspases present themselves in cells as inactive procaspases, with the prodomain and cleavage removal between both the large and small subunits forming the active tetramer. Both directly and indirectly, caspase activity is accountable for cellular protein cleavage, typically proteolysed during apoptosis. Apoptotic caspases are subdivided into initiators (caspases-8, -9, and -10), executioners (caspases-3, -6, and -7), and others (caspases-2 and -12) (Ashe & Berry, 2003; Elmore, 2007).

Independent caspase cascade pathways in apoptosis have also been described. These pathways may involve proteases, calpains, apoptosis inducing factors (AIF), or cathepsins. Interaction with AIF with cyclophilin leads to DNA fragmentation via DNase action (Bröker et al., 2005; Kroemer & Martin, 2005; Norberg et al., 2010; Ondroušková et al., 2008).

CHAPTER 3: MATERIALS AND METHODS

3.1 Research outline and approach

3.1.1 Overview and research methods

DBID was screened its anti-proliferation effect against two colorectal cancer cell lines, and its possible mechanism of action was elucidated. *In vitro*, antioxidant activities of the compound were investigated. The acute toxicity test and subacute toxicity were used to evaluate the safe usage of DBID compound in animal models. The effect of the DBID compound on the azoxymethane-induced colonic aberrant crypt foci in rats was investigate. The colon tissues homogenate were grossly and histopathologically examined for aberrant crypt foci (ACF). Moreover, the antioxidant enzyme activities, gene and protein expression were investigated. Figure 3.1 presents the schematic overview of this study. The following table (Table 3.1) summarises research methods used in each section.

Table 3.1: Research methods used in this study.

	Research Aspect	Methods	Assay/Technique/ etc.
In vitro studies	Cancer Study	Growth of cell lines -Cell culture in appropriate media	Culturing the colon cancer cell lines: HCT 116 and HT-29 and Normal colon cell: CCD841 CoN
		Cytotoxicity and antiproliferative effects	MTT assay
		Apoptosis Fluorescence microscopic examination	AO/PI staining
		Flow cytometry	Annexin V
		Apoptosis	Caspase activity
		Reactive oxygen species	ROS generation
		Apoptotic gene expression	Real Time-PCR
		Apoptotic protein expression	Western blotting
	Antioxidant Activity	Free radical scavenging assay	FRAP, DPPH radical scavenging assay
In vivo studies	Acute toxicity	Serum biochemical analysis	LFT, RFT and lipoid profile
		Histological evaluation of Liver and kidney	Haematoxylin and eosin (H&E) staining
	Subacute toxicity	Animals body weight	weighing weekly
		Serum biochemical analysis	LFT, RFT and lipoid profile
		Histological evaluation of Liver and kidney	Haematoxylin and eosin (H&E) staining
	Chemopreventive effects	AOM-induced ACF in rats	Topographic observation of the 2% methylene blue stained colon and Aberrant crypts scoring
			Haematoxylin and eosin (H&E) staining
			antioxidant activity of colon tissue homogenate
		Gene expression	Real Time-PCR
		Protein expression	Western blotting
			Immunohistochemistry

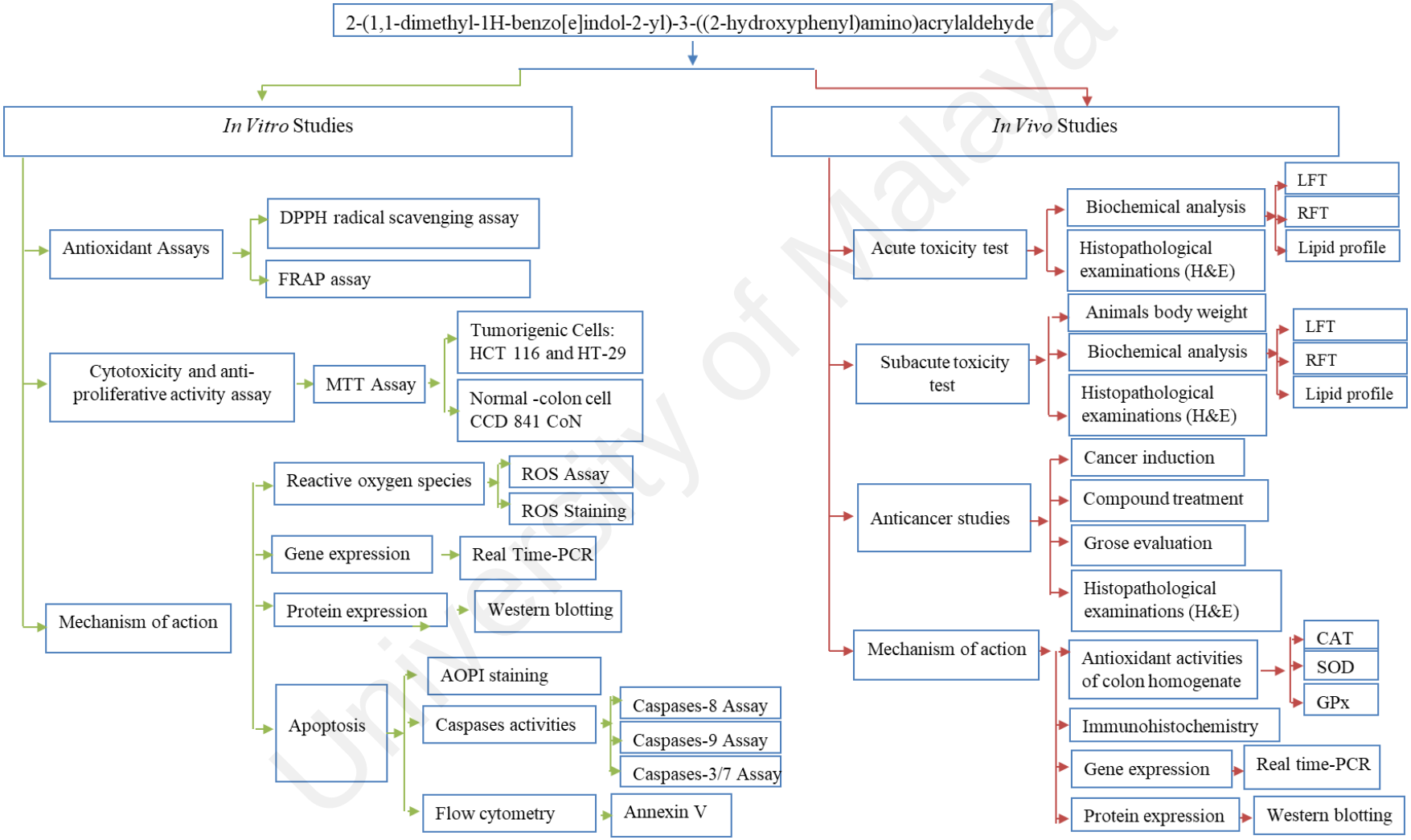

Figure 3.1: Schematic overview of the methodology used in this study.

3.2 Materials

3.2.1 Chemicals and equipment

The solvents and reagents utilised in this study were of analytical. Ultrapure MiliQ water was used. Appendix A-E show the chemicals, apparatus, kits, cell lines and software used in this study.

Compound:

The DBID compound was prepared by the Department of Chemistry, University of Malaya. Figure 3.2 shows the chemical structure of 2-(1,1-dimethyl-1H-benzo[e]indol-2-yl)-3-((2-hydroxyphenyl)amino)acrylaldehyde (DBID).

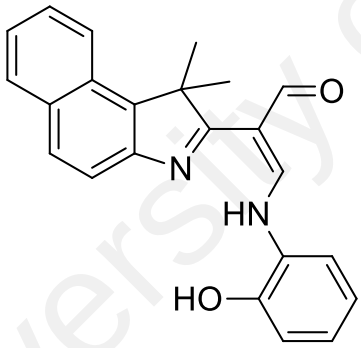

Molecular weight: 356

Formula: $C_{23}H_{20}N_2O_2$

Figure 3.2: Chemical structure of the DBID compound.

The new compound, DBID, has been synthesized by reaction of 2-(diformylmethylidene)-1,1-dimethylbenzo[e]indole with 2-aminophenol (Hajiaghaalipour et al., 2017).

3.3 *In vitro* cancer studies

3.3.1 Cell lines and growth media

3.3.1.1 HCT 116

HCT 116 cell line was purchased from American Type Culture Collection (ATCC), USA (ATCC® CCL-247™). This adherent cell line is categorised as a colon epithelial adenocarcinoma and has epithelial-like morphology. HCT 116 cell line was grown in media consisting of ATCC-formulated McCoy's 5A Medium (ATCC® 30-2007™) with a 10% FBS, 100 units/ml of penicillin-streptomycin supplement.

3.3.1.2 HT-29

This cell line was sourced from ATCC, USA (ATCC® HTB-38™), holding the categorisation of colon epithelial adenocarcinoma. The morphology of this adherent cell line is epithelial-like. The growth media that was used consisted of ATCC-formulated McCoy's 5A Medium (ATCC® 30-2007™) with 10% fetal bovine serum (FBS), 100 units/ml of penicillin-streptomycin supplement.

3.3.1.3 CCD 841 CoN

Normal human colon cell CCD 841 CoN (ATCC® CRL-1790™) was provided from ATCC, VA, USA. The cell line is categorized as a normal human colon epithelial cell. This adherent cell line is epithelial-like. To culture the CCD 841 CoN cell line, media consisted of ATCC-formulated Eagle's Minimum Essential Medium (ATCC® 30-2003™) supplemented with 10% FBS, 100 units/ml of penicillin-streptomycin was used.

3.3.2 Cell culture

Growth of the cells lines took place in a CO_2 water-jacketed incubator which was humidified at 37°C and consisted of 95% room air and the remaining 5% of CO_2. On a 48-hour cycle, and using trypsin-EDTA, the cells were passaged by trypsinization when they reach to 80-90% confluency in flask.

3.3.3 Cytotoxicity test (MTT assay)

The MTT (3-(4,5-dimethyl thiazol-2-yl)-2, 5-dimethyl tetrazolium bromide) assay is an indirect colorimetric assay to assess cell proliferation, cell viability, and/or cytotoxicity. The MTT assay can assess the quantity of viable cells that have been adapted to quantify the growth modulation of cells *in vitro*.

The DBID cytotoxicity and anti-proliferative effects were determined using the MTT assay, using a procedure that was described by Mosmann (1983). The tumorigenic cell lines used in this study were the human colon adenocarcinoma cells HT 116 and HT-29 while a normal human colon cell line (CCD 841 CoN) was utilized to identify DBID's cytotoxic effects.

Approximately 5000 cell/well in 96-well plates were seeded with cells and allowed to attach overnight. The media was changed and various concentrations (µg / ml) of the compound was used to treat the cells. Subsequently, it was incubated for a further 48 h.

DBID compound's effects on cell growth was examined by utilising the MTT assay. 20µl of MTT solution (5mg/ml in PBS) was added to each of the wells, which were then incubated at 37°C for a period of 4 h. The supernatant was then aspirated and the MTT-formazan crystals that were formed by metabolically viable cells dissolved in 100ml of dimethyl sulfoxide (DMSO). The absorbance was measured at 590 nm wavelength and the cell growth inhibition was calculated using the formula:

$$\text{Inhibition (\%)} = [(\text{OD}_{\text{blank}} - \text{OD}_{\text{sample}}) / (\text{OD}_{\text{blank}})] \times 100$$

Different concentrations (µg/ml) of the compound was used to treat the cells to obtain the IC_{50}. The IC_{50} is the concentration of the compound that prevents the 50% of cells growth.

3.3.4 Reactive oxygen species assay

3.3.4.1 Measurement of ROS generation

The intracellular reactive oxygen species (ROS) generation was measured using Cellular Reactive Oxygen Species Detection Assay Kit (Abcam, Cambridge, UK) according to the manufacturer protocol. The procedure was based on oxidation of DCFH-DA to form the fluorescent compound, 2′,7′-dichlorofluorescein (DCF) by intracellular ROS and other peroxides. 2',7'-dicholodihydrofluorescein diacetate (DCFH-DA) oxidises, forming 2',7'-dichlorofluorescein (DCF), a fluorescent compound.

The HCT 116 and HT-29 cells, two colon cancer cell lines, were seeded at a density of 5000 cells per well into 96-well cell plates. They were then cultured for a period of 24h and following that, were treated with the DBID compound at the IC_{50} concentration (triplicate). The ROS was measured at time points of 12h, 24h, 48h. The cells were washed with PBS after incubation and then in each well, 20μM of DCFH-DA was added. Absorbance was measured at 520 nm. H_2O_2 was utilised as positive control. Data was collected from the fluorescence reader.

3.3.4.2 ROS generation staining with the use of DHE

Dihydroethidium (DHE) fluorescent probe was utilised to measure DBID compound's effect on reactive oxygen species (ROS) generation in colon cancer cells. This process was measured, as described previously (Daghastanli et al., 2008; Gomes et al., 2005).

The HCT-116 and HT-29 cells were cultured on coverslips with complete medium and allowed to attach overnight. DBID compound at IC_{50} concentration (9.3 and 11.8 μg/ml for HCT 116 and HT-29, respectively) were then exposed to the cells for a period of 24h. DSMO was utilised as negative control. The treated cells were washed twice after incubation with PBS. They were then stained with DHE (0.5 μM of DHE in 1ml media) for 20 minutes at 37°C. The coverslips were then mounted with mounting medium (Dako,

USA) on the slides. A fluorescence microscope was used to measure ROS formation in treated and untreated cells (Olympus BX51).

3.3.5 Fluorescence microscopic examination

Apoptosis occurrence was qualitatively investigated. The method used was AO/PI double staining in order to investigate the HCT 116 and HT-29 cells morphological characterisation. This was done under a fluorescent microscope in order to analyse the viable cells, early, and late apoptosis.

The procedure was carried out using both the propidium iodide (PI) and acridine orange (AO) double staining dye. It was observed under a fluorescence microscope using the method that has been described previously (Hajiaghaalipour et al., 2015; Ng et al., 2013). Both the HCT 116 and HT-29 cells were seeded in a six well plate. They were then treated with IC_{50} concentration of DBID compound (9.3 and 11.8 µg/ml for HCT 116 and HT-29, respectively) determined by MTT assay and then underwent incubation for 24 h. After the time period, the cells were harvested and stained with an equal volume of fluorescent dye (AOPI). The cells were observed using a fluorescence microscope (Olympus BX51).

3.3.6 Flow cytometric annexin V

The Annexin V assay was conducted utilising FITC Annexin V Apoptosis detection kit (BD ApoAlert Annexin V, Clontech, USA) includes the reagents required for identifying a population of cells that have initiated apoptosis using staining procedure and analysis by flow cytometry. IC_{50} concentration of the DBID compound (9.3 and 11.8 µg/ml for HCT 116 and HT-29, respectively), which was determined by MTT assay, was used to treat the cultured cells in a 25-cm flask for a period of 24h, following which apoptosis was measured using the FITC Annexin V staining protocol. Cold PBS was used to wash the cells twice and cell pellet was resuspended in 1x Assay Buffer at a

concentration of 1 x 10^6 cells/ml. Subsequently, 100 µl of the solution was transferred to a 5 ml culture tube and added with 5 µl of both FITC Annexin V and PI before the cells were gently vortexed and incubated in the dark for a time period of 15 min at room temperature. After that, 400µl of 1x Binding Buffer was added to each of the tubes and analysed using flow cytometry within an hour.

In the flow cytometry analysis by Annexin-V/PI fluorescent staining, each quadrant for evaluation is indicated as follows: AN-/PI-: Viable spermatozoa with no signs on PS translocation; AN+/PI-: Viable spermatozoa showing PS translocation; AN+/PI+: Dead spermatozoa showing PS translocation; AN-/PI+: Dead spermatozoa with no signs of PS translocation.

3.3.7 Cellular caspase activities (Caspase -8, -9 and -3/7) assay

The HCT 116 and HT-29 cells were seeded in the white 96 well plate (SPL, Korea) at 25,000 cells / well. They were then incubated overnight at the temperature 37°C with 5% CO_2. IC_{50} concentration of the compound (9.3 and 11.8 µg/ml for HCT 116 and HT-29, respectively) was then used to treat the cells. For control and blank, untreated cells and media without any cells were used. The caspase activities was assessed for the different incubation times i.e. 4h, 8h, 16h, 24h, and 48h. Caspase -8, -9 and -3/7, activities were carried out utilising Promega Company commercial kits and used in accordance to the manufacturer's procedure (Promega, USA).

In brief, Caspase-Glo™ -8, -9 and -3/7 agents were prepared after treatment and then added directly to the cells in 96-well plates. They underwent 30 minutes of incubation before luminescence was recorded. MG-132 Inhibitor was added to the Caspase-Glo® -8 and -9 reagent in order to decrease non-specific background activity in cell-based assays. A luminometer was used to read the plates (Promega, USA).

The absorbance at 30 min was used for calculation. The data was averaged of in triplicate. Culture medium were used in the determination of background readings while the "no cell media" blank control value was subtracted from each value.

3.3.8 Gene expression assessed by Real Time Reverse transcription PCR

3.3.8.1 RNA extraction

RNeasy® plus mini kit (QIAGEN, Germany) was used to isolate RNA from the samples. 25 cm^2 flasks were utilised to grow both HCT 116 and HT-29 cell lines. Before the initiation of treatment, 6 x 10^6 cells were seeded in 5ml of growth media and were allowed to attach overnight. 24 hours before extraction of the total RNA, IC_{50} of the DBID compound (9.3 and 11.8 µg/ml for HCT 116 and HT-29, respectively) was used to treat the cells. HCT 116 and HT-29 cells which were untreated were utilised as controls. The extraction and purification processes was in accordance to manufacturer's protocol.

The grown cells in the cell-culture flasks were trypsinised after incubation for the indicated hours (4, 8, 16, 24, 48 h). They were then collected as a cell pellet prior to lysis. Buffer RLT was added to disrupt the cells. The cells were then homogenised by pipetting the lysate directly into a QIA shredder spin column placed in a 2ml collection tube. It was then centrifuged at full speed for 2 minutes. Following this, the homogenised lysate was transferred to a gDNA eliminator spin column where it was placed in a 2ml collection tube. It was then centrifuged for 30 sec at 10,000 rpm. The column was subsequently discarded and 350µl of 70% ethanol was added to the flow-through and then mixed well by pipetting. 700µl of the RNeasy spin column was transferred and placed in a 2ml collection tube which was then centrifuged for 15 sec at 10,000 rpm, following which the flow-through was discarded. Treatment with 80µl DNase (QIAGEN, Germany, Cat. No: 79254) was done to eliminate genomic DNA contamination. DNA removal was carried out with the addition of 10µl DNase I stock solution and 70µl buffer RDD directly to the

RNeasy spin column membrane. The mixing process should be done by gently inverting the tube. This mixture underwent incubation for a time period of 20 minutes at room temperature (20 – 30°C). 500µl of RPE washing buffer was used to wash the membrane twice. It was centrifuged for 15s at 10,000 rpm. RNA was eluted in RNase-free water and to prevent RNase activity, stored at -80°C. Purified RNA was used for reverse transcription.

3.3.8.2 RNA quantity and quality

The pure isolated RNA may be contaminated by DNA, protein or phenol that could inhibit the RNA downstream amplification. Therefore, evaluation of RNA integrity and quality is necessary. The quantity of the RNA was checked by using a Thermo Scientific NanoDrop-spectrophotometer at absorbance 260/280 and 260/230.

A260/280: ratio is about 2 indicates pure RNA and deviation from this amount indicates that the RNA contains protein impurities, since RNA has the highest absorbance at 260 and side chain amino acids such as tyrosine and tryptophan absorb at 280.

A260/230: Absorbance at 230 nm is for different salt buffers such as EDTA, carbohydrate, trizol and guanidine thiocyanate. An A260/230 value about 1.7 is a desired value for pure RNA.

The purity of the isolated RNA was checked by running 1% agarose gel electrophoresis. The agarose gel was run for 45 minutes in 90V, and then was observed under UV light. RNA sharp and clear bands can be observed in 18S and 28S rRNA.

3.3.8.3 Reverse transcription (RT)

In reverse transcription, RNA is reverse transcribed to cDNA. The process requires known primers, and reverse transcriptase, and RNA-dependent DNA polymerase.

The RNA was converted to cDNA according to the protocol of the cDNA kit (Applied Biosystemes, USA). The concentration used for all RNA in reverse transcription was 100 ng/µl RNA diluted in RNase free water. The cDNA obtained was kept at 4˚C for RT-PCR assay.

According to the manufacturer's guidelines total RNA converted to cDNA by adding up to 9 µl RNA (1000 ng) in RNAse free water, 10 µl of RT buffer, and 1 µl of RT enzyme. In brief, 9 µl of extracted RNA (concentration of 100 ng/µl of RNA diluted in 9 µl RNAse free water) was mixed with 10 µl of RT buffer and 1µl of RT enzyme. The mixture was mixed thoroughly and briefly centrifuged to spin down the contents and eliminate air bubbles. Then the mixtures were placed in a thermal cycler under the following conditions according to the protocol of the kit.

The mixtures were processed in thermal cycler in the following conditions at 25˚C for 10 min, 37˚C for 120 min and 85˚C for 5 seconds, respectively. Then, the samples were kept a 4˚C.

3.3.8.4 Real Time-PCR

TaqMan® Gene Expression Master Mix (Product No. 444556) assay was performed according to the reaction setup instructions generated by the StepOne software (Ver. 2.0, Applied Biosystems). In this study, the expression of selected genes expressed by the respective cells was investigated. Apoptosis-related cysteine peptidase specific primers; caspase 3 (Casp3, Assay ID: Hs00234387_m1), caspase 8 (Casp8, Assay ID: Hs01018151_m1), caspase 9 (Casp9, Assay ID: Hs00609647_m1), apoptosis regulator; BCL2 (BCL2, Assay ID: Hs00608023_m1), BCL2 associated X (BAX, Assay ID: Hs00180269_m1), tumor protein p53 (TP53, Assay ID: Hs01034249_m1) and BH3 interacting domain death agonist (BID, Assay ID: Hs00609632_m1) and two endogenous

controls, β-actin (ACTB, Assay ID: Hs99999903_m1) and Glyceraldehyde-3-Phosphate Dehydrogenase (GAPDH, Assay ID: Hs03929097_g1) were used in this study (TaqMan®, MGB probes, FAM™ dye-labelled).

All TaqMan probes used in this study were FAM/MGB probe. The probes were labelled with the 6-carboxyfluorescein, acronym (FAM) reporter dye at the 5' end and a TaqMan dihydrocyclopyrroloindole tripeptide minor groove binder, acronym (MGB) probe quencher at the 3' end. These genes were purchased from Applied Biosystems, USA.

To prepare the reaction cocktail, 50 ng of total RNA in 1 µl was used as template. Each reaction tube contained 5 µl fast advanced master mix, 0.5 µl reverse transcriptase, 3.5 µl nuclease free water and 1 µl sample. Thus, the total volume was 10 µl per reaction. For the non-template control (NTC) reactions, 1 µl of RNase free water was used in place of the sample. The mixture was transferred into a fluorescence-compatible fast reaction plate (MicroAmp™) and capped with optical caps (Product No. 4323032). In the reaction plate, 3 replicates of each sample along with 3 replicates of endogenous control were used. Expression of endogenous control was used to normalize fluorescence signals for target assay.

After preparing the reaction plate, the plate was centrifuged briefly and loaded into Applied Biosystem StepOnePlus™ Real Time-PCR system. The relative expression of each gene is compared to the endogenous control housekeeping genes. The relative expression of the investigated genes was normalized with the endogenous control.

Data were analyzed according to the comparative Ct ($2^{-\Delta\Delta Ct}$) method by Wong and Medrano (2005), the amplification of the target and of the reference genes were measured in the samples and reference. CT values used the means of triplicate measurements. The

relative quantity of target in each sample was determined by comparing normalized target quantity in each sample to normalized target quantity in the reference.

ΔCT= CT (target gene) - CT (reference gene)

ΔΔCT= ΔCT (treated sample) - ΔCT (untreated sample)

Fold change = $2^{-\Delta\Delta Ct}$

3.3.9 Protein expression by western blotting

3.3.9.1 Protein extraction

HCT 116 and HT-29 cells were plated in a 25 cm flask and treated with IC_{50} of DBID (9.3 and 11.8 µg/ml for HCT 116 and HT-29, respectively) for 24 h. Total protein of the cells was extracted with using PRO-PREP (Intron, UK) solution kit. This solution included highly denature ionic detergent such as sodium dodecyl sulphate (SDS), lithium dodecyl sulphate and sodium deoxycholate that can isolate protein as a monomeric for any protein molecular weight analysis and western blot. It also contains zwitterioninc detergent CHAPS (3-[(3-Choamidopropyl) dimethylammonio]-1- propanesulfonate) which is more effective in disrupting protein interaction. Total protein was isolated by following the protocol:

After incubation time, the cells were harvested and washed with PBS. 400 µl of extraction solution was added to the pallet and homogenised using an ultrasonic cell disruptor (Branson) by putting on ice. After 5-10 minutes homogenising, samples were incubated at –20^{o} C for 30 minutes to promote cell lysis. Then the samples were centrifuged 15 minutes, at 4 ° C, 13000 rpm to separate supernatant. The supernatant was then transferred into the new 1.5 ml eppendorf tube and stored in –20° C.

3.3.9.2 Protein quantification

Protein quantification was performed to determine samples concentration by using Micro BCA protein assay kit (Thermo Scientific™ - US). This kit contains Micro BCA Reagent A (MA), Micro BCA reagent B (MB), Micro BCA reagent C, and Bovine Serum Albumin (BSA) as Standard Ampules at 2.0mg/mL in a solution of 0.9% saline and 0.05% sodium azide. The Kit is a detergent-compatible bicinchoninic acid formulation for the colorimetric detection and quantitation of total protein. A purple-colored reaction product is formed by the chelation of two molecules of BCA with one cuprous ion (Cu^{+1}). This water-soluble complex exhibits a strong absorbance at 570 nm wavelength that is linear with increasing protein concentrations. The samples concentration were calculated from a linear plot of BCA standard concentration (Axis X) of the intensity by changing of color in absorbance. This absorbance obtained from the reaction between BSA and BCA reagents. Standard concentrations of BSA were prepared at 10, 8, 6, 4, 2, 1, 0.5, and 0 µg/ml. The samples then were diluted 1 in 50 with PBS buffer. 50µl of total protein samples or standard as a serial dilution were added to 50 µl of BCA reagents in a greiner UV-transparent 96 well plate (Thermo Scientific™ - US) in triplicate. The plate was incubated for 2 hours at 37°C, then the intensity of changed colors were qualified by using a plate reader at wavelength of 570 nm. Standard curve was generated by serial dilution and samples protein concentration calculated from the standard curve (Appendix G).

3.3.9.3 Western blotting

SDS-PAGE running: Polyacrylamide gel contains two different parts (resolving and stacking) with separate formulation. Resolving part is used at the bottom of gel caster with a pH of 8.8 and stacking part is placed above the resolving with a pH of 6.8. In this study, resolving gel with 14 % for (Bax (ab32503), Bcl2 (ab59348), Caspase 3 (ab13847) and beta actin (ab8227)) was used. Stacking gel is used to pack protein together after

loading and are mostly prepared in 4 %. The gel was prepared in gel cast and kept overnight at 4° C. The compositions of each gel are shown in Table3.2.

Table 3.2: Composition of 12% resolving and 4% stacking gel.

Stock solution	Resolving gel 12%	Stacking gel 4%
Acrylamide	8.3 ml	0.665 ml
4X resolving	4 ml	_
4X Stacking	_	1.25 ml
10% SDS	0.2 ml	50 µl
10% APS	0.1 ml	25 µl
TEMED	7 µl	5 µl
Double distilled H2O	6.4 ml	3 ml

The following day equal volume of samples (20 µg) were mixed with loading dye, then boiled for 5 minutes and loaded in the gel. Gel cast was then placed inside the electrophoresis tank and bathed in migration buffer with the recommended time as instructed by the manufacturer. Prestained protein marker was loaded into the one of the empty wells to assess protein size bands. Rabbit polyclonal beta actin (Abcam, UK) was used as loading control, to check whether all samples have been loaded equally, and to compare the expression of different samples. Electrophoresis was disconnected when the front dye reached the bottom of the gel.

Transfer to membrane: The samples were separated by electrophoresis, the protein transferred to PVDF (BIORAD, UK) membrane for immunoblotting. A hydrophobic membrane needs to prewet into pure methanol (2 minutes) and then into the twobin buffer (5 minutes) which contains 20% methanol. The presence of methanol in twobin buffer (transfer buffer) is to promote dissociation of SDS from the protein and improve adsorption of protein onto the membrane (Pettegrew et al., 2009). The PVDF membrane was placed next to the gel. The two were sandwiched between absorbent materials, and clamped between solid supports to maintain tight contact between the gel and membrane

without air bubbles. Samples transformation can perform in wet or semi-dry conditions. In this study, wet condition tank is used. The gel membrane sandwich was placed in wet transfer tank for electro blotting at constant voltage of 100 volts for 90 minutes. After transferred membrane was exposed and washed with PBST (phosphate buffer saline-tween 20) 3 times in 5 minutes.

Blocking step: To block the membrane, two blocking solutions were traditionally used: non-fat milk or BSA (5%). Milk is cheaper but is not recommended for studies of phospho-proteins, as it causes high background because the phospho-specific antibody detects the casein present in the milk. BSA was used to block the membrane 90 minutes at 4 ° C under agitation. Washing with PBST 3 times in 5 minutes is necessary on this step before incubation with primary antibody.

Incubation with antibodies: primary antibody was diluted 1:1000 in PBST buffer and incubated with membrane 60 minutes at 4°C under agitation. After washing with PBST buffer, secondary antibody (attached to horseradish peroxidase-HRP) was diluted 1:2000 and incubated for 60 minutes under agitation.

Visualizing: to visualize the target protein band Opti-4CN^{TM} Substrate kit was used. This kit is colorimetric (HRP) substrate and detected band can be seen by the naked eye. Primary and secondary antibodies used in this study are shown in Table 3.3.

The visualized blots of target protein, membrane were captured by a gel documentation system (Vilber Lourmat, from Fisher Scientific, USA). The density of each band was determined using Image J software (National Institutes of Health, USA). The ratio of each target band over Beta actin was calculated and considered as the expression level of the target proteins.

Table 3.3: Primary and secondary antibodies that have been used in western blot.

Target protein	Primary antibody	Secondary anti body
Anti-Bcl-2 antibody Product code: ab59348	Rabbit polyclonal to Bcl-2	Goat anti-rabbit HRP Product code: ab205718
Anti-Bax antibody Product code: ab32503	Rabbit monoclonal to Bax	Goat anti-rabbit HRP Product code: ab205718
Anti-Caspase-3 antibody Product code: ab13847	Rabbit polyclonal to Caspase-3	Goat anti-rabbit HRP Product code: ab205718
Anti-beta Actin antibody Product code: ab8227	Rabbit polyclonal to beta Actin	Goat anti-rabbit HRP Product code: ab205718

3.4 Antioxidant analysis

3.4.1 Ferric reducing antioxidant power (FRAP)

The FRAP assay was carried out according to the method of Benzie and Strain (1996) with slight modification: the volumes were scaled down to accommodate microtiter plate volumes. The FRAP reagent was prepared by mixing acetate buffer, TPTZ (2,4,6 tripyridyl-S-triazine) and $FeCl_3.6H_2O$ at a ratio of 10:1:1. To a volume of 0.005 ml of the DBID compound, 0.095 ml of FRAP reagent were added. After 4 min, the absorbance of the blue color was measured against a blank sample containing distilled water. A standard curve was prepared using different concentrations of $FeSO_4.H_2O$ (Appendix H).

3.4.2 1,1-Diphenyl-2-picrylhydrazyl (DPPH) radical scavenging activity

The DPPH radical scavenging activity was determined using the method developed by Cos et al. (2002) with some modifications. The DBID compound (5 µl) was added to 195 µl of a 0.004% MeOH solution of DPPH. Trolox was used to construct a standard curve by using different concentrations (0 – 200 µg/ml). Absorbance at 517 nm was determined after 30 min, and the percentage of inhibition was calculated as [(A0 - A1)/A0] ×100,

where A0 is the absorbance of the control (dH_2O), and A1 is the absorbance of the sample/standard. A graph of the DPPH radical scavenged (%) vs. concentration of sample was plotted (Appendix I). IC_{50} denotes the effective concentration of samples used to reduce 50% of available DPPH radicals.

3.5 *In vivo* studies

3.5.1 Animal and ethical issues

Adult SD (Sprague Dawley) male and female rats (6-8 weeks of age, 180-200 g of weight) were provided by the animal house service center of the University of Malaya. All procedures were approved by the Faculty of Medicine, Institutional Animal Care and Use Committee (FOM IACUC), of the University Malaya (UM) with ethic number: 2015-180804/BMS/R/MAA. All of the animals had been cared for in accordance with the criteria of the National Academy of Science's Guide for the Care and Use of Laboratory Animals (Clark, 2010). Six rats per cage were housed in an animal room in a clean and well ventilated standard environment of 12:12 h light:dark cycle with controlled temperature and humidity. Food and water were available and rats had free access to standard laboratory diet (Reeves et al., 1993) and tab water *ad libitum*.

3.5.2 Acute toxicity evaluation

The demonstration of the safety usage of the synthetic compound required that the acute toxicity of the compound be determined (Figure 3.5). Twelve female SD rats were assigned evenly into groups categorized according to the OECD guideline (OECD Guideline, 2001). Prior to the dosing, these animals were fasted overnight, but had free access to water. A single dose of the synthetic compound (300 mg/kg) was administered to the animals by oral gavage. After dosing, food was withheld for another 3 to 4 h. Following the administration, the animals were observed for 30 min and 2, 4, 8, 24 and 48 h; this was to monitor any possible onset of toxicological symptoms or clinical

symptoms. According to the guideline, if 0-1 animal died in the tested dosed (300 mg/kg) the animal would be treated for higher concentration of the compound (2000 mg/kg), but if 2-3 animals died in the tested dosed (300 mg/kg), a new group (n=3) would be assigned and treated with 50 mg/kg. At this dose (50 mg/kg), if 0-1 animals died the safe dose would be categorized in >50-300, but if 2-3 animals died next group would be treated with 5 mg/kg and the safe dose category would be determined (>0-5). If only 0-1 of the animals administered with 2000 mg/kg of the compound died, the safe value would exceed 2000 mg/kg, but if 2-3 animals died, then dosing proceeded at 300-2000 mg/kg. Any signs of behavioural changes, toxicity, and mortality were recorded over a period of 2 weeks. On day 15, the animals were sacrificed. Following the sacrificing of the rats, the blood and organs (liver and kidney) were collected. This was for serum biochemical analysis and histopathological evaluation for signs of toxicity. Cardiac puncture under anaesthesia was used as the method of terminal blood sampling.

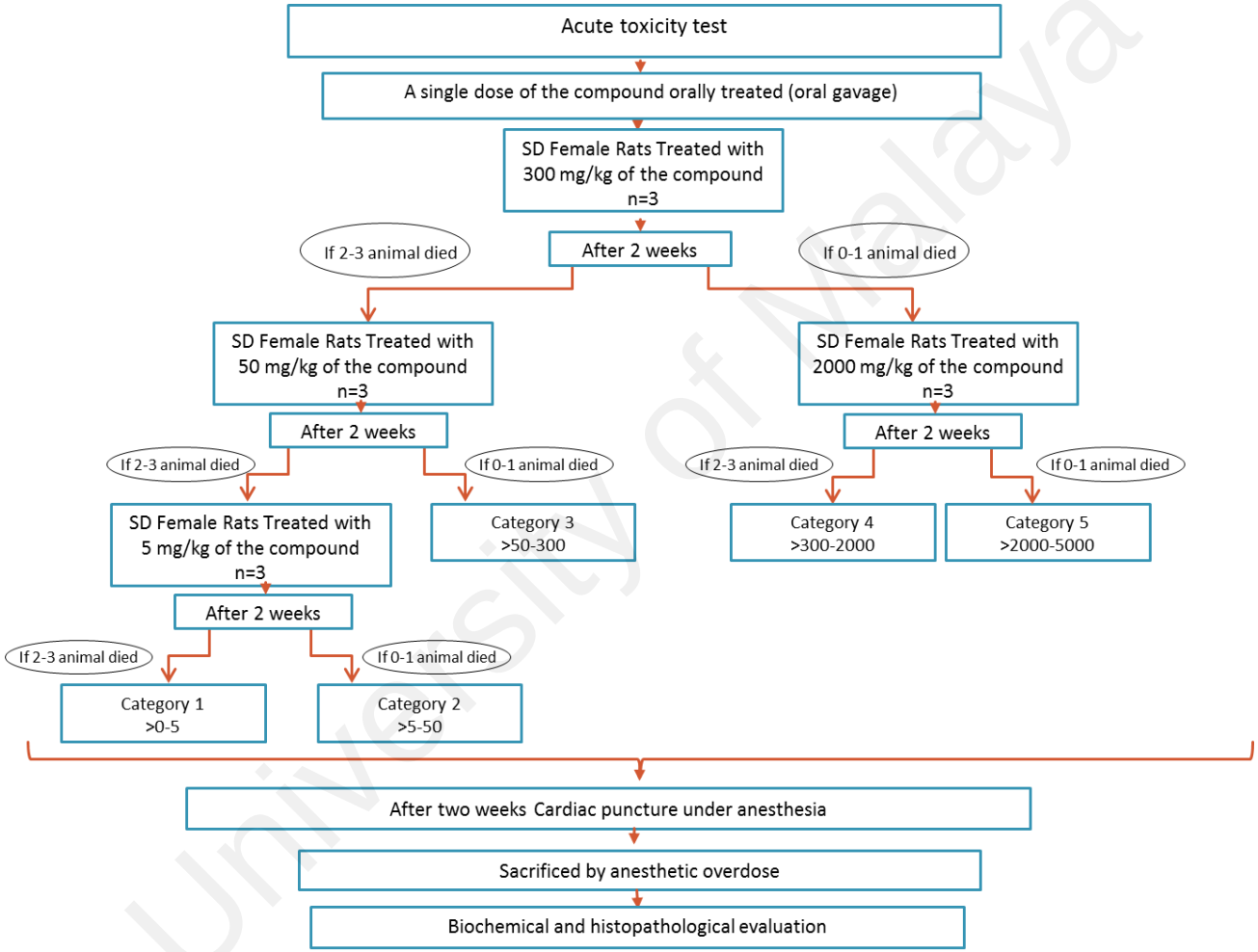

Figure 3.3: The flowchart of acute toxicity test for the DBID compound.

3.5.3 Subacute oral toxicity evaluation

In the assessment and evaluation of the toxic characteristics of the compound, the determination of oral toxicity using repeated doses was carried out after initial information on toxicity has been obtained by acute toxicity testing (Figure 3.6). Forty male and female Sprague Dawley rats were assigned into four groups categorized according to the OECD guideline no. 407, Repeated Dose 28-day Oral Toxicity Study in Rodents rodent, OECD guideline for the testing of chemicals (OECD Guideline, 2008).

Groups of five male and five female SD rats were orally administrated by oral gavage with Tween 20 (10%) (vehicle as control), 10, 20, and 40 mg BDID/kg body weight/day for 28 days to investigate the subacute oral toxicity. This division was random, splitting the rats into four groups of ten rats each (five males and five females in each group). The maximum volume of liquid to be administered at one time did not exceed 1ml/100g body weight. All of the animals were observed closely, each day for any possible onset of toxicological symptoms or clinical symptoms and the body weight of rats were recorded weekly until the end of experiment.

During the period of experiment, animals were given ad libitum access to food and tap water. The animals were observed for 28 days and sacrificed on day 29. Following sacrificing the rats by overdosing anesthesia, cardiac puncture was used as the method of terminal blood sampling for serum biochemical analysis and then the liver and kidney organs were also collected for histopathological evaluation of toxicity.

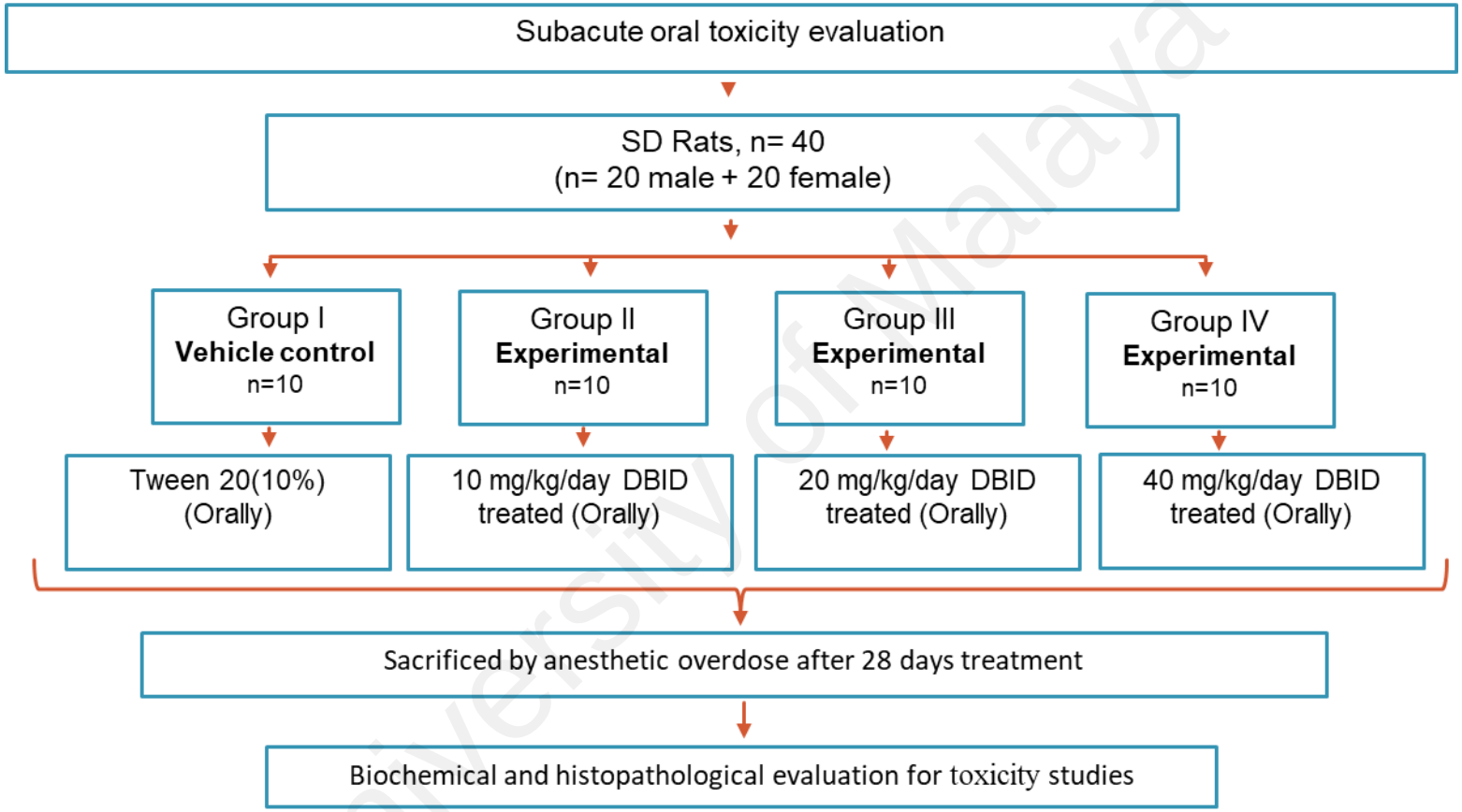

Figure 3.4: The flowchart of subacute toxicity test for the DBID compound.

3.5.4 Chemopreventive effects of DBID on colon cancer in an animal model

3.5.4.1 Chemicals

Azoxymethane:

Azoxymethane (AOM) is a known carcinogenetic agent using for the study of colon carcinogenesis in rodents. AOM is the metabolic derivative from 1,2-dimethylhydrazine via azomethane as an intermediate compound. It is generally used to induce colon cancer with specific induction pattern similar to the pathogenesis of human sporadic colon cancer. The azoxymethane has been widely used to study the molecular biology, prevention, and treatment of colon cancer. It has been known to be used in studies to evaluate the efficacy as preventative measure for azoxymethane-induced carcinogenesis (Escribano et al., 2004; Fiala et al., 1987; Lijinsky, 1985). The AOM was purchased from Sigma-Aldrich (MO, USA).

5-Fluorouracil:

5-Fluorouracil (5-FU) is used as an anticancer drug to especially treat colon cancer, breast cancer, and head and neck cancer since 1957 (Grem, 2000). It is a heterocyclic aromatic organic compound similar to pyrimidine molecules of DNA and RNA. 5-Fluorouracil is classified as an antimetabolite medication which interferes with cells making DNA and RNA, in order to stop the growth of the cancer cells (Ji et al., 2015; Noordhuis et al., 2004; Rutman et al., 1954). The 5-fluorouracil was obtained from Sigma-Aldrich (MO, USA). It is an analogue of uracil with a fluorine atom at the C-5 position instead of hydrogen (Figure 3.5).

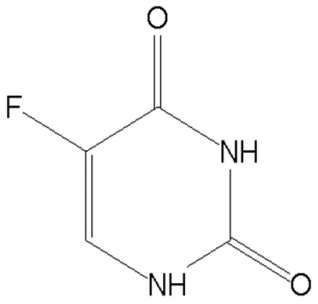

Figure 3.5: Chemical structure of 5-Fluorouracil (Zhang et al., 2008).

3.5.4.2 Animal study groups

Twenty-four male Sprague Dawley rats were randomly divided into four groups of six rats each. The animals were anesthetized prior to AOM (carcinogen) injection. Azoxymethane (AOM)-induced aberrant crypt foci (ACF) in animal model is a well-known procedure in colon cancer studies. The rats that were in cancer groups were injected subcutaneously with the colon-specific carcinogen (AOM) at 15 mg/kg once a week for two weeks. In addition, six rats were assigned as normal control group which received no AOM injection and were orally administrated with Tween 20 during the experiments. After AOM injection, these four groups were continued (two-month) to be orally administrated with tween 20 (10%)(vehicle), 20 mg/kg and 40 mg/kg synthetic compound once a day and weekly intravenous injection of 5-Fluorouracil (35 mg/kg), respectively. All of these animals were given food and water ad libitum. After ten weeks of experiment, all the animals were sacrificed and the colon tissue was collected and examined histologically for the presence of aberrant crypt foci (ACF). Liquid nitrogen was used to prepare colon tissue samples for tissue homogenization process.

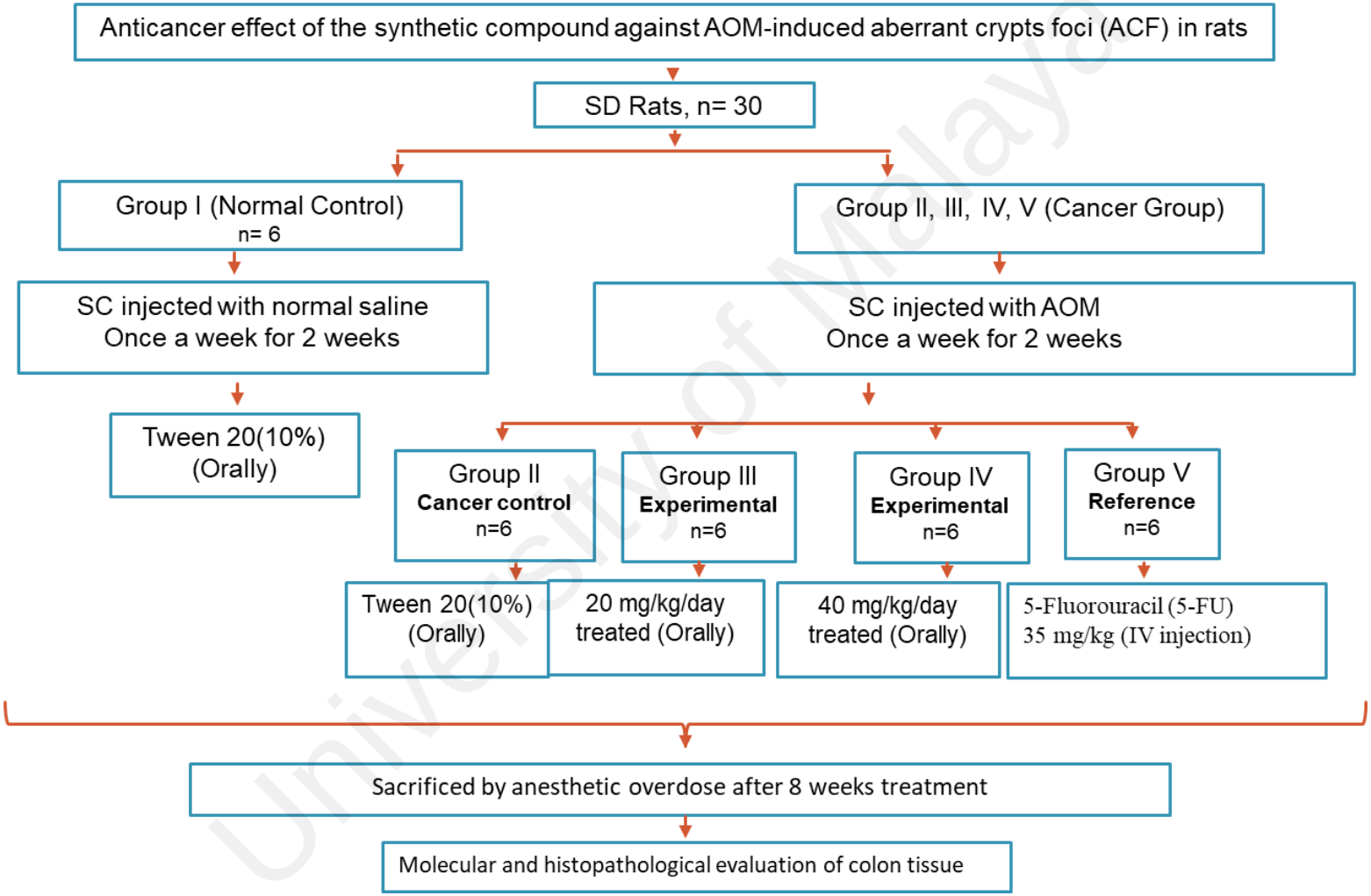

Figure 3.6: The flowchart of the chemopreventive study against colon cancer.

3.5.4.3 Scoring of aberrant crypts

The animals were euthanized using an overdose of ketamine and xylazine, and colon tissues were separated. Then they were flushed with cold phosphate buffered saline (PBS). Subsequently, the colon specimens were longitudinally opened from anus to rectum and stained with 2% methylene blue to observe and record the incidence of aberrant crypts foci (ACF) under dissecting microscope. The numbers of crypts per sample were detailed and the ACF score was calculated based on the number of aberrant crypts foci in each focus.

3.5.4.4 Histological evaluation of the colon

The colon tissues of all groups were immediately fixed after animal dissection in 10% buffered formalin and proceeded by using tissue-processing machine (Leica, Germany) prior to embedded in paraffin blocks. Then the paraffin blocks were cut into 5 μm sections and stained with hematoxylin and eosin (H&E). The slides were examined using an Olympus BX60 light microscope and captured using an Olympus XC10 camera (Tokyo, Japan) for histological evaluation.

Haematoxylin and eosin stain (H&E):

Hematoxylin and eosin stain (H&E stain or HE stain) is a routine and popular staining method in histology. The hematoxylin and eosin stain uses two separate dyes, one staining the nucleus and the other staining the cytoplasm and connective tissue. Hematoxylin has a deep blue-purple color that will stain the nucleic acids within the nucleus, leaving it a deep purplish-blue color.

Eosin is an aqueous or alcoholic solution of eosin Y, which stains the cytoplasmic material including connective tissue and collagen, and leaves an orange-pink

counterstain. This counterstain acts as a sharp contrast to the purplish-blue nuclear stain of the nucleus, and helps identify other entities in the tissues.

In the procedure, the tissue samples from each rat were fixed in 10% buffered formalin for 24 h then processed in a paraffin tissue processing machine. The next step the tissue is kept in a melted paraffin bath for a few hours. Wax is infiltrated in the tissue and increases hardening, making sectioning of the tissue easy. Then tissue is transferred to a mould in the process of embedding with melted paraffin and allowed to cool and solidify to obtain blocks for sectioning. Then approximately 5 μm thick paraffin wax embedded tissue sections were prepared for staining with H&E for histological evaluation.

In brief, the sections were deparaffinized in three changes of xylene, 3 minutes each. Then, were dehydrated in 2 changes of absolute alcohol for 5 min, 95% alcohol for 2 min, and 70% alcohol for 2 min, respectively. The slides were washed briefly in distilled water for 5 min, and then were stained with hematoxylin solution for 6 min. The excess stains were removed by using running tap water, and acid alcohol before immersing in lithium carbonate solution. The slides were washed and stained with Eosin. After that, the slides were rinsed in 95% alcohol (2 changes), absolute alcohol and 2 changes of xylene before mounting with mounting medium. The protocol below shows the procedure for the H&E preparation and staining:

1. Deparaffinize in Xylene I and II and III - 5 minutes each
2. Rehydrate
    a. EtOH 100% - 3 minutes
    b. EtOH 100% - 3 minutes
    c. EtOH 95% - 3 minutes
    d. EtOH 95% - 3 minutes
    e. EtOH 70% - 3 minutes
3. Rinse in distilled water - 5 minutes

4. Stain in hematoxylin - 6 minutes (Filter before each use to remove oxidized particles)
5. Rinse in running tap water - 20 minutes
6. Decolorize in acid alcohol -1 to 3 seconds (Discard after each use)
7. Rinse well in tap water - 5 minutes
8. Immerse in lithium carbonate -3 Seconds
9. Rinse in tap water - 5 minutes
10. Counterstain in Eosin - 15 seconds
11. Dehydrate
    a. EtOH 95% - 3 minutes (Discard after each use)
    b. EtOH 95% - 3 minutes
    c. EtOH 100% - 3 minutes
    d. EtOH 100% - 3 minutes
12. Clear in Xylene I and II - 5 minutes
13. Mount with Cytoseal in fume hood.

3.5.4.5 Localization of proteins by immunohistochemistry (IHC)

Immunohistochemistry technique was used to identify the location of proteins in the tissue. Location of target was identified by light microscope. Immunohistochemical analysis of tissue sections were performed as previously described by Bardi et al. (2014). In the procedure, colon tissues were fixed overnight in 10% buffered formalin before processing. Then the tissues were embedded with the paraffin wax and were cut were cut into 5 µm sections prior to staining. The sectioned tissues (5-µm thickness) were deparaffinized in xylene and rehydrated in reducing concentration of ethanol. Tri-EDTA buffer (10mM Tris Base, 1mM EDTA solution, 0.05% Tween 20, pH 9.0) was used for antigen retrieval 10 min, and then 1% H_2O_2 in methanol was applied to neutralize the endogenous peroxidase. Endogenous peroxidase was blocked using hydrogen peroxide blocking solution for 5 min followed by rinsing of the samples.

Sections were then blocked with 1.5% blocking serum (serum from the same source of secondary antibody) for the non-specific binding prior to incubation with primary

antibody. 1:100 diluted primary antibody in blocking serum was used and incubated in 4°C overnight. The day after, sections were rinsed 3 times 5 minutes each in PBS, then incubated with biotinylated secondary antibody for 1 hour at room temperature, and were then exposed to AB enzyme 1 hour and the sections washed 3 times, 5min each. Location of protein was detected with DAB (Diaminobenzidine HCl) (Santa Cruz, USA) which can bind to antibodies attached to protein and detected dark-brown stain. Sections were rinsed 5 min with deionized water, then counterstained with hematoxylin for nuclear staining and rinsed to eliminate extra hematoxylin. Slides were dehydrated with different dilution of ethanol and xylene, wiped off excess xylene and covered with 1 drop mounting medium.

Olympus BX60 light microscope with an attached Olympus XC10 camera (Tokyo, Japan) was used to view the slides and capture the photos. Dark brown stained were obtained based on the expression of target proteins.

3.5.4.6 mRNA expression analysis by Real Time PCR (qPCR)

The separated colon tissues (0.5 cm of the middle part) were immediately washed with cold phosphate buffered saline and were kept in five volume of RNA Later® prior to RNA extraction. RNA later® solution was used to stabilize and protect tissues cellular RNA (Ambion, L/N: 1206029). Samples can be preserved in RNA Later® solution at 20°C or below for up to 2 years. Total RNA was extracted from 30 mg tissues (wet weight) that were floating into the RNA later® solution using the RNeasy® plus mini kit (QIAGEN, Germany). The details of the procedures are described in Section 3.3.8.

The Total RNA was isolated from 30 mg of colon tissue by using RNeasy® plus mini kit (QIAGEN, Germany), and assessed for quality and quantity using absorption measurements (Thermo Scientific Nanodrop 2000 Spectrophotometer, Massachusetts,

USA) and agarose gel as the most common method to evaluate RNA integrity. Reverse transcription into cDNA was performed by using Two-Step qRT-PCR kit, High capacity RNA to cDNA by Applied Biosystems, USA.

The relative quantification of the genes was performed using the TaqMan® Gene Expression Master Mix by following the manufacturer's protocol. The expression of two endogenous controls Actb (Rn00667869_m1) and Gapdh (Rn01775763_g1) were used in this study. Apoptosis-related cysteine peptidase specific primers; BCL2 (Rn99999125_m1), BAX (Rn01480161_g1) and Casp3 (Rn00563902_m1) were purchased from TaqMan® (MGB probes, FAM™ dye-labelled). All experiments samples were loaded in three biological replicates. The ΔΔCt method was used to determine the relative expression and perform comparative Ct values analysis via differences between the treated and untreated groups.

3.5.4.7 Protein expression analysis by western blotting

The colon tissue samples were washed with cold phosphate buffered saline and 1 cm of the middle part of colon tissue were collected from rat and kept in -80 °C prior to tissue homogenization. 50 mg of colon tissue (wet tissue) was separated and soaked into 400 µl of extraction solution. The tissues were homogenised using an ultrasonic cell disruptor (Branson) by putting on ice to disrupt tissues. After 10 minutes homogenising, samples were incubated at –20º C for 30 minutes to promote cell lysis. This step was performed two times to increase protein concentration. The samples were centrifuged 15 minutes at 4 ° C and 13000 rpm to separate supernatant. The supernatant then transferred into the new 1.5 tube and stored in –20° C.

From 50 mg colon tissue, the total amount of protein was extracted. The total protein concentration was determined by using lysis buffer (Pro-Prep Solution Kit, Intron, UK) and Micro BCA Protein Assay kit (Thermo Scientific™ - US), respectively.

Through the use of 14% sodium dodecyl sulphate polyacrylamide gel electrophoresis, the western blot analysis was then processed. The blotted proteins were subsequently transferred into a polyvinylidene fluoride membrane (Bio-Rad, UK). After that, they were blocked with 5% non-fat milk in TBS-Tween buffer before subjected to specific primary and secondary antibodies (Abcam, UK). The specific primary antibodies including b-actin, Bax, Bcl-2 and Caspase-3 were purchased from Abcam Company, UK. From Amersham Biosciences Corp (NJ, USA) the secondary antibodies conjugated to horseradish peroxidase had been obtained. The visualization of the protein bands utilized a colorimetric DAB substrate kit (Bio-Rad, UK), that was subsequently quantified through the utilization of the ImageJ 1.8.0 software (National Institutes of Health, Bethesda, MD, USA). The details of the procedures are described in Section 3.3.9.

3.5.4.8 Antioxidant enzymes activities of colon tissue homogenate

After washing the colon tissue samples with cold phosphate buffered saline, 1 cm of the middle part of colon tissue were collected from rat and kept in -80 °C prior to tissue homogenization. The activity levels of glutathione peroxidase (GPx), superoxide dismutase (SOD) and catalase (CAT) were determined by using commercial kits according to manufacturer's protocol (Cayman Chemical, USA).

(a) ***Catalase assay***

The assay is based on the reaction of CAT with methanol in the presence of H_2O_2 producing formaldehyde, which is measured calorimetrically using 4-amino-3-hydrazino-5-mercapto-1, 2, 4-triazol (Purpald) as the chromogen. Purpald forms a bicyclic heterocycle with aldehydes which, upon oxidation, changes from colorless to a purple color (Johansson & Borg, 1988; Sinha, 1972).

The assay was conducted according to the instruction provided with the commercially purchased kit from Cayman Company (item no. 707002). This assay was performed according to the protocol in the kit.

100 µl of diluted assay buffer, 30 µl of methanol, and 20 µl of the samples were mixed together. The reaction was initiated by adding 20 µl of diluted hydrogen peroxide to all the wells being used. The plate was covered with the plate cover and incubated on a shaker for 20 min at room temperature, and then 30 µl of diluted potassium hydroxide and 30 µl of catalase purpalad (Chromogen) were added to each well to terminate the reaction. The well was covered with the plate cover and incubated for 10 min at room temperature on a shaker. A volume of 10 µl of potassium periodate was added to each well and incubated for 5 min at room temperature on a shaker. The absorbance was read up at 540 nm with microplate reader.

CAT activity in each sample was expressed in nmol/min/ml using the following equation:

First the formaldehyde concentration of the sample (µM) was calculated by using the equation obtained from linear regression of the standard curve:

formaldehyde (µM) – [sample absorbance – (y-intercept) /Slop] X (0.17ml/0.02 ml)

Then the CAT activity was calculated by using the following formula:

CAT activity (nmol/min/ml) = (µM of sample/20 min) X sample dilution

One unit is defined as the amount of enzyme that caused the formation of 1.0 nmol of formaldehyde per min at 25 °C.

(b) ***Superoxide dismutase***

Cayman's SOD kit assay utilizes tetrazolium salt for detection of superoxide radicals generated by xanthine oxidase and hypoxanthine. The assay was conducted according to the instructions provided with the commercially purchased kit from Cayman Company (item no. 706002).

A volume of 200 µl of the diluted radical detector and 10 µl of the samples were mixed together in the 96-well plate. The reaction was initiated by adding 20 µl of diluted xanthine oxidase to all the wells. The 96-well plate was shaken for a few seconds to mix and covered with the plate cover, then it was incubated on a shaker for 20 min at room temperature. The absorbance was read up at 450 nm using a microplate reader.

SOD activity was calculated using the following formula:

SOD activity (U/ml) = [(sample LR - y-intercept) /Slop × (0.23ml/0.01 ml)] × sample dilution

One unit of SOD is defined as the amount of enzyme needed to exhibit 50% dismutation of the superoxide radicals.

(c) ***Glutathione peroxidase***

The GPx activity was measured through a coupled reaction with glutathione reductase. The assay was conducted according to the instruction provided with the commercially purchased kit from Cayman Company (item no. 703102).

A volume of 100 µl of assay buffer, 50 µl of co-substrate mixture, and 20 µl of the samples were mixed together in the 96-well plates. The reaction was initiated by adding 20 µl of cumene hydroperoxide to all the wells being used and shaken for a few seconds

to mix. The absorbance was read once every min at 34 nm using a microplate reader for at least 5 time points.

GPx activity was calculated using two formulas:

$$\Delta A_{340}/\text{min} = |A_{340}\,(\text{time 2}) - A_{340}\,(\text{time 1})| \,/\, (\text{time 2 (min)} - \text{time 1 (min)})$$

Time 1 = absorbance at 0 min, time 2 = absorbance at 5 min, and A_{340} = change in absorbance per min obtained from the standard curve, so:

The activity of GPx (nmol/min/ml) = (ΔA_{340} min/ 0.00373 μM^{-1}) X (0.19 ml / 0.02 ml) X sample dilution

3.6 Statistical analysis

Experimental results were presented as means ± standard deviation. Each of the measurements and of the analyses were carried out, without exception, in triplicate for *in vitro* studies.

Data in *in vivo* studies were expressed as mean ± SD of six animals for anticancer investigation (n=6).

This study used SPSS version 18 statistical software and Excel 2007 for the statistical and graphical evaluations. One-way analysis of variance (ANOVA) with Tukey's multiple comparisons and the Student's t-test were carried out. p-value < 0.05 was considered as significant.

CHAPTER 4: RESULTS

4.1 *In vitro* cancer studies

4.1.1 *In vitro* inhibition of cell proliferation (MTT Assay)

The 3-(4,5-dimethylthiazol-2-yl)-2,5-diphenyl tetrazolium bromide (MTT) assay is an indirect colorimetric assay to assess the number of viable cells and has been adapted to measure the growth modulation of cells *in vitro*. Two colon cancer cell lines were selected to determine the antiproliferative activity of the DBID compound. In addition, normal colon cell (CCD 841 CoN) was included in order to examine the cytotoxicity of the compound on normal cells. The cells were treated with the different concentrations of compound for 48 h. The antiproliferative activity of HCT 116 and HT-29 cells by the new synthetic compound (DBID) are shown in Figure 4.1 and the IC_{50} values of the compound is shown in Table 4.1

Figure 4.1 shows that antiproliferative activity of the compound increases in a dose-dependent manner and the range of percentage of inhibition in treated HCT 116 cells with the compound were from 12.3 % to 93.7 %, while the range in HT-29 cells treated with the same compound were from 8.7 % to 86.9 %. Also, Table 4.1 shows that the DBID compound at a concentration of 9.32± 1.2 µg/ml and 11.85± 2.7 µg/ml inhibited 50 % of HCT 116 and HT-29 proliferation, respectively. The IC_{50} of the 5-fluorouracil as reference control in HCT 116 and HT-29 cells were 2.37 ± 0.93 µg/ml, 3.9±1.26 µg/ml, respectively.

Although the DBID compound inhibited the growth of both the cancer cell lines tested, HCT 116 cell line was more sensitive to the compound since they inhibited the growth of the cells at lower IC_{50} (IC_{50} =9.32 µg/ml) when compared to HT-29 cells (IC_{50} =11.85 µg/ml). The HT-29 cells seemed more resistant to the inhibitory effects of the compound ($p > 0.05$).

A normal colon cell line (CCD 841 CoN) was used to measure the cytotoxcity of DBID compound in normal cells. The IC_{50} value of the compound on normal colon cells (189.73± 4.1 µg/ml) was significantly higher than the IC_{50} values obtained in DBID treated cancer cell lines (HCT 116 and HT-29 cells).

The data showed that DBID compound at concentrations of 9.3 and 11.8 µg/ml can inhibit 50% of HCT 116 and HT-29 proliferation *in vitro*, respectively. These results showed the high ability of the compound to inhibit proliferation of both cell lines. This indicates that, while the DBID compound was cytotoxic to cancer cells, but was not relatively cytotoxic to normal cells.

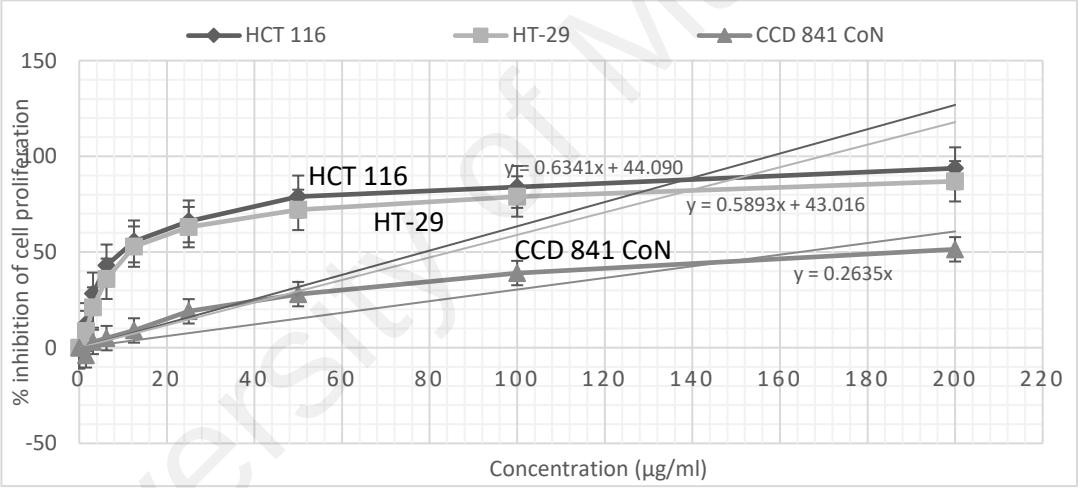

Figure 4.1: The percentage inhibition of cell proliferation.

Results were means ± SD (n=3).

Table 4.1: IC_{50} values of DBID on cancer and normal colon cell lines.

Compound	**HCT-116**	**HT-29**	CCD 841 CoN
DBID (µg/ml)	9.32± 1.2 ^{a}	11.85± 2.7 ^{a}	189.73± 4.1^{b}

Results were means ± SD (n=3). Different letters (a and b) in a column are significantly different ($p < 0.05$) as tested by One-way ANOVA.

4.1.2 Reactive oxygen species (ROS) production

Intracellular ROS generation was evaluated using intracellular peroxide-dependent oxidation of DCFHDA to form fluorescent DCF. H_2O_2 was used as a positive control. The two tumorigenic cells were treated with DBID for 12h, 24 h and 48 h ethidium derived fluorescence time-dependently increased showing the capacity of DBID to cause intracellular oxidation.

Figure 4.2 and shows that the generation of ROS in HCT 116 cells treated with the DBID compound increased in a time-dependent manner and the highest formation of ROS in treated cells was generated after 24 h treatment of the compound. At 48 h after treatment, a slight reduction of ROS in both cells indicated that the cells had transitioned to the late phase, that being apoptosis.

Figure 4.3 shows that when HT-29 cells were treated with the compound, the intracellular ROS increased in a time-dependent manner and the highest formation of ROS in treated cells was generated after 24 h treatment of the compound.

Quantification of the generated fluorescent intensity demonstrated significant ROS production at 12 h and 24 h in HCT 116 and HT-29, respectively. The generation of ROS in HCT 116 and HT-29 cells following DBID treatment were also examined using the oxidative-sensitive dihydroethidium probe which converts to fluorescent ethidium and intercalates into DNA as a result of ROS generation. When cancer cells (HCT 116 and HT-29) were treated with DBID for 24 h, ethidium derived fluorescence increased showing the capacity of DBID to cause intracellular oxidation (Figure 4.4). The generated fluorescent intensity demonstrated significant ROS production after 24 h DBID treatment in both cells. The production of ROS in HCT 116 and HT-29 cells, following DBID treatment at IC_{50} concentration compared to the untreated cells (control), was elevated

after 24 h incubation. This result showed that DBID can promote oxidative stress in both cancer cell lines; HCT 116 and HT-29 cells upon treatment.

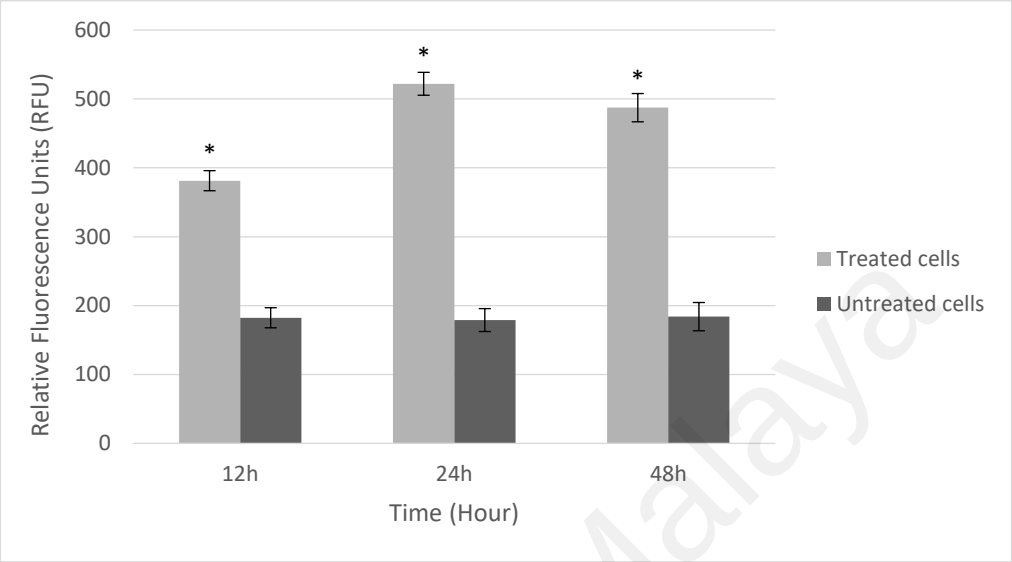

Figure 4.2: Intracellular ROS generated in HCT 116 cells treated with DBID.

Results are expressed as mean ± standard deviation. *p<0.05 compared to the control (untreated cells) as tested by the Student's t-test.

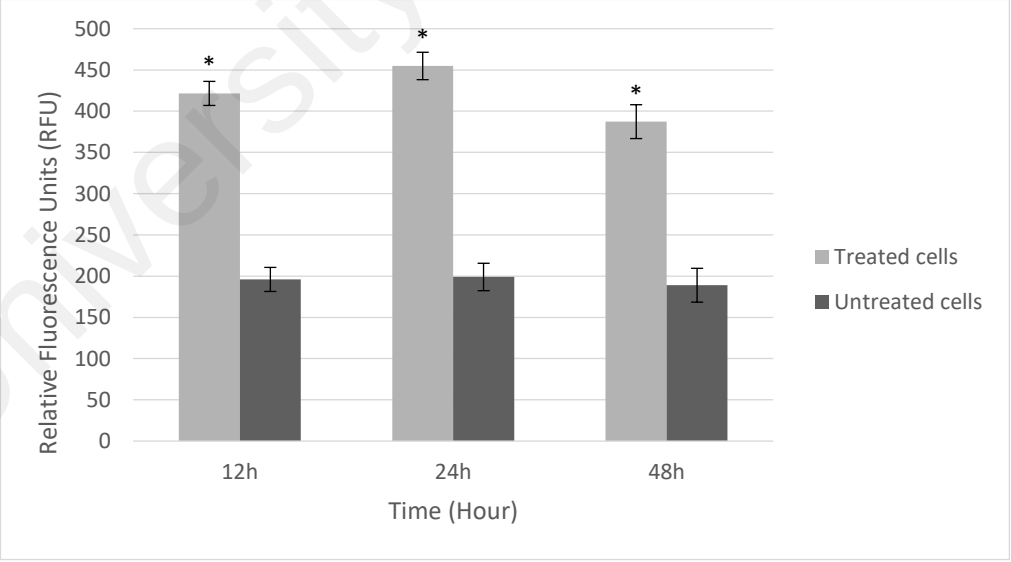

Figure 4.3: Intracellular ROS generated in HT-29 cells treated with DBID.

Results are expressed as mean ± standard deviation. *p<0.05 compared to the control (untreated cells) as tested by the Student's t-test.

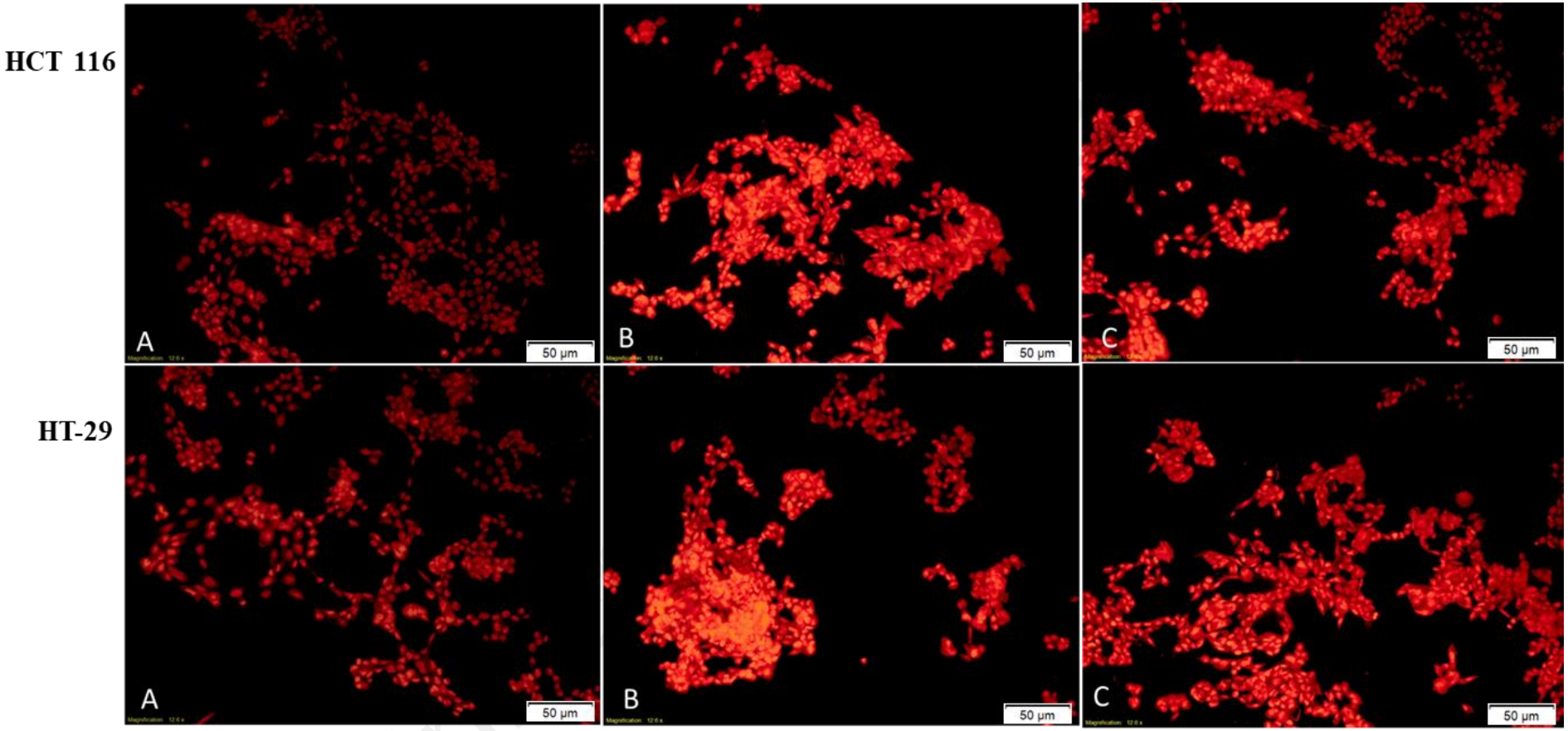

Figure 4.4: Effect of DBID on ROS generation in colon cancer cells.

First row shows the HCT 116 cells and second row shows the HT-29 cells. (A) Untreated cells, (B) DMSO as negative control and (C) cells treated with IC_{50} concentration of DBID compound for 24h then stained with DHE dye (red) (magnification: 20X).

4.1.3 Fluorescence microscopic examination

Acridine orange and propidium iodide, known as nucleic acid binding dyes, were used to investigate the morphological characterization of the HCT 116 and HT-29 cells under a fluorescent microscope to analyze the viable cells early apoptosis and late apoptosis. AO penetrates the plasma membrane of viable and early apoptotic cells and stained nucleated cells generate a green fluorescence while PI only enters cells with compromised membranes and produce an orange/red fluorescence in dying, dead, and necrotic nucleated cells stained with PI (Mironova et al., 2007; Von Bertalanffy, 1963).

The occurrence of apoptosis was qualitatively investigated by using fluorescence microscopy and the two dyes of AO/PI. As shown in Figures 4.5 and 4.6, a normal configuration with green nuclei and an intact structure was observed in untreated cells while the cells treated with DBID showed bright green nuclei indicating condensation of chromatin in the nucleus and interpolated propidium iodide (orange fluorescence) amongst the fragmented DNA and nuclear fragmentation. As shown in Figures 4.5 and 4.6, apoptosis characteristics e.g. cell shrinkage, membrane blebbing and chromatin condensation were observed in HCT 116 and HT-29 cells treated with DBID, respectively. AO/PI staining of both colon cancer cells (HCT 116 and HT-29 cells) treated with DBID exhibited that the cells had undergone remarkable morphological changes in apoptotic bodies. The results of this study suggest that the activation of the caspase pathway can trigger apoptosis in HCT 116 cells treated with DBID.

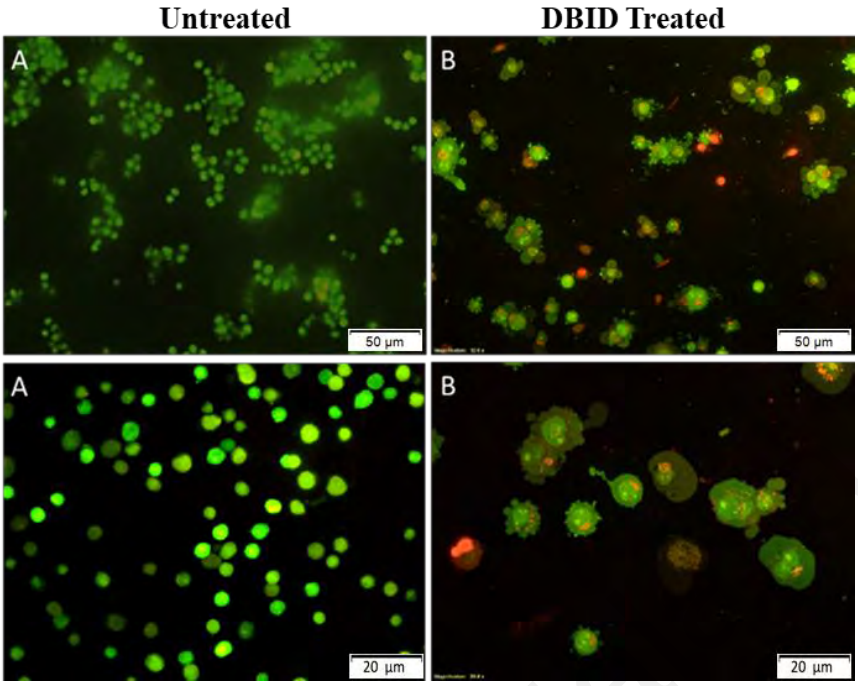

Figure 4.5: Morphological charges of untreated and DBID-treated HCT 116 cells.

Fluorescence microscopic examination by using double fluorescent dye (AO/PI) staining method on cells after 24 h incubation treated with DBID. From left to right; (A) untreated HCT 116 cells, (B) 9.3 µg/ml DBID-treated. The following photo shows different magnification in the rows (magnification: 20X and 40X).

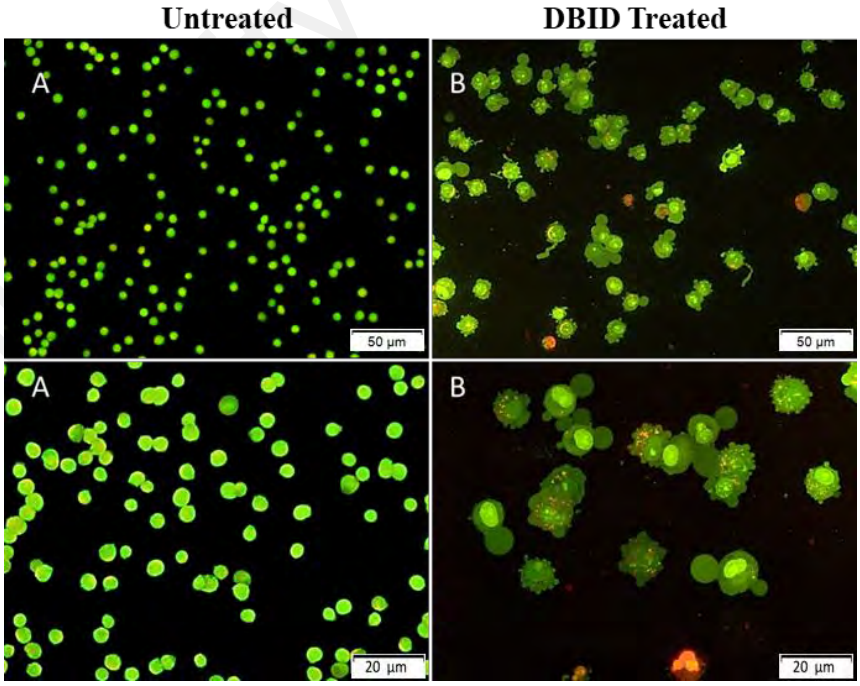

Figure 4.6: Morphological charges of untreated and DBID-treated HT-29 cells.

Fluorescence microscopic examination by using double fluorescent dye (AO/PI) staining method on cells after 24 h incubation treated with DBID. From left to right; (A) untreated HT-29 cells, (B) 11.8 µg/ml DBID-treated. The following photo shows different magnification in the rows (magnification: 20X and 40X).

4.1.4 Annexin V assay

Annexin V/ propidium iodide (PI) flow cytometry was performed to confirm the presence of apoptosis. Annexin V is used to detect apoptosis by targeting the loss of plasma membrane asymmetry by specific interaction with phosphatidylserine (PS) on the cell surface. The intact cell membrane of viable cells is not permeable to PI and represent AV-/PI- staining. The loss of plasma membrane asymmetry and strong affinity of AV-FITC with PS leads to AV+/PI- staining in the early apoptotic cells, whereas AV+/PI+ represents late apoptotic. Necrotic stage is represented by AV-/PI+ as a result of PI penetration through the membranes and intercalation into nucleic acid due to loss of plasma and nuclear membrane integrity. The flow cytometry of Annexin V results and analysis for HCT 116 and HT-29 cells are presented in Figure 4.7 (A and B) and Figure 4.8 (A and B), respectively. As shown in figures, both cancer cells treated with DBID underwent significant apoptosis after 24 h post DBID treatment compared with untreated cells ($p<0.05$). More than 40% of treated cells were detected as apoptotic cells after 24 h in both cells (Figure 4.7(B) and Figure 4.8 (B)). In addition, treatment with DBID showed no significant concurrent increase in necrotic cells. Consistent with AOPI stating results, flow cytometric Annexin V analysis of DBID treated cells clearly demonstrated that antiproliferation and apoptosis in HT-29 treated cells are closely related.

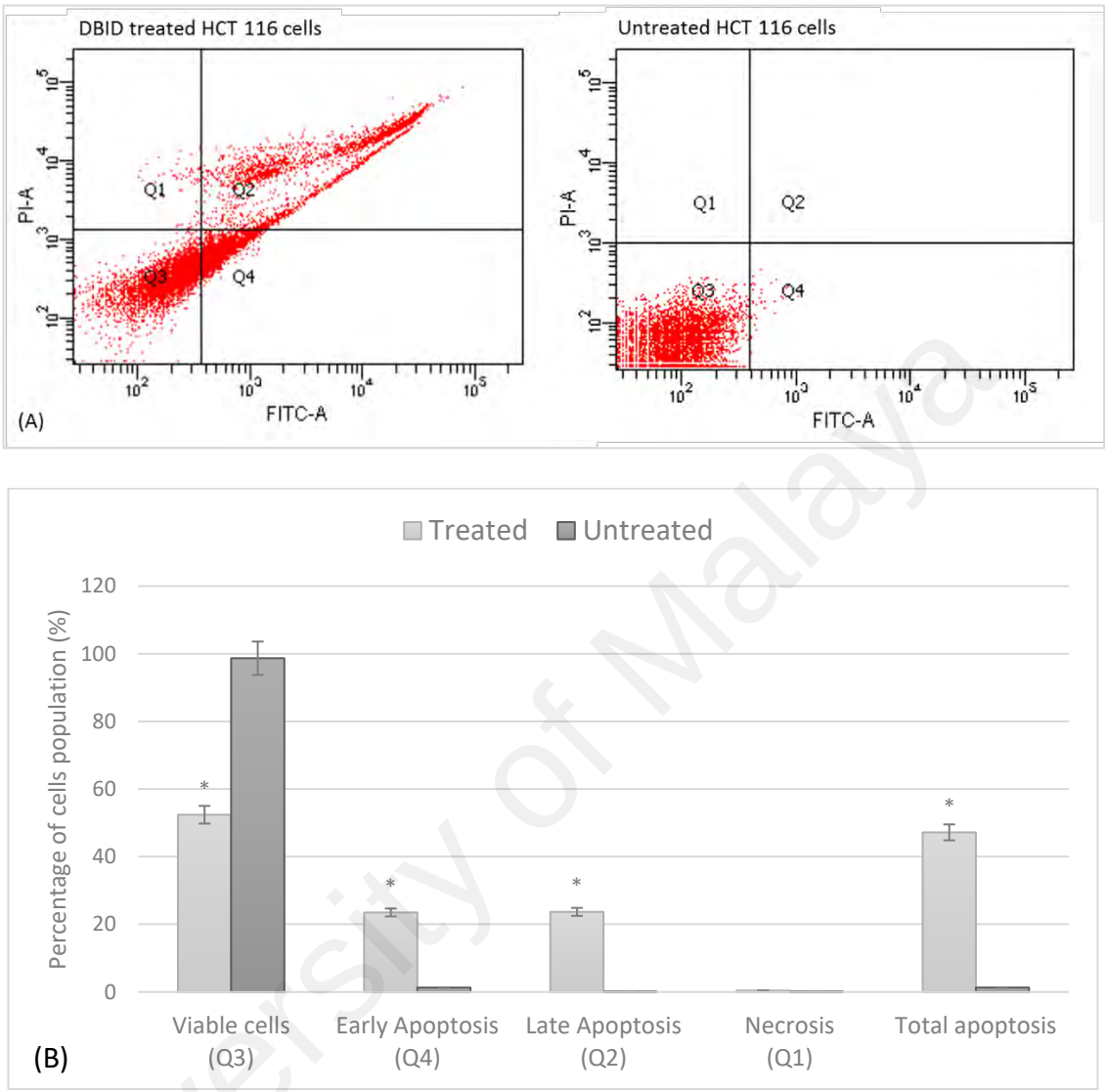

Figure 4.7: Flow cytometric annexin V/PI in HCT 116 cells.

(A) HCT 116 cells (DBID treated and untreated) were stained with Annexin V/PI (B) flow cytometric analysis of the percentage level of the four quadrants representing viable cells (Annexin V-PI-), Early apoptosis (Annexin V+PI-), Late apoptosis (Annexin+PI+) or Necrotic (Annexin V-PI+) stages in treated and untreated cells. Values shown are percentages of each quadrant. *P<0.05, as tested by the Student's t-test.

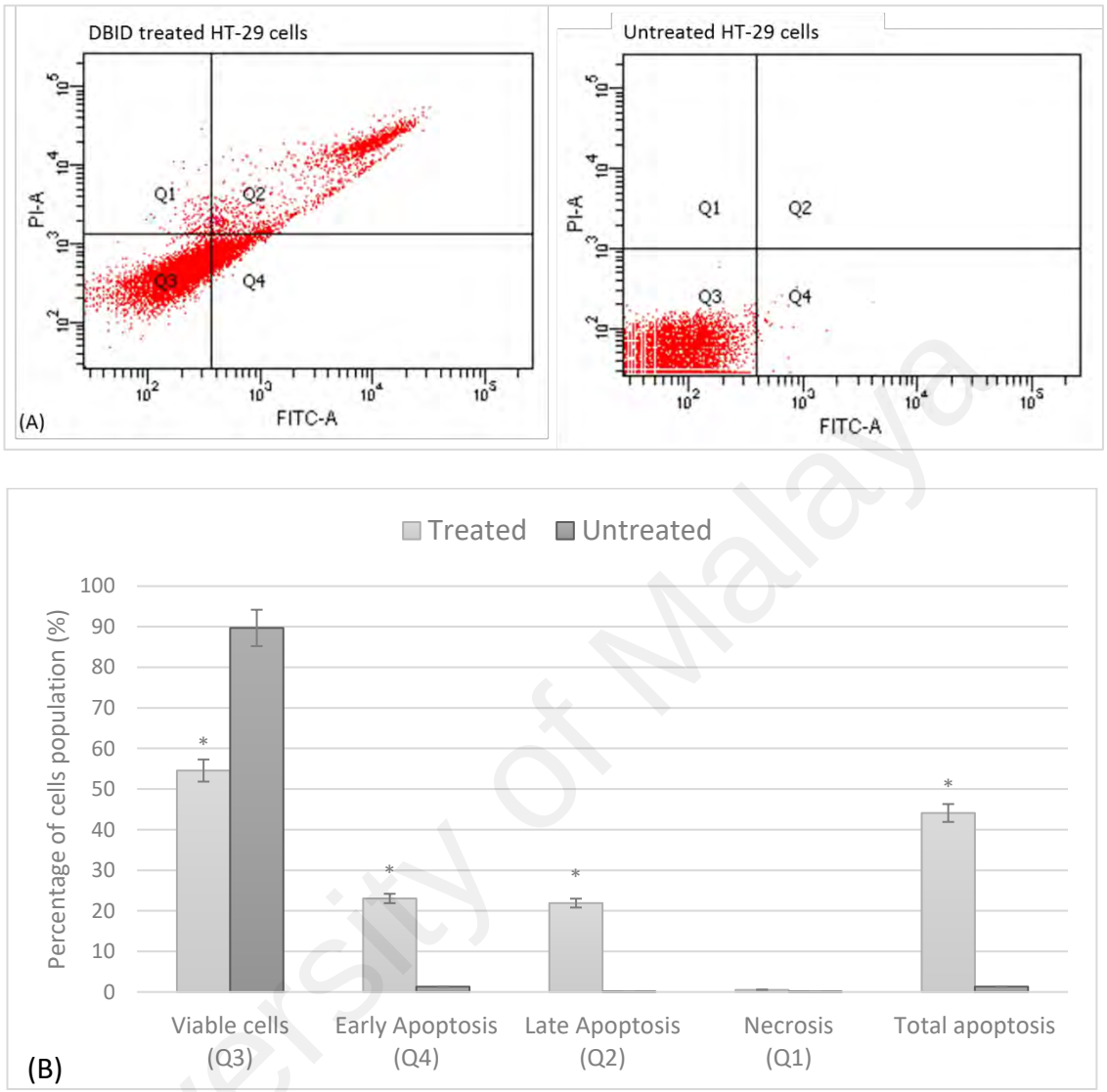

Figure 4.8: Flow cytometric annexin V/PI in HT-29 cells.

(A) HT-29 cells (DBID treated and Untreated) were stained with Annexin V/PI (B) flow cytometric analysis of the percentage level of the four quadrants representing viable cells (Annexin V-PI-), Early apoptosis (Annexin V+PI-), Late apoptosis (Annexin+PI+) or Necrotic (Annexin V-PI+) stages in treated and untreated cells. Values shown are percentages of each quadrant. *P<0.05, as tested by the Student's t-test.

4.1.5 Caspase activity

To investigate whether (and through which pathways) the antiproliferative activity shown by the DBID compound induction of apoptosis, the effect of DBID on caspase activity was assayed. Figures 4.9 and 4.10 show the activity of caspase -8, -9 and -3/7 in treated HCT 116 and HT-29 cells.

As shown in Figure 4.9, the activation pattern of caspases-8 and -9 were more or less similar in HCT 116 cells. The compound significantly increased the activities of caspase -8, -9 at 4 h and decreased in a time-dependent manner (Figures 4.9). The results showed that the maximum activity of the caspase-8 and -9 in HCT 116 was after 4 h incubation by 3.4 and 6.4 fold, respectively. The increment was highly significant ($p<0.01$) up to 16 h incubation time in caspase-8 and significant ($p<0.05$) after 24 and 48 h. The increments of caspase-9 was highly significant ($p<0.01$) up to 24 h incubation time and significant ($p<0.05$) after 48 h. The caspase-3/7 showed an increase up to 24 h incubation time and then decreased after 48 h. The activation of caspase-3/7 showed that the compound was able to induce apoptosis in the treated HCT 116 cells.

As shown in Figure 4.10, the compound increased the activities of caspases -8, -9 and -3/7 in HT-29 cells, compared to the control. The compound increased the caspase -3/7 activity and decreased the caspase-9 activity in a time-dependent manner and caspase -8 showed an increase up to 16 h incubation time and then reduced after 24 and 48 h. There was a highly significant increase in the activities of caspase-3/7 compared to control after 24 h incubation time by 3 fold ($p <0.01$).

The results showed that the compound was able to induce apoptosis by activation of caspase-3/7. The treatment was able to activate the death receptor pathway by activating caspase-8. The caspase-8 results showed that the compound produced significant increase, while 16 h time period induced the highest levels of caspase -8 activity by 2.8

fold. ($p<0.01$). The activity of caspase-9 in treated cells was highly significant compared to the untreated cells ($p<0.01$). The maximum activity was shown in 4 h by 2.9 fold and although it decreased in 16 h, the activity of the caspase-9 was still highly significant in comparison to the untreated HT-29 cells.

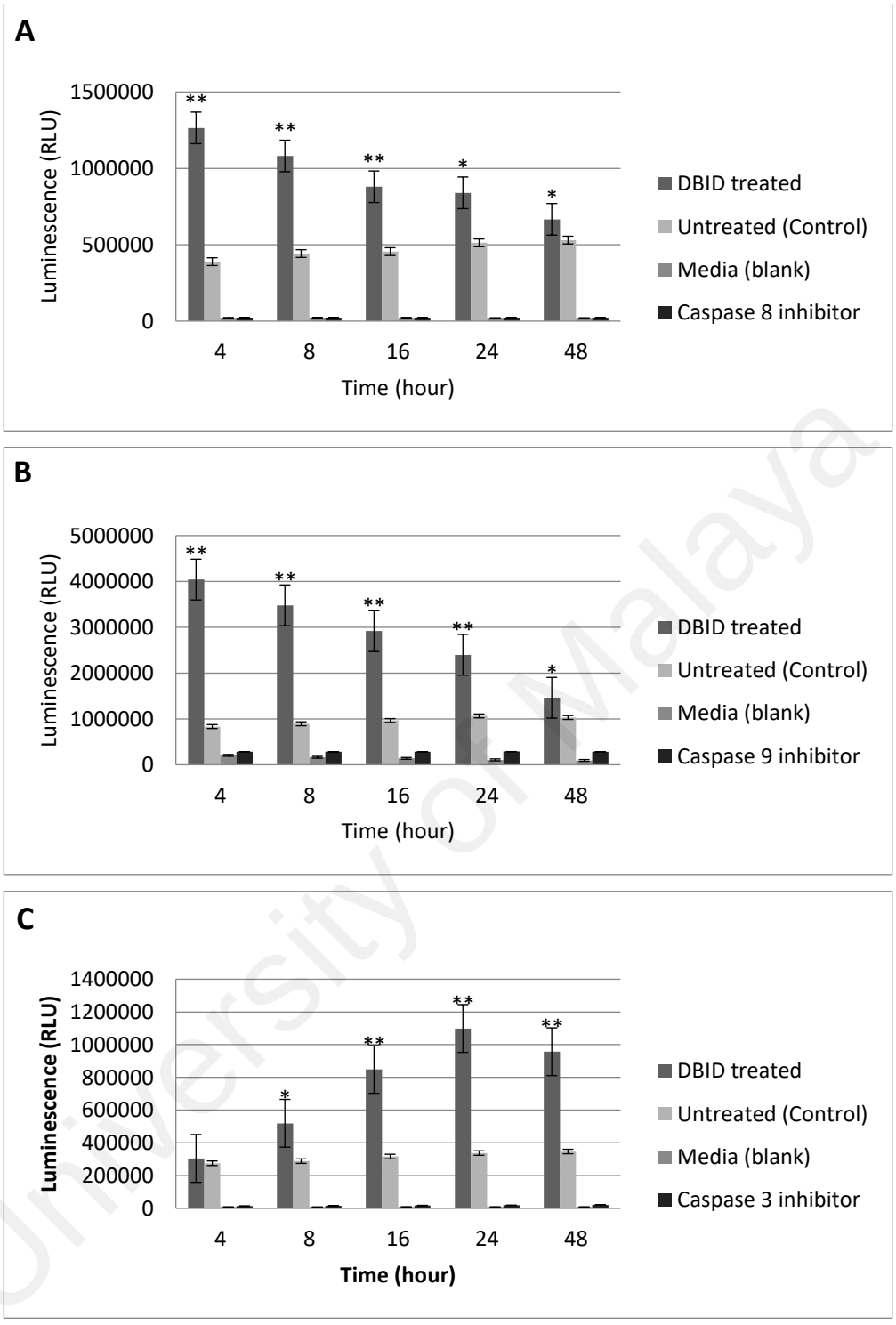

Figure 4.9: The effect of DBID on caspase activity in HCT 116 cells.

The activity of (A) Caspase-8 (B) Caspase -9 and (C) Caspase -3/7. The cells were treated with 9.3 µg/ml of DBID. Data shown are the mean values of the triplicates. * $p<0.05$ and **$p<0.01$ indicate significant differences from untreated cells as tested by the Student's t-test.

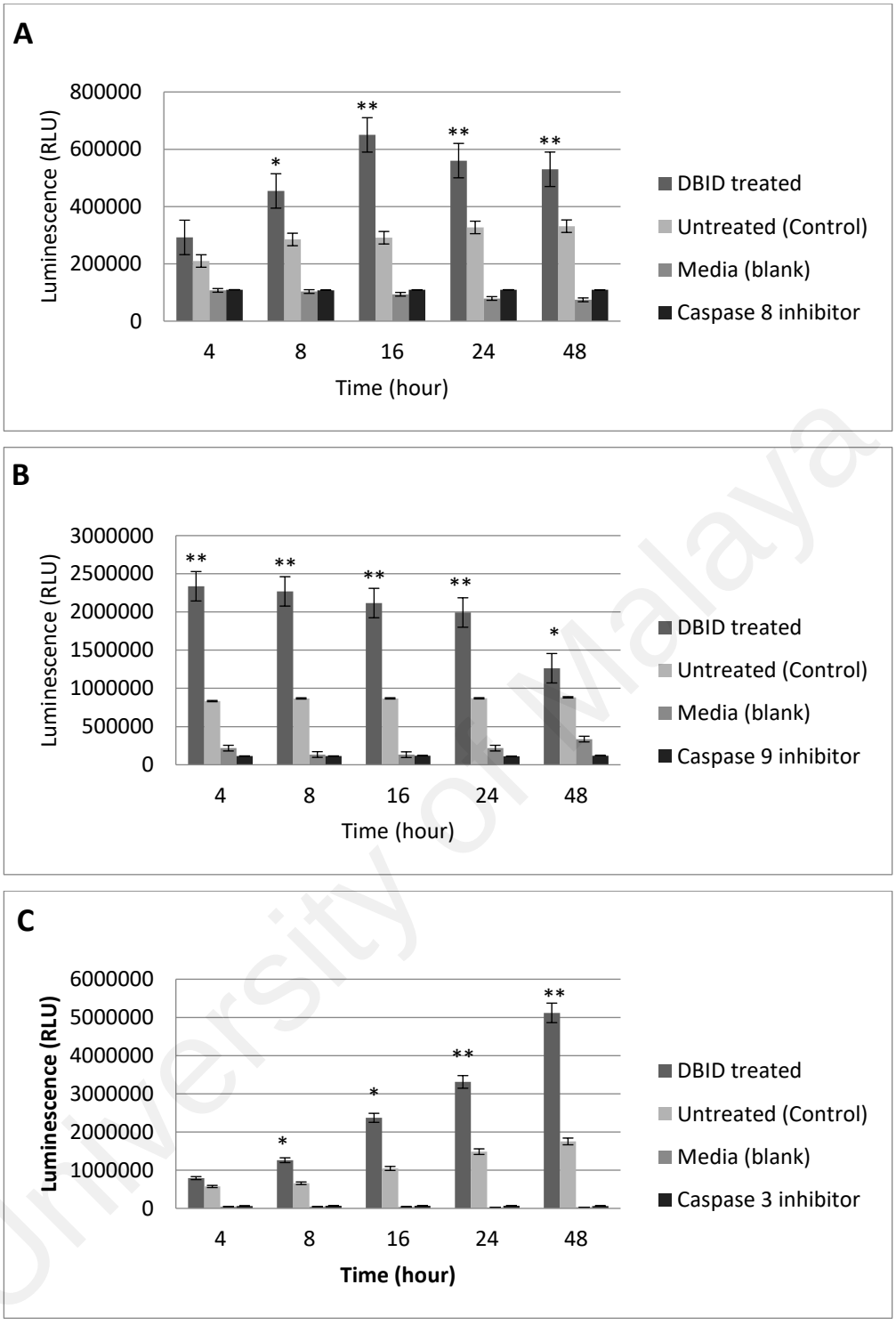

Figure 4.10: The effect of DBID on caspase activity in HT-29 cells.

The activity of (A) Caspase-8 (B) Caspase -9 and (C) Caspase -3/7. The cells were treated with 11.8 µg/ml of DBID. Data shown are the mean values of the triplicates. * $p<0.05$ and **$p<0.01$ indicate significant differences from untreated cells as tested by the Student's t-test.

4.1.6 Study of gene expression by Real Time-PCR

To further study the pathways involved in the treated HCT 116 and HT-29 cells, the cells were treated with the IC_{50} concentration of the compound. The expression of CASP8, CASP9, CASP3, BCL2, BAX, TP53 and BID was assessed using RT-PCR technique. The comparison of expression of these genes demonstrates the molecular response of these cells toward the compound treatments. The results were expressed as fold changes over the respective controls. Fold variation values less than 1 were expressed as negative values. The statistical analysis of Real Time-PCR results for a given gene were expressed as a difference from the ΔCT value obtained between treated versus untreated cell lines; the ΔΔCT value.

Figure 4.11 shows that CASP8, CASP9, CASP3, BAX, TP53 and BID were significantly overexpressed in treated HCT 116 cells by a mean factor of 1.89, 2.43, 2.95, 2.91, 5.3 and 2.42, respectively. The expression of BCL2 was significantly downregulated in DBID treated cells by a mean factor of 0.62.

Figure 4.12 shows that CASP8, CASP9, CASP3, BAX, TP53 and BID were significantly overexpressed in treated HT-29 cells by a mean factor of 1.67, 2.79, 2.48, 3.7, 4.1 and 1.47, respectively. The apoptosis regulator gene, BCL2, was slightly down regulated in DBID treated cells by a mean factor of 0.89. This decrease was not statistically significant.

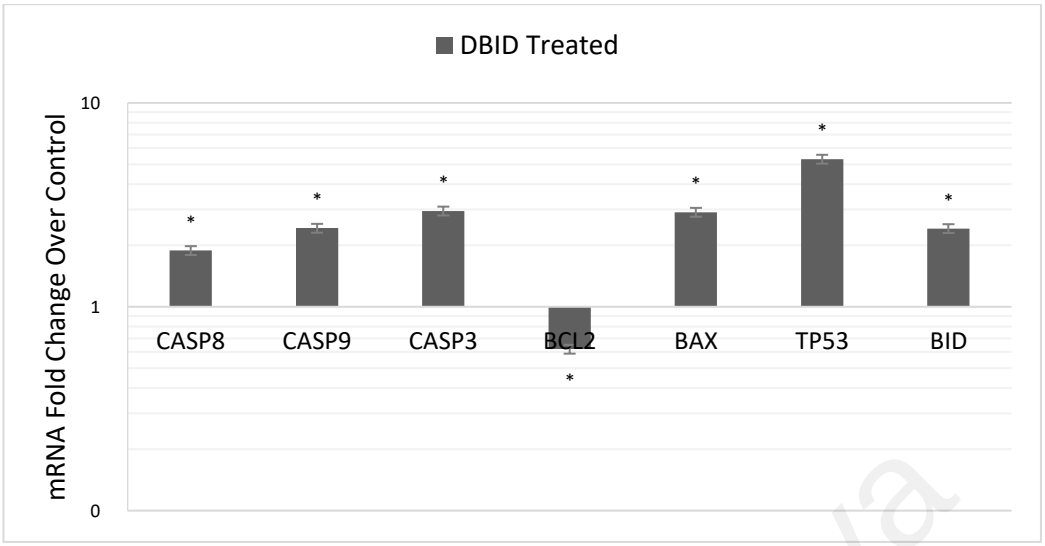

Figure 4.11: Gene expression analysis of HCT 116 cells treated with DBID.

Results are expressed as mean ± standard deviation of three replicates. *P<0.05 indicate significant differences from untreated cells as tested by the Student's t-test.

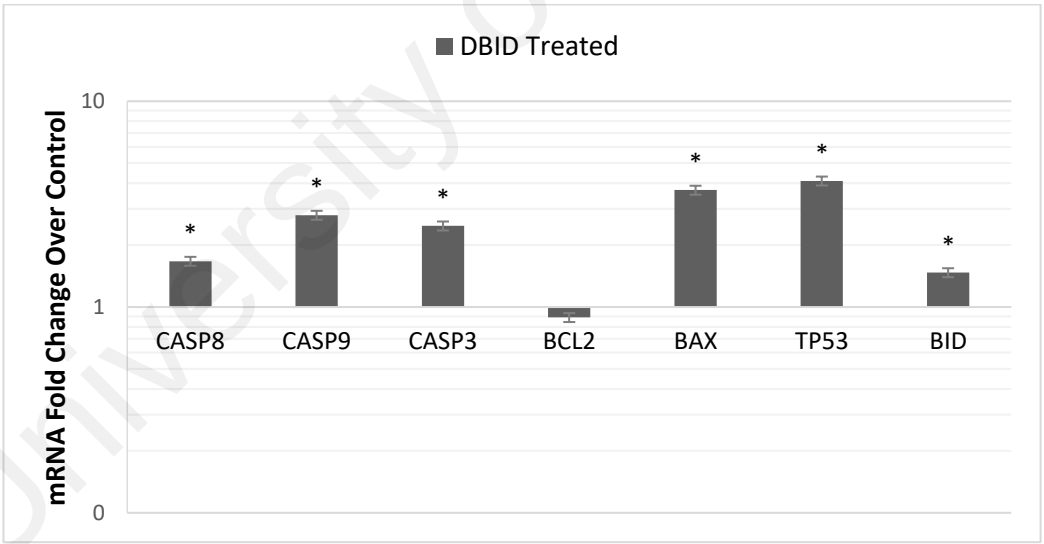

Figure 4.12: Gene expression analysis of HT-29 cells treated with DBID.

Results are expressed as mean ± standard deviation of three replicates. *P<0.05 indicate significant differences from untreated cells as tested by the Student's t-test.

.

The purity of the isolated RNA was checked by running 1% agarose gel electrophoresis (Figure 4.13). Agarose gel is commonly performed to evaluate RNA integrity. The RNA samples were assessed by adding of Ethidium-Bromide and evaluated by electrophoresis in TBE buffer.

Figure 4.13: RNA gel electrophoresis.

4.1.7 Protein expression by western blot

Figures 4.13(A) and 4.13(B) show the expression of apoptotic proteins in both HCT 116 and HT-29 cells lines, respectively.

The protein blot expression analysis by Image J scanning verified that the expression of Caspase-3 and Bax proteins were up-regulated following DBID treatment after 24 h in both HCT 116 and HT-29 cells lines. The western blot analysis also showed that the DBID compound significantly down-regulated the expression of Bcl2 in both cells.

As shown in Figure 4.14(A) the DBID compound significantly increased the protein expression level of caspase-3 and Bax by 2.26±0.2 and 1.7±0.17 fold, respectively, in the HCT 116 treated with DBID compared with the untreated cells. Bcl2 expression decreased significantly by 0.53±0.06 and 0.66±0.10 fold in the HCT 116 and HT-29 cells, respectively, under DBID compound treatment compared with the untreated cells. The expression of Caspase-3 and Bax also significantly increased by 1.8±0.18 and 1.98±0.15 fold, respectively, in the HT-29 treated with DBID compared with the untreated cells (figure 4.14(B)).

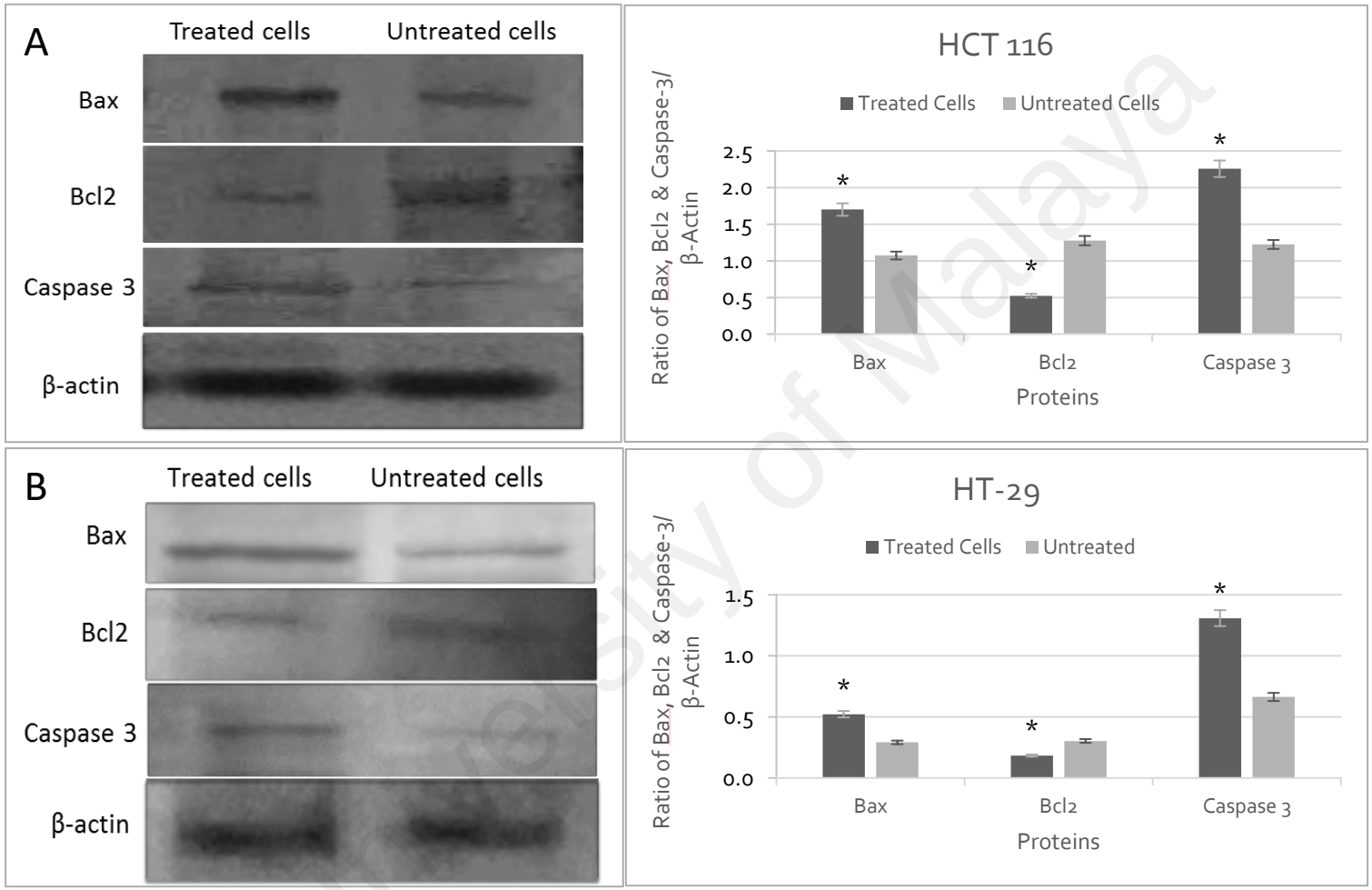

Figure 4.14: Western blot analysis of colon cancer cells treated with DBID.

(A) HCT 116 cell (B) HT-29 cells. The blots were scanned and analyzed using ImageJ software. *Indicates significant differences from untreated cells ($p < 0.05$).

4.2 *In vitro* antioxidants activities of the compound

The FRAP assay measures the ability of antioxidants to reduce the ferric 2, 4, 6-tripyridyl-S-triazine complex [Fe (III)-(TPTZ)2]$^{2+}$ to intensely blue colored ferrous complex [Fe(II)-(TPTZ)2]$^{2+}$ in acidic medium. The reduction capacity of a compound may serve as a significant indicator of its potential antioxidant activity (Meir et al., 1995). Table 4.2 indicates the antioxidant capacities of the compound using the FRAP assay. The FRAP value belonging to the compound was 4.93±1.3 mmol Fe^{2+}/g, while the FRAP value for quercetin as a powerful antioxidant was higher (6.29±1.7 mmol Fe^{2+}/g). However, the difference between the FRAP values of quercetin and DBID was not statistically significant ($p>0.05$). $FeSO_4.7H_2O_2$ was used as the standard (Appendix G).

2,2-diphenyl-1-picrylhydrazyl (DPPH) free radical scavenging method has been widely applied for the determination of antioxidant activity of a compound. The colorimetric property of DPPH is used as an indicator of antioxidant capacity of chemical and biological compounds (Huang et al., 2005).

The results presented in Table 4.2 revealed that the DPPH radical scavenging ability of quercetin, a known antioxidant, was similar to the compound ($p>0.05$). As shown in Table 4.2, DBID compound showed IC_{50} values of 45.3±0.9 µg/ml while the IC_{50} value of quercetin (pure flavonoid), which was used as the positive control in DPPH assay, had a IC_{50} value of 39.3±0.78 µg/ml. Trolox was used as the standard in this assay (Appendix H). The DBID compound possesses the high ability of donating H^+ almost the same as quercetin as a positive control in scavenging the DPPH free radicals. It is expected that positive control (quercetin) as a pure compound would show higher antioxidant activity in FRAP and DPPH free radical scavenging assays. Similar to FRAP, observing a same pattern in DPPH results also confirms the capability of antioxidant activity of the compound (DBID).

Table 4.2: Antioxidant activities of DBID compound and control.

Assays	DBID	Quercetin
Ferric reducing antioxidant power (mmol/g Fe^{2+}/g)	4.93±1.3	6.29±1.7
DPPH radical scavenging activity (IC_{50}, µg/ml)	45.3±0.9	39.3±0.78

Assays were performed in triplicate and the results are presented as means ± SD. IC_{50} is defined as the concentration of the compound that could reduce 50% of the reagent colour.

4.3 *In vivo* studies

4.3.1 Acute toxicity study

The animals' health conditions were observed throughout the experiment, and the results obtained from this observation revealed no mortality or behavioural changes, such as signs of weakness, tremors or uncontrollable movements. The effect of the DBID compound on the liver and kidney was examined through the histological study as shown in Figure 4.15. Histological examination of liver and kidneys exhibited normal cellular architecture, without any changes in colour or any morphological disturbances.

Table 4.3 presents the serum biochemical parameters that were probed using the collected blood. The biochemical parameters of renal and liver function test and lipid profile showed that the values are within the normal range with no differences between treated group and control group. The acute toxicity results showed that the safe value of oral administration of DBID exceeded 2000 mg/kg body weight.

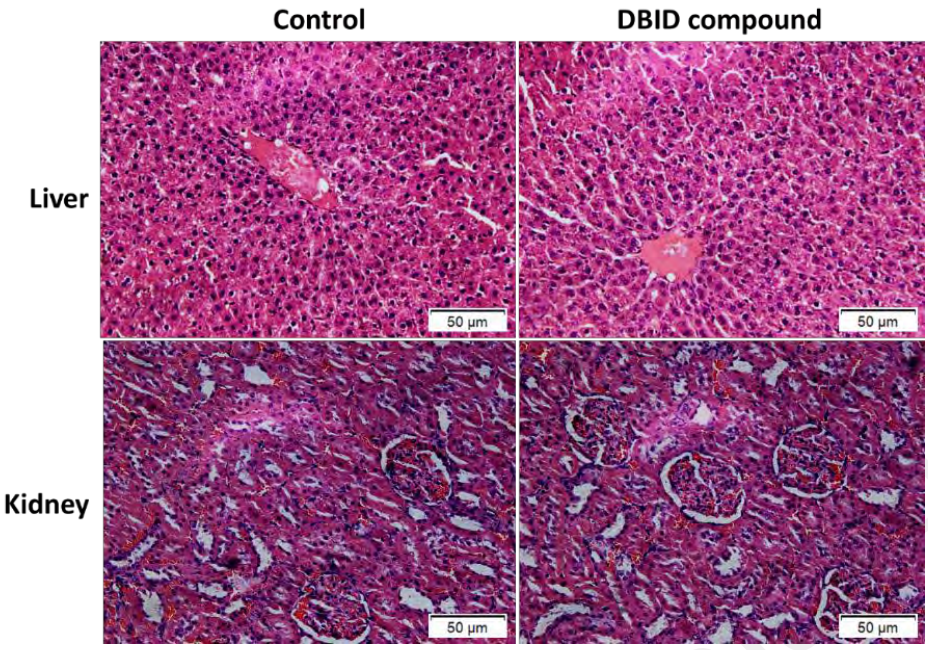

Figure 4.15: Histological examination of liver and kidney in acute toxicity study.

Vehicle group that received 10% tween 20 (Control). DBID compound group that received 2000 mg/kg DBID compound. There was no notable difference between the vehicle group and the experimental group. H & E stain; magnification, 20X.

Table 4.3: Serum biochemical screening in acute toxicity test.

Biochemical parameters	Units	Control	DBID 2000 mg/kg
LFT			
Albumin	g/ L	35.7± 3.2	34.5±3.5
Total bilirubin	mmol/L	<2	<2
Alkaline phosphatase	U/ L	179.3±43.14	167.00±113
Alkaline aminotransferase	U/ L	79±28.8	74.00±11.3
G-glutamyl transferase	U/ L	0.06±0.7	0.04±0.4
RFT			
Sodium	mmol/L	140.7±5.8	140.00±2.8
Potassium	mmol/L	5.3±2.4	5.45±1.2
Chloride	mmol/L	99.67±4.0	100.50±0.7
Carbon Dioxide	mmol/L	31.33±1.1	33.50±0.7
Anion gap	mmol/L	14.7±1.1	12.50±0.7
Urea	mmol/L	6.23±1.4	6.50±0
Creatinine	umol/L	27.33±2.5	22.00±0
Lipid profile			
Triglyceride	mmol/L	0.73±0.5	1.35±1.3
Total cholesterol	mmol/L	1.90±0.2	2.20±2
HDL cholesterol	mmol/L	0.45±0.1	0.74±0.6
LDL cholesterol	mmol/L	1.12±0.3	0.85±0.7

Results are expressed of three parallel measurements as mean ± SD (n=3). *The significant value was set at $p< 0.05$ as tested by the Student's t-test.

4.3.2 Subacute toxicity study

During the period of administration, the animals were observed closely each day for signs of toxicity. Table 4.4 presents the weekly records of the animals' body weight. The rats' body weights in control showed no significant differences compared to treated groups ($p>0.05$). The experimental animals in this study showed no mortality or any signs of toxicity in DBID oral administration for 28 days. The results obtained from serum biochemical analysis showed that the values are within the normal range with no significant differences between the groups (Table 4.5).

Figure 4.16 illustrates the histological examination of liver and kidney in rats orally administrated with vehicle and 10, 20, and 40 mg BDID/kg body weight/day. The histopathological examination of liver and kidney in all the groups revealed normal cellular architecture, without any changes in colour or any morphological disturbances. The subacute toxicity results showed no significant toxicity in repeated dose of DBID at three different concentrations (10, 20, and 40 mg BDID/kg body weight/day) for 28 day treatments.

Table 4.4: Rats' body weight in subacute toxicity study.

Animal body weights during the subacute toxicity experiment				
Groups	**Week 1**	**Week 2**	**Week 3**	**Week 4**
Control group (Vehicle)	225±12	270±26	339±34	417±28
DBID Compound (10 mg/kg)	219±11	267±24	326 ±32	409±38
DBID Compound (20 mg/kg)	235±15	281±31	362±31	429±34
DBID Compound (40 mg/kg)	228±18	274±22	347±35	424±37

The values are expressed as the mean± SD (n=10). There are no statistically significant differences between the groups ($p > 0.05$) as tested by One-way ANOVA.

Table 4.5: Serum biochemical analysis in subacute toxicity study.

Biochemical parameters	Units	Control group (Vehicle)	10 mg/kg DBID	20 mg/kg DBID	40 mg/kg DBID
LFT					
Albumin	g/ L	33 ± 2	35 ± 1	34 ± 2	35 ± 2
Total bilirubin	mmol/L	<2	<2	2	<2
Alkaline phosphatase	U/ L	131 ± 11	134 ± 17	141 ± 13	133 ± 19
Alanine Aminotransferase	U/ L	60 ± 9	59 ± 16	60 ± 12	59 ± 18
G-glutamyl transferase	U/ L	0.4 ± 0.7	0.5 ± 0.4	0.5 ± 0.6	0.5 ± 0.9
RFT					
Sodium	mmol/L	141 ± 2	140 ± 3	142 ± 2	141 ± 4
Potassium	mmol/L	5 ± 2	5 ± 1	5 ± 2	5 ± 2
Chloride	mmol/L	100 ± 7	101 ± 4	100 ± 6	100 ± 5
Carbon Dioxide	mmol/L	28 ± 4	29 ± 6	28 ± 4	29 ± 7
Anion gap	mmol/L	15 ± 3	16 ± 2	17 ± 8	15 ± 4
Urea	mmol/L	5 ± 0.9	5 ± 0.7	5 ± 0.2	5 ± 0.9
Creatinine	umol/L	26 ± 3	27 ± 5	22 ± 8	26 ± 4
Lipid profile					
Triglyceride	mmol/L	0.8 ± 0.5	0.9 ± 0.3	0.9 ± 0.7	0.8 ± 0.9
Total cholesterol	mmol/L	2 ± 0.7	2 ± 0.6	2 ± 0.4	2 ± 0.8
HDL cholesterol	mmol/L	0.5 ± 0.3	0.5 ± 0.7	0.5 ± 0.5	0.5 ± 0.7
LDL cholesterol	mmol/L	1 ± 0.2	1 ± 0.7	1 ± 0.8	1 ± 0.9

Values are expressed as mean ± SD (n=10). There are no statistically significant differences between the groups ($p > 0.05$) as tested by One-way ANOVA.

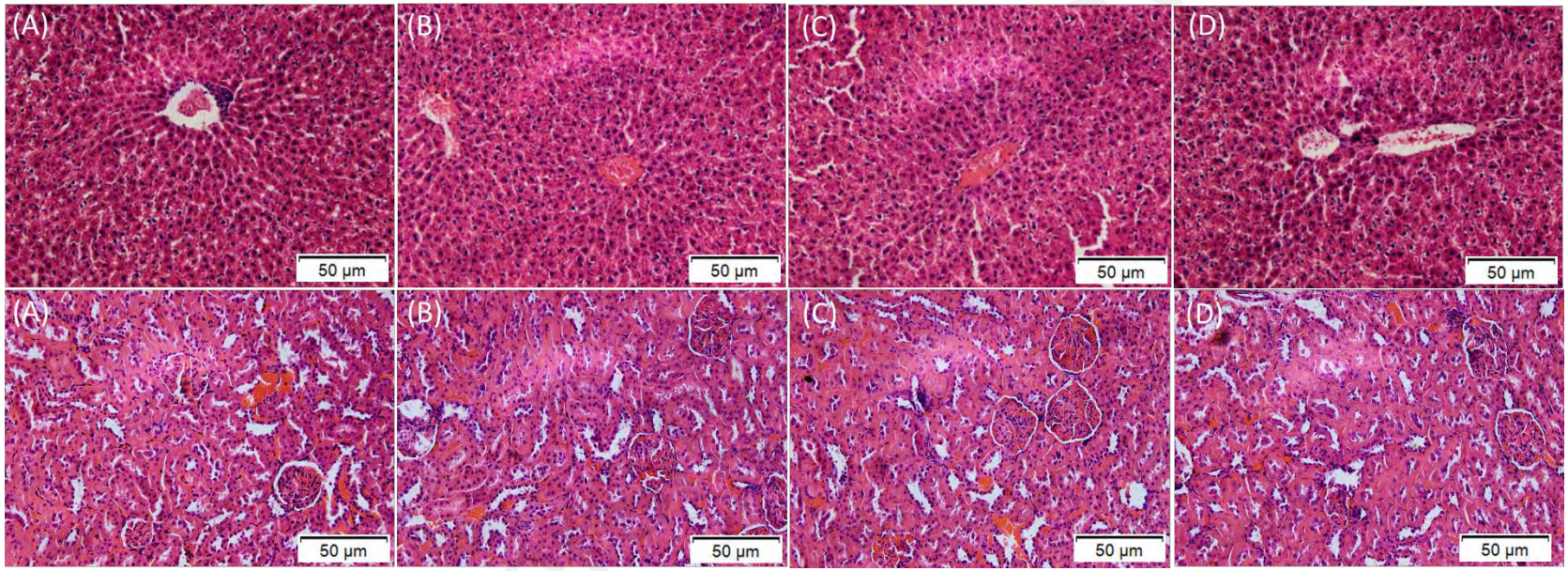

Figure 4.16: Histological examination of liver and kidney in subacute toxicity study.

(A) Vehicle control, (B) DBID 10 mg/kg/d, (C) DBID 20 mg/kg/d, (D) DBID 40 mg/kg/d. There was no notable difference between the vehicle group and other experimental groups. H & E stain; magnification, 20X.

4.3.3 Chemopreventive effects of DBID against colon cancer

4.3.3.1 ACF frequency

In this study, azoxymethane-induced aberrant crypt foci was performed as colorectal carcinoma model in rats. The tumour quantification analysis of the colon tissues, following staining with methylene blue, was performed immediately after sacrificing the animals. Figure 4.17 displays topographic views of the stained colon tissues of the different groups. The average total number of ACF in comparison with the AOM treated group are illustrated in Table 4.6. As shown in Figure 4.17 and table 4.6, significantly greater number of ACFs were recorded in the cancer control group while the reference treated group and the compound treated groups showed significant inhibition in AOM-induced colonic ACF ($p<0.05$). A significant inhibition in the number of AOM-induced ACF formation was observed in DBID compound in a dose-dependent manner and 5-Fluorour.

The groups with high dose of DBID administration significantly inhibited the incidence of the ACF up to 70% and the 5-Fluorouracil as reference control induced up to 73% inhibition in treated rats compared to cancer control group. Furthermore, DBID compound significantly reduced the number of AOM-induced ACF formation in a dose-dependent manner. The group administrated with low-dose and high-dose of DBID decreased the mean number of ACF by 27±1.9 and 23±1.4 in treated group, respectively.

Table 4.6: The effect of DBID compounds on AOM-induced colonic ACF in rats.

	Number of foci containing					
Groups	1 crypt	2 crypt	3 crypt	4 crypt and more	Total ACF	Inhibition %
Normal control group (sham group)	0	0	0	0	0.0	0
15 mg/kg AOM (cancer control group)	11.7±3.1[a]	25±3.6[a]	18.3±3.1[a]	27±2.6[a]	82±10.8[a]	-
AOM+ DBID Compound (20 mg/kg)	5.7±2.1[b]	8.3±3.1[b]	4.7±1.5[b]	8.7±2.1[b]	27±1.9[b]	65.14
AOM+ DBID Compound (40 mg/kg)	4.7±2.5[b]	7.3±2.5[b]	4.3±2.3[b]	6.7±2.5[b]	23±1.4[b]	70.58
AOM+(5-FU) 35 mg/kg (reference group)	4.3±2.1[b]	6.7±2.5[b]	3.7±2.1[b]	6.3±2.5[b]	21±1.4[b]	73.18

The values are expressed as mean ± SD (n=6). Different letters (a and b) in a column are significantly different ($p < 0.05$) as tested by One-way ANOVA.

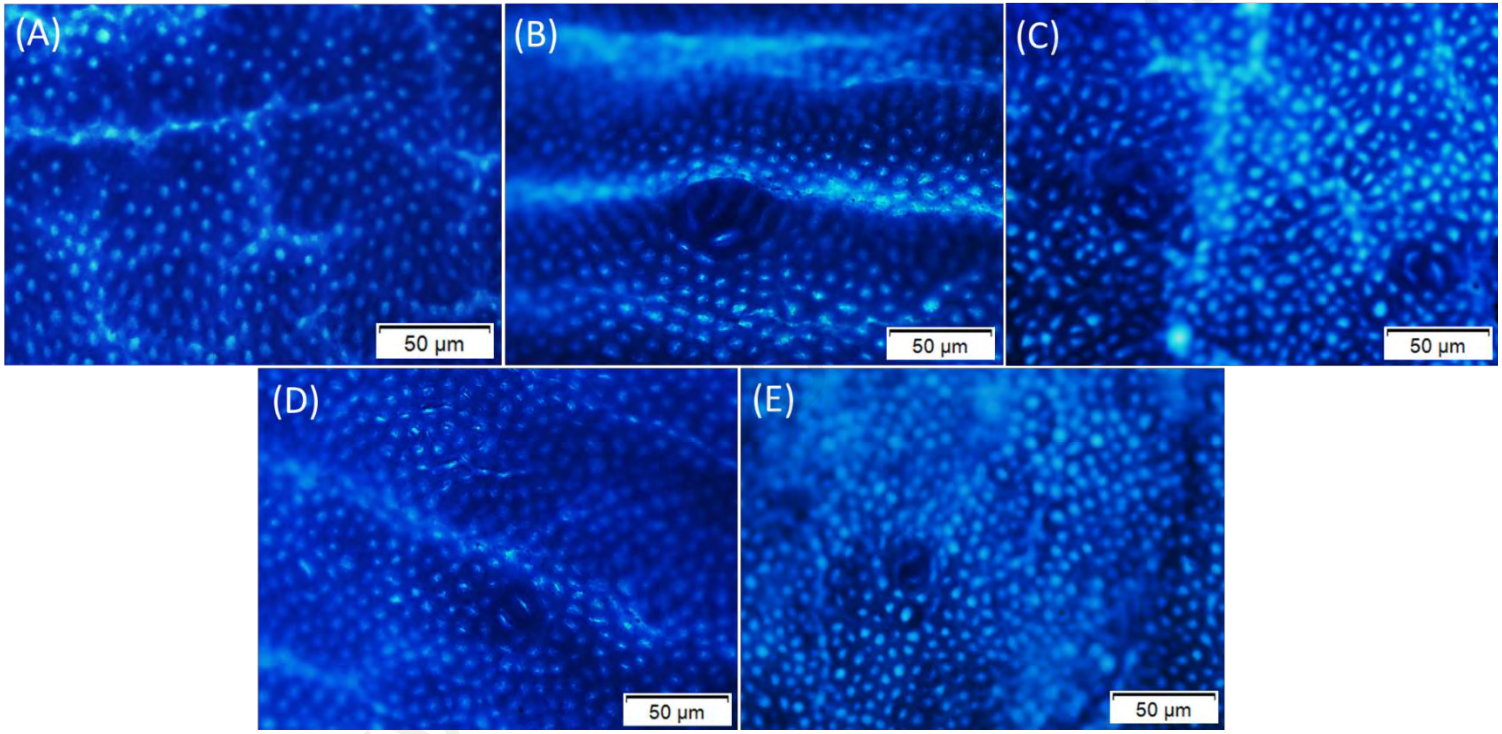

Figure 4.17: Topographic views of the methylene blue-stained colon.

(A) Normal colon mucosa, (B) cancer control group, (C) treatment group with low dose compounds, (D) treatment group with high dose of compounds and (E) Reference control group. Aberrant crypts were distinguished from the surrounding normal crypts by the increased size, increased distance from the basal to lamina surface of cells, and the easily discernible pericryptal zone (methylene blue stain; 20X magnification).

4.3.3.2 Histological analysis of aberrant crypt foci

The colon tissue stained with haematoxylin and eosin showed narrow lumens in epithelial cells, elongated nuclei, loss of cell polarity, increased mitotic activity, lack of goblet cells in dysplastic ACFs while circular shaped cells and basal locations of the nuclei were observed in normal control group (Figure 4.188). Azoxymethane (AOM)-induced aberrant crypt foci (ACF) formation and pathological changes in the colonic mucosal tissues in cancer groups. It was elucidated that the numbers of cells with pathological differences was reduced in reference control or compound treated groups. DBID dose-dependently decreased AOM-induced aberrant crypt foci (ACF) formation and pathological changes in the colonic mucosal tissues.

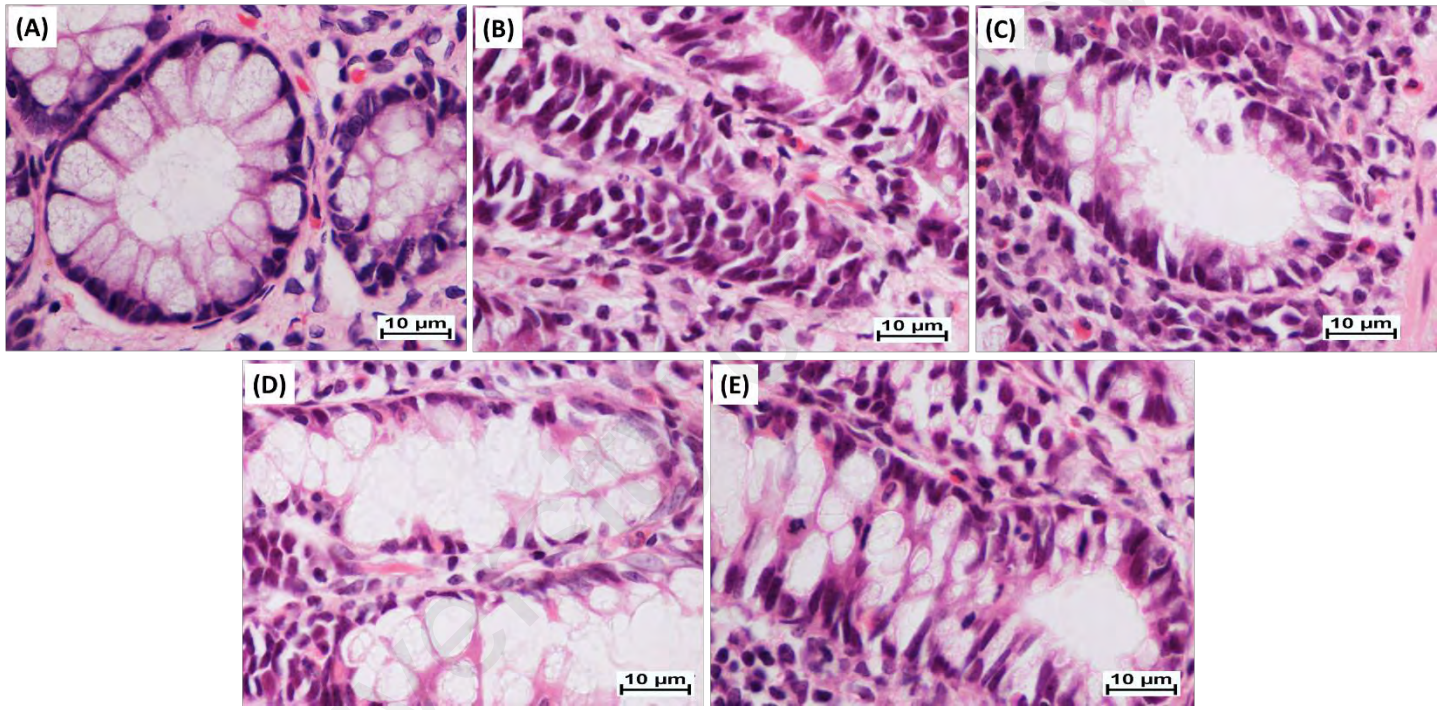

Figure 4.18: Histological study of colon tissues.

(A) Normal colon mucosa, (B) cancer control group, (C) treatment group with low dose compounds, (D) treatment group with high dose of compounds and (E) Reference control group. The section was cut parallel to the muscle layer. H & E stain; 100X magnification.

4.3.3.3 Immunohistochemistry analysis

In order to investigate the mechanisms by which DBID compound evoke apoptosis, the colon specimens from normal control group, AOM control group and colon sections of the rats treated with high and low dose of DBID compound were subjected to immunohistochemistry analysis. Photomicrographs of ACF exhibiting grades of nuclear morphology from colons of rats were captured. All sections were cut parallel to the muscle layer. The presence of elongated and stratified nuclei were noted throughout the crypt.

The Bax and Bcl2 were evaluated as cell proliferation markers in the colon specimens. Sections of colon samples from the control groups and treatment groups with DBID are shown in Figures 4.19 and 4.20, respectively. The immunohistochemical Bax staining of the colon sections from the azoxymethan group revealed a lower number of positive cells than those from the azoxymethan plus treatment groups, while the immunohistochemical Bcl-2 staining of the colon sections from the azoxymethan group revealed a higher number of positive cells than those from the azoxymethane plus treatment groups.

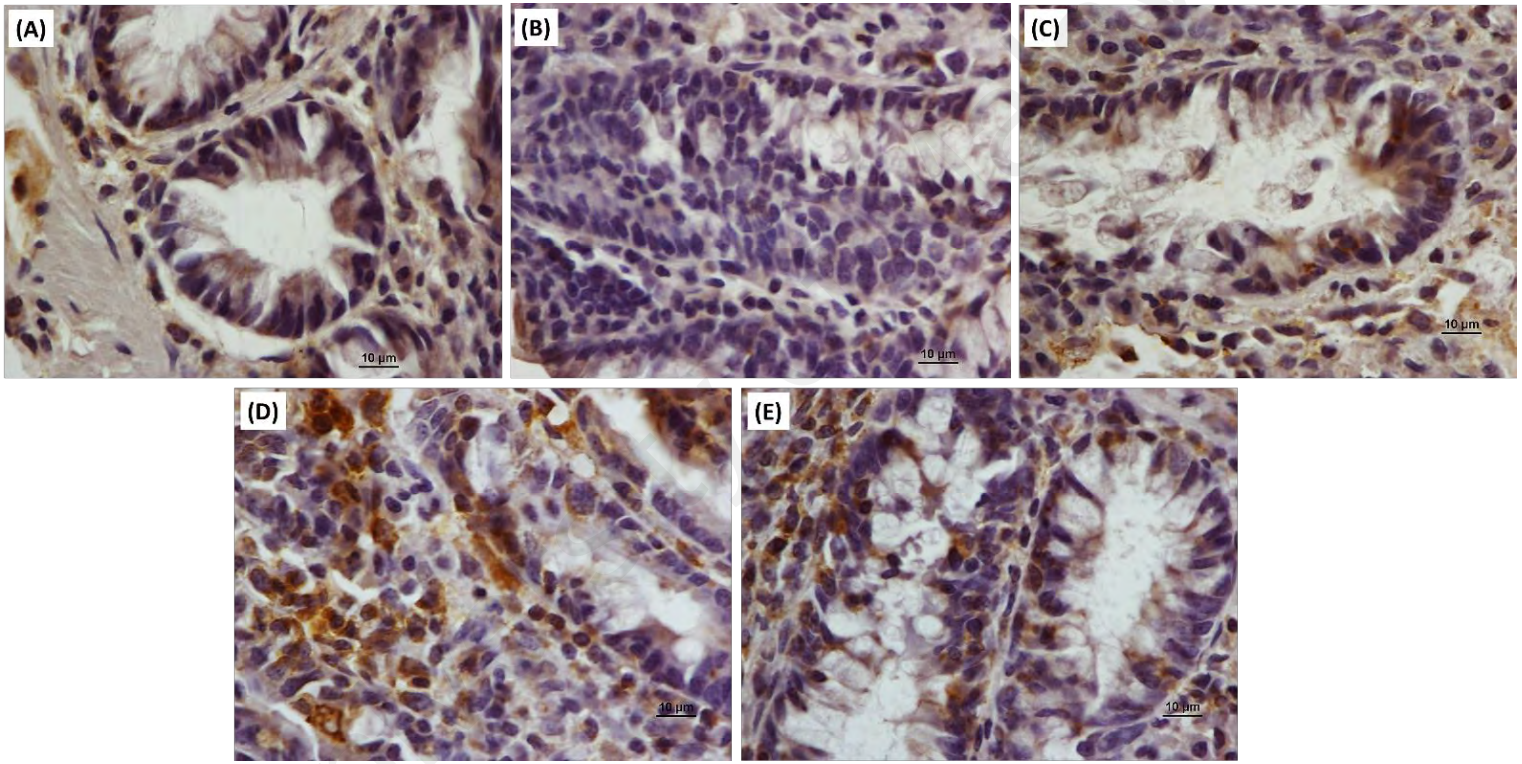

Figure 4.19: Immunohistochemical expression of Bax in colon tissues of rats.

Five groups of rats were included (A) normal control, (B) cancer control, (C) low dose of DBID, (D) high dose of DBID and (E) 5-FU treatment control. The Bax protein expression is illustrated as brown staining; 100X magnification.

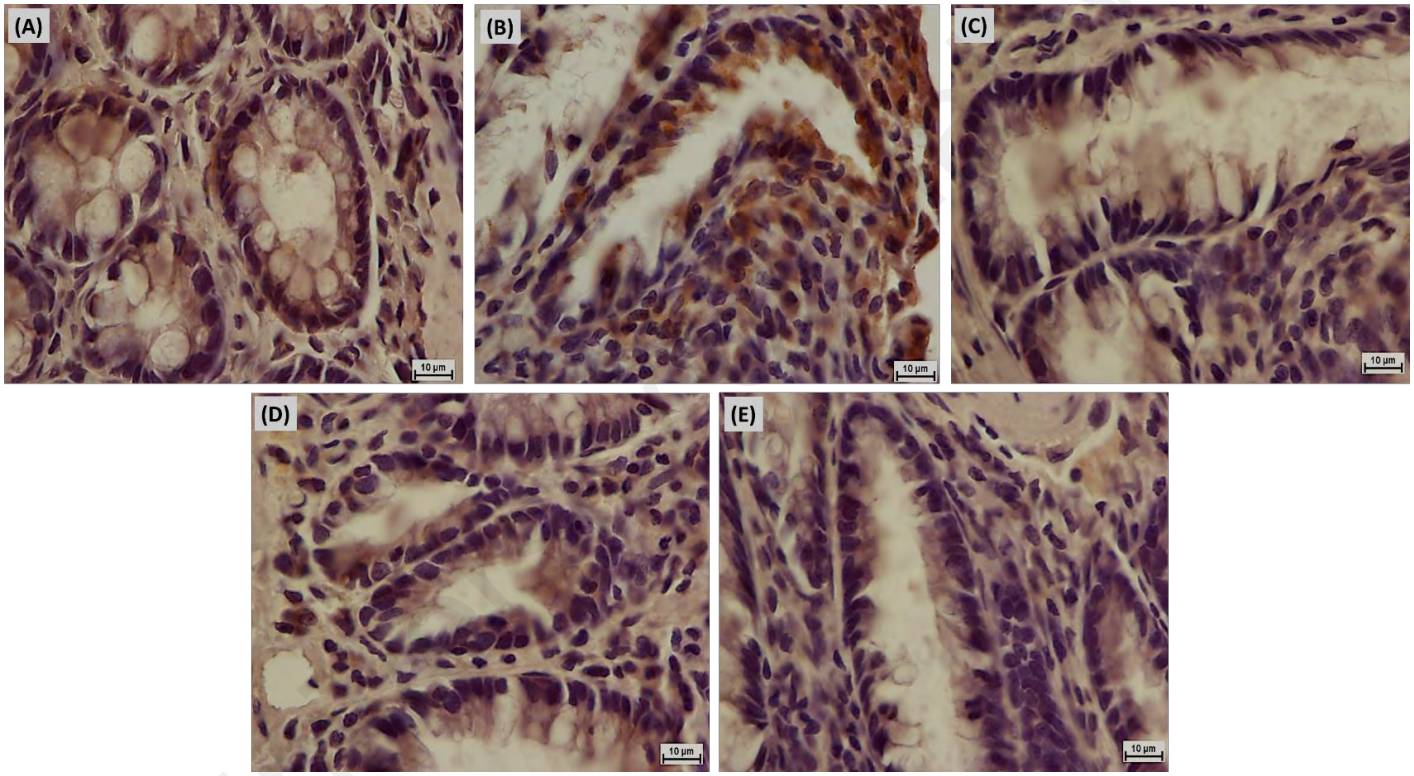

Figure 4.20: Immunohistochemical expression of Bcl2 in colon tissues of rats.

Five groups of rats were included (A) normal control, (B) cancer control, (C) low dose of DBID, (D) high dose of DBID and (E) 5-FU treatment control.The Bcl-2 protein expression is illustrated as brown staining. 100X magnification.

4.3.3.4 Gene expression by Real-Time-PCR

In Figure 4.21, following DBID (40 and 20 mg/kg) and reference (5-Fluorouracil) treatment, the expression of BAX mRNA in the colon tissue were 3.45, 3.19 and 3.48 fold higher as compared to normal control (sham). Treatment with DBID resulted in a dose-dependent increase in CASP3 mRNA expression (5.61 to 4.52 fold) following treatment with 40 to 20 µg/kg DBID. Treatment with DBID at 40 and 20 mg/kg resulted in a significant reduction (0.45 and 0.52 fold) in BCL2 mRNA expression as compared to cancer control (1.27 fold) and normal control (1.0 fold) groups ($p<0.05$). The purity of the isolated RNA was checked by running 1% agarose gel electrophoresis (Figure 4.22).

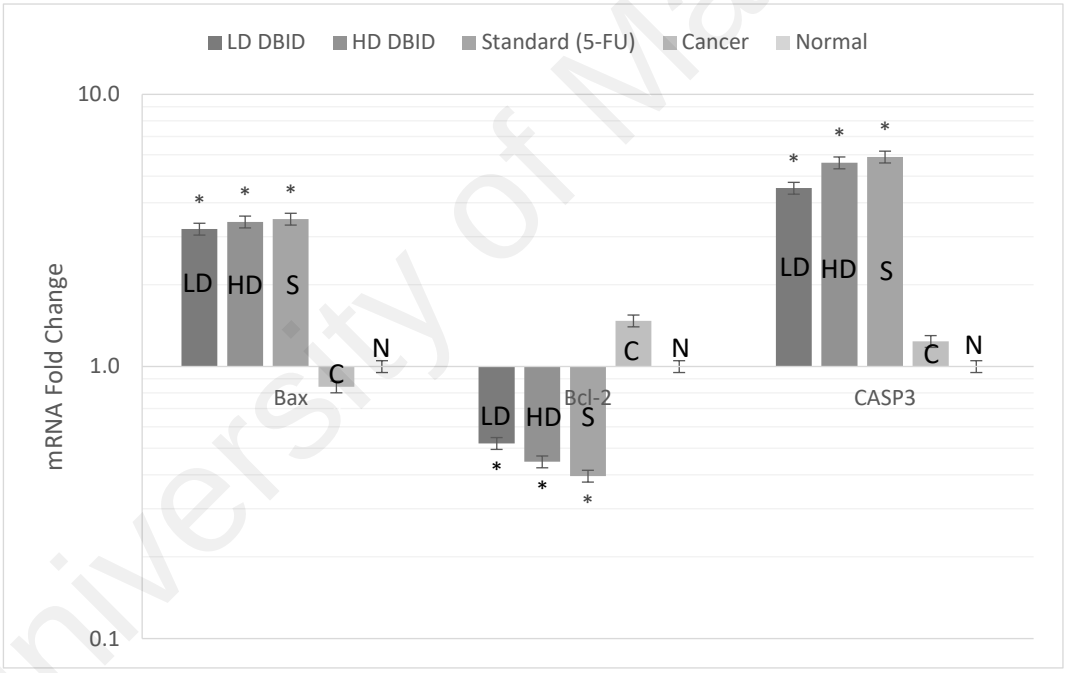

Figure 4.21: Gene expression analysis of rat colon tissue by using Real Time-PCR.

The mRNA expression of BAX, BCL2 and CASP3 in rat colon tissue was investigated. Relative mRNA expression was calculated using the $2^{-\Delta\Delta CT}$ method. The results are representative of reactions run in triplicate and expressed as mean ± Std. Dev. * shows significant difference from normal control ($p< 0.05$).

Figure 4.22: RNA gel electrophoresis.

4.3.3.5 Protein expression by western blotting

In order to further investigate the chemopreventive activity of this compound in colon cancer and the mechanism underlying this effect, the expressions caspase 3, pro-apoptotic (Bax) and anti-apoptotic (Bcl-2) in the different groups were analysed. As shown in Figure 4.23, western blot analysis revealed that the expression of caspase 3 and Bax proteins in colon tissue were up-regulated by DBID and reference drug (5-Fluorouracil), which were significantly higher than cancer control and normal control ($p<0.05$). The expression of Bcl-2 protein in colon tissue was significantly down-regulated by DBID and 5-Fluorouracil compared to cancer control. Consistent with gene expression studies, the western blotting results revealed that the DBID compound altered the Bax/ Bcl2 ratio by increasing the expression of Bax protein and down-regulating the expression of Bcl-2. Furthermore, a significant expression of caspase 3 as an executioner caspase in caspase cascade, leading to apoptosis process, was observed.

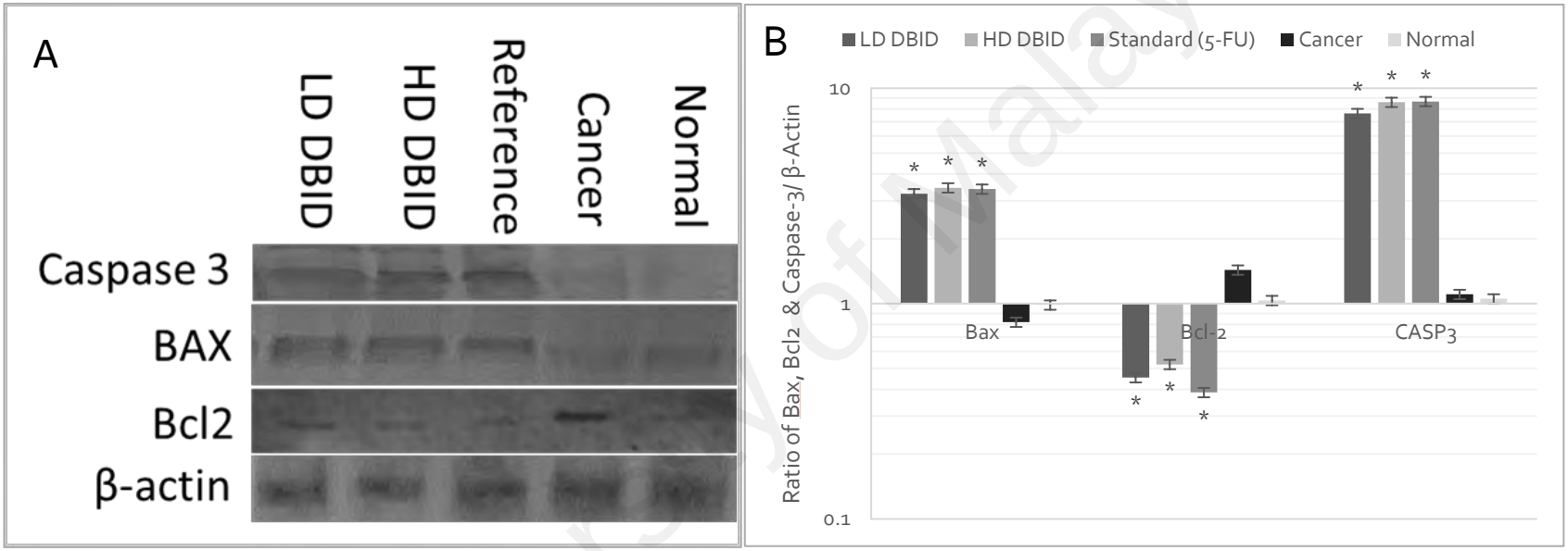

Figure 4.23: Western blot analysis of colon tissue homogenate.

The blots were scanned and analyzed using ImageJ software. The protein expression of treatment group with 20 mg/kg DBID compound (LD DBID), treatment group with 40 mg/kg DBID compound (HD DBID), 35 mg/kg 5-fluorouracil (Reference), Cancer control group (Cancer) and Normal control group (Sham). Western blot analysis confirmed up-regulation of Bax and Caspase-3 and down-regulation of Bcl-2 at the protein level.

4.3.3.6 Antioxidant enzyme activities of colon tissue homogenate

The activities of catalase (CAT), superoxide dismutase (SOD), and glutathione peroxidase (GPx) are shown in Figure 4.24. In general, the antioxidant activities were significantly elevated in groups treated with DBID and 5-fluorouracil, while the antioxidant activities were reduced in the cancer control group. In our study, the upregulation of antioxidant enzymes, catalase, superoxide dismutase, and glutathione peroxidase enzymes following administration of DBID was observed in colon tissue homogenate ($p<0.05$).

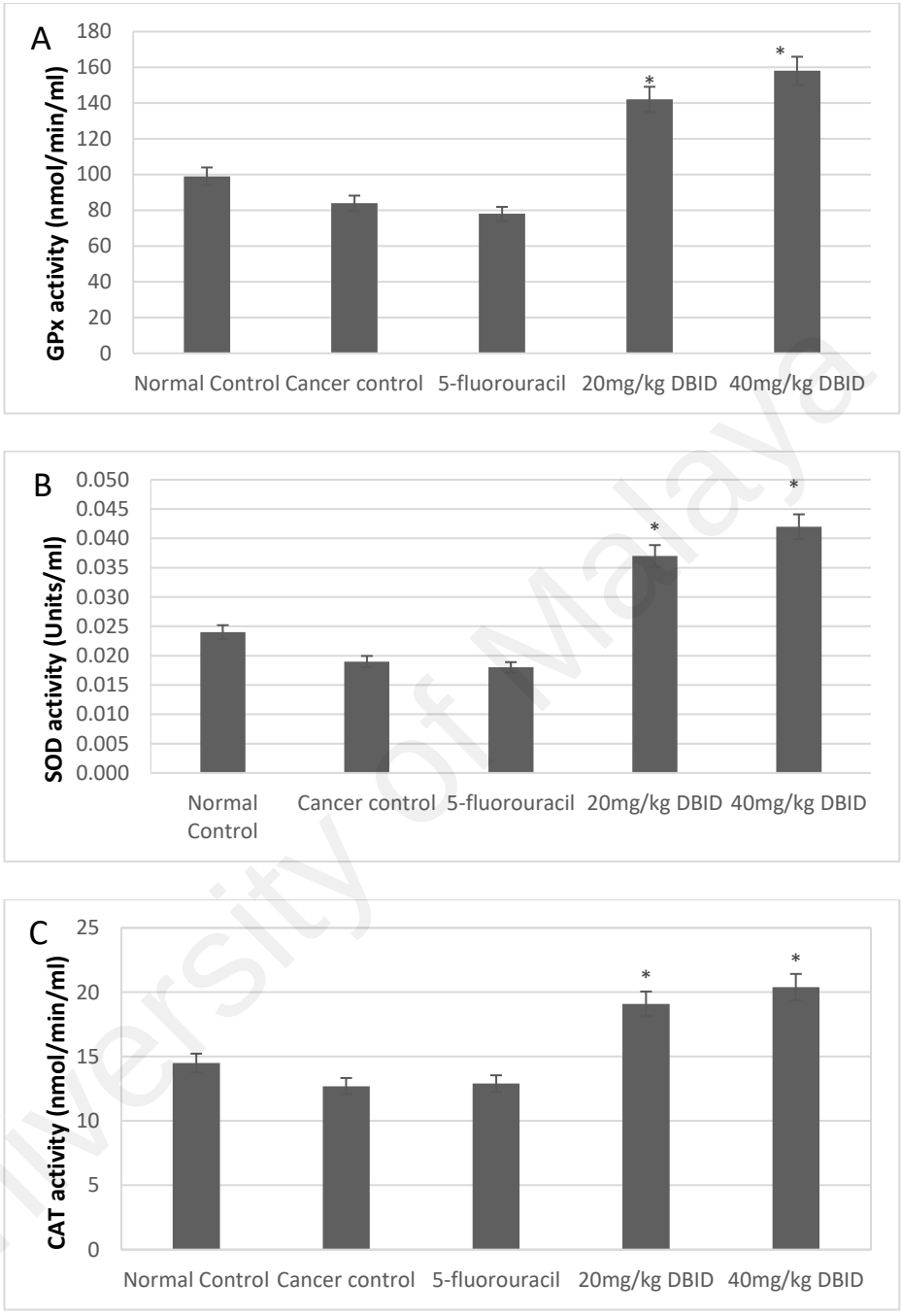

Figure 4.24: The antioxidant activity of colon tissue homogenate.

The activities of glutathione peroxidase (A), superoxide dismutase (B), and catalase (C) in colon tissue homogenate are presented as mean ± SD (n=6). *The significant value was set at <p 0.05, compared with cancer control group.

CHAPTER 5: DISCUSSION

5.1 *In vitro* cancer studies

5.1.1 Inhibition of cell proliferation

The MTT assay has been widely adopted for monitoring the cytotoxicity of various substances that would either inhibit or stimulate cell growth.

These results (Figure 4.1 and Table 4.1) showed the high ability of the DBID compound to inhibit of proliferation of the cell lines. The DBID compound inhibited the proliferation of HCT 116 and HT-29 cells with an IC_{50} of 9.32±1.16 and 11.85± 2.7µg/ml, respectively. These results showed that HCT 116 cells was more sensitive to be inhibited by DBID compared to HT-29 cells ($p>0.05$), which could be due to differences in the structure of the two cell lines. HCT116 cells have no ability to differentiate; however, HT29 has retained intermediate capacity to differentiate. (Yeung et al., 2010). HCT 116 cells and HT-29 cells were treated with the DBID compound. DBID treatment induced stronger antiproliferative effect in HCT-116 cells (IC_{50} = 9 µM) than in HT-29 cells (IC_{50} =12 µM). This data showed the toxicity of the compound on these two types of colon cancer cell lines. The IC_{50} value of the compound on CCD 841 CoN as normal colon cells were significantly higher than the cancer cell lines (IC_{50}>150 µg/ml).

The findings of this study showed the strong inhibitory effect of the DBID compound against the tumorigenic cell lines, HCT116 and HT-29, without being relatively cytotoxic on normal cells (CCD 841 CoN). Many studies have proposed the anticancer effect of heterocyclic compounds (Cholody et al., 2005; Hajrezaie et al., 2014b; Sashidhara et al., 2010; Weinstein et al., 1997; Zahedifard et al., 2015a).

5.1.2 Reactive oxygen species (ROS) assay

Within living cells, reactive oxygen species are continuously produced. This is a natural consequence of metabolic reactions as well as other biochemical reactions, though the ROS concentration is critical in cells and tissue. Under oxidative stress conditions, excessive ROS leads to numerous impairments, both biochemical and physiological. All this promotes the process of cell death. The important role of intracellular ROS in apoptosis induction has been reviewed by Simon et al. (2000). It has been suggested that the disproportional increase in intracellular ROS leads to release cytochrome C from mitochondria which trigger caspase activation. Understanding the role of reactive oxygen species (ROS) in apoptosis opens new approaches for controlling cancer growth.

This biochemical difference between normal and cancer cells may thus be a strategy for modulating cellular ROS to selectively kill cancer cells. It has been hypothesized that ROS associated with oncogenic transformation would make the cells highly dependent on its antioxidant systems to eliminate the harmful effects of ROS (Pelicano et al., 2004; Trachootham et al., 2009).

The result obtained when intracellular ROS was estimated showed that the production of ROS in HCT 116 and HT-29 cells following DBID treatment compared to the untreated cells (control) was elevated. This result showed that DBID can promote oxidative stress in both cancer cell lines, HCT 116 and HT-29 cells, upon treatment (Figures 4.2-4.4).

Previous studies have suggested that the reactive oxygen species are responsible as part of the signalling process involved in the activation of a crucial mechanism for the elimination of cancer cells such as apoptosis (Chung et al., 2003; Liou & Storz, 2010; Ricci et al., 2003). A similar effect was observed with the DBID compound in HCT 116 and HT-29 cells (Figure 4.2-4.4). The present results propose the apoptosis inductions

through the production of intracellular ROS formation in cells treated with DBID compound.

Induction of apoptosis should be studied by investigating the signalling pathway of apoptosis such as activation of caspase proteins (especially caspase-8), releasing of cytochrome c, etc. ROS activate caspase enzymes which cause apoptosis in cell.

5.1.3 Apoptosis and caspase activity

Figure 4.5 and 4.6 showed the morphological characterization of the HCT 116 and HT-29 cells under a fluorescent microscope after staining with AO and PI, nucleic acid binding dyes, to elucidate the viable cells, early apoptosis and late apoptosis. AO/PI staining of both cells treated with DBID exhibited remarkable morphological changes of treated cells in apoptotic bodies e.g. cell shrinkage, membrane blebbing and chromatin condensation.

The morphological characteristics of apoptosis, as a result of treatments with the DBID, was similar to the previously reported compounds affecting on cancer cell proliferation that eventually leads to apoptotic cell death (Abd Ghafar et al., 2013; Ashwaq et al., 2016; Assayaghi et al., 2016). Apoptosis is typically accompanied by the activation of a class of death proteases (caspases) and widespread biochemical and morphological changes to the cell. These changes almost invariably involve chromatin condensation and its margination at the nuclear periphery, extensive double-stranded DNA fragmentation, and cellular shrinkage and blebbing. DBID induced apoptosis in both cell lines.

Consistent with AOPI stating results, flow cytometric Annexin V results for DBID treated HCT 116 and HT-29 cells, presented in Figure 4.7 (A and B) and Figure 4.8 (A

and B), respective, clearly demonstrated that antiproliferation and apoptosis in treated cells are closely related.

Apoptosis is typically accompanied by the activation of caspase proteins. Caspases are cysteine-aspartic proteases or cysteine-dependent aspartate-directed proteases. This would be a family of cysteine proteases that have essential and necessary roles to play in apoptosis. Caspase-9 is known as an indicator for the activation of a branch caspase cascade, namely, the intrinsic (mitochondria mediated) apoptotic pathway and caspase-8 is a marker for the extrinsic (receptor) pathway of apoptosis. Caspase-3 is activated in apoptotic cells by both the extrinsic and intrinsic pathways (Fulda & Debatin, 2006).

As shown in Figures 4.9 and 4.10, there was significant change in the activation of caspase-8 and caspase-9 in treated HCT 116 and HT-29 cells during the investigated time points. The compound significantly increased the activities of caspase-3/7, -8 and -9 compared to untreated cells. This suggests that both intrinsic or mitochondrial pathways mediated by the activation of caspase -9, and extrinsic or death receptor pathways mediated by the activation of caspase -8 triggered the apoptosis induction in treated cells. The caspase -8 and -9 as initiator caspases and caspase-3/7 as executioner caspases were involved in the mechanism of apoptosis induced by the compound on HCT 116 and HT-29 cells, thought it showed some differences in the caspase activation pattern.

The results described above suggests that apoptosis and activation of caspase-3 occurred through both of the extrinsic and intrinsic pathways in treated HCT 116 and HT-29 cells with the DBID compound. In line with these results, the cytotoxic effect and antiproliferative activity of heterocyclic compounds synthetic compounds, against colon cancer cells by activating caspases and inducing apoptosis had been previously demonstrated by other studies (Hajrezaie et al., 2015; Zahedifard et al., 2015b). Similarly,

it was shown in this study that the DBID compound induced apoptosis via the intrinsic pathway and the extrinsic pathway in treated HCT 116 and HT-29 cells.

The extrinsic pathways are associated with the triggering of death receptors (DR) on the cell surface. The binding of the ligand to the receptor leads to the triggering of DR, and the use of DR proteins can cause the auto activation of caspases via proteolytic domains in the pro–caspases. Three of the known DR ligands, TNF-α, Fas, and TNF-related apoptosis induce TNF-related apoptosis-inducing ligand (TRAIL). TNF-α enhances the proliferation of chemically induced breast cancer cells. In that pathway, activation of two main proteins, namely, FasL and TRAIL, led to the activation of caspase-8. Active heterotetramer caspase-8 is released from the DISC and is free to cleave pro–caspase-3 to caspase-3. With the amplification of apoptotic signals from the DRs and the activation of caspase-8, BID proteins (a Bcl-2 family protein) are activated. The functions of these Bcl2 family proteins are very critical in the homeostasis of apoptosis, particularly in the intrinsic pathway (Jin & El-Deiry, 2005; Schultz & Harringto, 2003; Wajant et al., 2005).

Bcl2 family members share one or more of the four characteristic domains of homology known as the Bcl2 homology (BH) domains (named BH1, BH2, BH3 and BH4). Alternatively, the BH3-interacting domain death agonist proteins (BID) (from the Bcl2 protein family) are cleaved to truncated-BID (BID) proteins, which induce Bax-mediated mitochondrial cytochrome c release. Both events commit the cell to apoptosis (Gross et al., 1999; Hengartner, 2000).

Reports reveal that the reactive oxygen species (ROS) plays an important role in inducing apoptosis through activation of the intrinsic or mitochondrial mediated pathway. Mitochondria contain apoptosis-inducing factors, the second mitochondria-derived

activator of caspases/direct IAP binding protein with low pI (Smac/DIABLO) and cytochrome c, which are all pro apoptotic. An increase in the oxidative stress in the mitochondria resulted into a leakage of cytochrome C from the mitochondrial intermembrane space to the cytoplasm (Circu & Aw, 2010; Matés & Sánchez-Jiménez, 2000).

The released cytochrome C forms a multi-protein complex called the apoptosome, which consists of cytochrome C, apoptotic protease activating factor 1 (Apaf-1), pro–caspase-9, and ATP. The formation of the apoptosome leads to the activation of caspase-9 and eventually the caspase cascade that activates effector caspases (i.e., caspase-3 and caspase-6) (Cain et al., 2002; Fan et al., 2005; Hengartner, 2000).

Generally, the reactive oxygen species are responsible as part of the signalling process involved in the activation of a crucial mechanism for the elimination of cancer cells such as apoptosis (Chung et al., 2003; Liou & Storz, 2010; Ricci et al., 2003). Several anticancer agents depend on this form of cell death for their efficacy (Liou & Storz, 2010; Trachootham et al., 2009). The present results propose the apoptosis inductions through the production of intracellular ROS formation in cells treated with DBID compound.

5.1.4 Gene and protein expression

The gene expression study of some of these genes involved in apoptosis by using Real Time-PCR technique showed the overexpression of CASP3, CASP9, CASP8, TP53, BID and BAX and downregulation of BCL2 in HCT and HT-29 cells treated with DBID compared with untreated cells (Figures 4.11 and 4.12).

The activation of caspases is known as a hallmark of apoptosis, which proposes new therapeutic agents for the treatment of cancer cells (Beauparlant & Shore, 2003; Hensley et al., 2013; Jiang et al., 2001; Philchenkov et al., 2004). Bcl-2 protein family is important

in the regulation of apoptosis when the stimuli are intrinsic in nature, Bax and Bid proteins are mainly found in the cytosol. At the onset of apoptosis, the localization of some Bcl2 proteins is altered. For example, Bax protein translocates from the cytosol to the mitochondrial membrane after treatment with an apoptotic stimulus. The increase in the Bax and Bcl2 ratio has been documented as a key factor showing induced apoptosis (Gross et al., 1999; Norberg et al., 2010; Schultz & Harringto, 2003).

Tumor protein p53 is involved in diverse functions, particularly in suppressing the pathogenesis of tumors. The p53 tumor suppressor gene (TP53) encodes the tumor protein p53, a transcriptional factor that binds to DNA and activates the expression of downstream genes, which mediates cellular stress responses i.e. cell-cycle arrest, senescence and apoptosis (Vazquez et al., 2008).

As explained above, BID, a pro-apoptotic member of the Bcl-2 family mediates the activation of caspase-9 by caspase-8 through the mitochondrial pathway. The ability of DBID to activate Bax can be inhibited by the anti-apoptotic Bcl-2 proteins resulting in apoptosis inhibition by sequestering DBID, leading to reduced Bax activation (Cory et al., 2003; Li et al., 1998). Moreover, the intrinsic or mitochondrial pathway is mediated by the alteration of the pro-apoptotic (Bax) and anti-apoptotic (Bcl2) ratio. Bcl2L (Bcl2-Like), BclXL (Bcl2 related protein long isoform) and other anti-apoptotic Bcl2 family members reside in the outer mitochondrial membrane and prevent cytochrome C release (Parrish et al., 2013). These results revealed that the treatment with DBID promotes apoptosis by alerting the Bax/ Bcl2 ratio by increasing the expression of Bax protein and down-regulating the expression of Bcl2 as well as upregulating the genes involved in apoptosis. There are some reports of synthetized compounds activating caspases (intrinsic and extrinsic pathway) and up-regulating the apoptotic genes and inducing apoptosis in

cancer cell lines (Asselin et al., 2001; Beauparlant & Shore, 2003; Hensley et al., 2013; Jiang et al., 2001; Olsson & Zhivotovsky, 2011; Philchenkov et al., 2004).

The western blot analysis of caspases-3, Bax and Bcl2 also verified that the DBID compound significantly up-regulated the protein expression level of caspase -3 known as an executioner caspase and pro-apoptotic Bax, while the expression of anti-apoptotic Bcl2 protein was down-regulated in both cells (Figure 4.14). The observations of gene expression study and cellular caspase activities measurements were in line with the western blot results which proposed the involvement of caspase cascades and apoptosis regulatory proteins in DBID mediated apoptosis in HCT 116 and HT-29 cells. These findings of the current study are consistent with previous studies reported by several researchers (Asselin et al., 2001; Beauparlant & Shore, 2003; Hensley et al., 2013; Jiang et al., 2001; Olsson & Zhivotovsky, 2011; Philchenkov et al., 2004).

5.2 *In vitro* antioxidant activity

Antioxidants have the ability to delay or inhibit the oxidation processes, which occur under the influence of many types of ROS. Antioxidants have long been known to offer protection against cancer, mainly offering protection against carcinogens and mainly via the prevention of mutation (Lobo et al., 2010; Valko et al., 2007).

In the defence system of the organism, antioxidants are active to attack free radicals. In laboratory techniques, a variety of *in vitro* chemical methods to evaluate the antioxidant activity of products and ingredients exist, which usually use methods such as spectrometry, chromatography, and electrochemical techniques. These methods differ in the mechanism of generation of different radical species and/or target molecules and in the way end products are measured. Ferric reducing antioxidant power (FRAP) and 1, 1-diphenyl-2-picryl hydrazyl radical (DPPH) were used in this study (Huang et al., 2005; Karadag et al., 2009).

These results (Table 4.2) indicated that the DBID compound had the high antioxidant ability in reducing ferric ions. The power of the compound in reducing ferric tripyridyl (Fe^{+3}) to ferrous form (Fe^{+2}), which was measured by the change of absorbance at 593 nm. The FRAP value of the DBID compound was 4.93±1.3 mmol Fe^{2+}/g while the frap value of quercetin as a pure flavonoid was 6.29±1.7 mmol Fe^{2+}/g as shown in Figure 4.2.

The effect of antioxidant on DPPH radical scavenging is due to their hydrogen donating ability or radical scavenging activity. Thus, DPPH assay was used to evaluate the ability of antioxidants to scavenge quenched DPPH radical.

The data listed in Table 4.2 indicated that the DBID compound was almost as potent as the pure flavonoid, quercetin, in scavenging the DPPH radical. The DBID compound showed IC_{50} values of 45.3±0.9 µg/ml and the IC_{50} value of quercetin was 39.3±0.78 µg/ml. The results obtained in this study showed that the DPPH radical scavenging activities of the DBID compound possess the high ability of donating H^+.

The accumulation of free radicals in the body leads to oxidative stress which plays an important role in the development of many chronic and degenerative diseases, one of which is cancer. Oxidative stress may cause DNA, protein, and/or lipid damage, leading to changes in chromosome instability, genetic mutation, and modulation of cell growth that ultimately leads to cancer (Dreher & Junod, 1996; Kehrer et al., 2010). DBID compound showed high antioxidant activity in FRAP and DPPH free radical scavenging assays. It was concluded that the compound has a good potency to scavenge the free radicals.

5.3 *In vivo* studies

5.3.1 Acute and subacute toxicity study

In drug development process, the toxicity testing of new compounds is required. There are various experimental animal models and methods for toxicity screening of substances. Acute toxicity test is a known method to determine the effect of a single dose which is administered at different dose levels, and the effect is observed for 14 days (Parasuraman, 2011).

The acute and subacute toxicity tests were performed to screen for any possible toxic effect of the compound in an animal model by following the Organization for Economic Cooperation and Development (OECD) test guidelines (OECD Guideline, 2001). From the results obtained as in (Figure 4.15 and Table 4.3), it was concluded that the safe dose of DBID compound exceeded 2000 mg/kg since there was no mortality or any signs of toxicity or any abnormalities in serum biochemical and histologic indicators of kidney and liver. In a previous study conducted by Pahari et al. (2010), mortality at 1750 and 2000 mg/Kg body weight has been reported in the acute toxicity of the indole derivative synthesized compound in albino rats.

For further investigation of toxicity, subacute oral toxicity of the compound in an animal model following the OECD guideline for the testing of chemicals was performed (OECD Guideline, 2008). Repeated dose toxicity or **s**ubacute toxicity includes the general toxicological effects occurring as a result of repeated daily dosing of a substance for a specified period. Repeated dose toxicity testing is generally carried out for a minimum of 28 days and administered daily through the oral route (Parasuraman, 2011).

The results show **s**ubacute toxicity results showed no significant changes in body weight of rats (Table 4.4) and no signs of toxicity or any abnormalities during the period of experiment in repeated oral amination of DBID compound at concentration of 10, 20,

and 40 mg/kg body weight/day for the period of 28 days (Figure 4.16, Table 4.5). Based on observations obtained from the repeated dose toxicity test, it was concluded that the safe repeated doses of DBID compound for 28 days exceeded 40 mg/kg, while there was no mortality or any signs of toxicity or any abnormalities in serum biochemical and histologic indicators of kidney and liver.

5.3.2 The chemopreventive effect of DBID against colon cancer

Azoxymethane (AOM) induced aberrant crypt foci (ACF) formation and pathological changes in the colonic mucosal tissues in cancer groups. The groups treated with DBID compound and 5-Fluorouracil showed significant suppression of the lesion formation (Figure 4.17, Table 4.6). In line with previous studies, the results showed that the new benzo indole compound (DBID) significantly suppressed the number of ACF in the colon compared to cancer control group (Hajrezaie et al., 2014a; Zahedifard et al., 2015b). Many studies have reported the chemopreventive effect of heterocyclic compounds (Faraj et al., 2014a; Faraj et al., 2014b; Hajrezaie et al., 2014a; Zahedifard et al., 2015a).

Antioxidants and oxidants are continuously balanced by externally supplied antioxidants and antioxidant enzymatic systems in the body. This balance has been suggested as a critical concept in maintaining a healthy biological system and protecting the body against disease (Pham-Huy et al., 2008; Valko et al., 2007).

The reactive oxygen species (ROS) generation is considered to be the primary cause of damaging effects. Recent published reports have shown vital role of reactive oxygen species and oxidative stress in tumour development (Kehrer et al., 2015). The antioxidant potential properties of the compound prohibited the generation of ROS in the colonic cells as presented by its ability to quench and scavenge DPPH and Ferric reducing antioxidant power (Table 4.2). We postulated that the presence of DBID compound with AOM

balanced the levels of the colonic intracellular antioxidant capacity. These results are in accordance with previous reports (Hajrezaie et al., 2014a; Hue et al., 2009).

On the other hand, DBID was able to increase the antioxidant enzymes i.e. SOD, CAT and GPx activity (Figure 4.24). There is a network of antioxidant enzymes in cells that can protect cells against oxidative stress (Kim et al., 2014). Superoxide dismutase is an enzyme that catalyzes the conversion of the superoxide anion oxygen and hydrogen peroxide. The low antioxidant capacity and the oxidant-antioxidant imbalance have been shown to have a key role in multistage carcinogenesis (Fridovich, 1997; Fukai & Ushio-Fukai, 2011). Catalases are enzymes that catalyze the conversion of hydrogen peroxide to water and oxygen, using either an iron or a manganese cofactor (Goyal & Basak, 2010). Glutathione peroxidase is an enzyme containing four selenium cofactors that catalyze the breakdown of hydrogen peroxide and organic hydroperoxides. Glutathione peroxidase (GPx) is the general name of enzyme groups which have peroxidase activity and protect the organism from oxidative damage (Hofmann et al., 2002). In our results, the antioxidant enzymes were upregulated following the administration of DBID in colon tissue homogenate.

The production of ROS combined with a decreased antioxidant enzyme level is a significant marker for tumour cells (Khan et al., 2010; Pelicano et al., 2004; Trachootham et al., 2009). The role of reactive oxygen species (ROS) in the pathogenesis and development of colorectal cancer has been suggested in many clinical studies (Kubiak et al., 2011; Mahmood, 2010; Strzelczyk et al., 2012). Positive therapeutic impact of targeting the antioxidant capacity of tumour cells and limiting the injury caused by oxidative stress have been shown as an anticancer strategy (Ayala et al., 2014; Pljesaercegovac et al., 2008). Based on the results obtained in this study, DBID was able to increase the SOD, CAT and GPx activity.

Increasing the activation of antioxidant enzymes such as superoxide dismutase (SOD), catalase (CAT), and glutathione peroxidase (GPx) is another factor to protect against cancer (Mates, 2000; MatÉs et al., 1999). It was shown that the DBID compound, by increase of the activities of GPX, SD, and CAT in colon tissue homogenates, protected against colon cancer in rats.

Moreover, the expression of Bax and caspase 3 proteins and genes were upregulated in DBID and 5-Fluorouracil treated groups whereas the Bcl2 expression was down regulated (Figures 4.19 - 4.23). The intrinsic or mitochondrial pathway is mediated by the alteration of the pro-apoptotic (Bax) and anti-apoptotic (Bcl2) ratio. Bcl2L (Bcl2-Like), BclXL (Bcl2 related protein long isoform) and other anti-apoptotic Bcl2 family members reside in the outer mitochondrial membrane and prevent cytochrome c release. In fact, cytochrome c release from the mitochondria is regulated by Bcl2 family proteins. Released cytochrome c interacts with Apaf-1 (apoptotic protease activating factor-1), ATP and pro-caspase 9, forming an apoptosome complex. The apoptosome cleaves pro-caspase 9 into its active form, caspase-9, which in turn stimulates the effector caspase-induced DNA breakdown, causing apoptosis. The activation of initiator caspases (caspase-2, caspase-8 and caspase-9) in turn causes the activation of executioner caspases-3, -6 and -7 and ultimately leads to DNA fragmentation, DNA budding and chromatin condensation which are characteristics of cells undergoing apoptosis (Parrish et al., 2013; Xiong et al., 2014). In line with RT-PCR results, the western blotting and Immunohistochemistry (IHC) staining results confirmed that the treatment with DBID induced apoptosis by alerting the Bax/ Bcl2 ratio and upregulating of caspase 3 genes and proteins expression. It was suggested that DBID is effective against free radicals involved in the formation of colorogenic lesions in Azoxymethane (AOM)-induced aberrant crypt foci (ACF) formation and pathological changes in rats and has a chemopreventive effect.

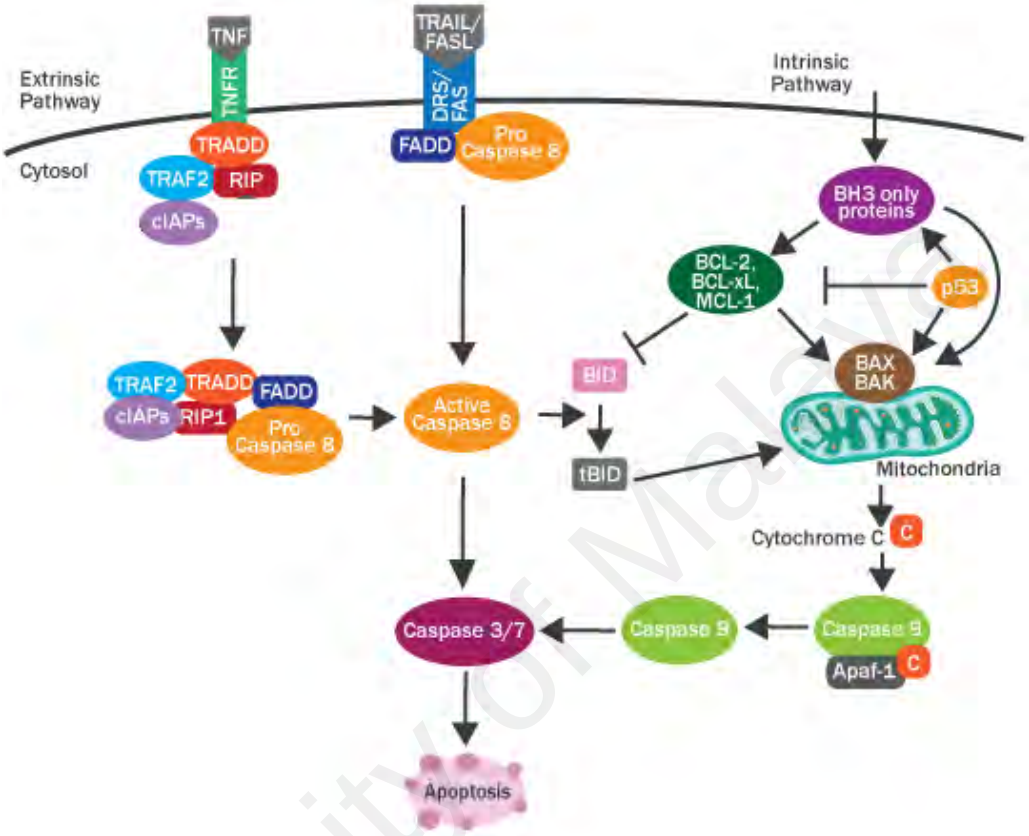

Figure 5.1: The proposed model of mechanisms derived from this study.

CHAPTER 6: CONCLUSION

6.1 Conclusion

This study determined the anticancer and antioxidant activities of 2-(1,1-dimethyl-1H-benzo[e]indol-2-yl)-3-((2-hydroxyphenyl)amino)acrylaldehyde, abbreviated as DBID.

6.1.1 *In vitro*

Evidence provided in the present study showed the antiproliferative activity of a new benzo indole derivative (DBID) against two colon cancer cell lines, HCT 116 and HT-29, without being toxic to the normal colon cell (CCD 841 CoN).

The quantitative and qualitative investigation of caspase activities by using luminescence spectrophotometry, fluorescence microscopy (AO/PI), flow cytometry analysis, gene expression and western blot validation provided in the present study, proposed that the antiproliferative effects of DBID on colon cancer cell lines could be due to the occurrence of apoptosis through the induction of cellular caspase activities as demonstrated by generating intracellular ROS, initiating both the intrinsic and the extrinsic apoptosis pathways. The DBID generated ROS, which was followed by the activation of caspase-8, -9 and -3.

6.1.2 *In vivo*

This study has provided results, specifically *in vivo* evidence, that a new benzo indole derivative (DBID) prevented the AOM-induced colon cancer in rats by suppression of aberrant crypt foci (ACF) formation and upregulation of antioxidant enzyme activities as well as its potent antioxidant activity. Moreover, the effect of DBID compound on colon cancer could be due to the induction of apoptosis through the induction of cellular caspase activities as demonstrated by initiating both the intrinsic and the extrinsic apoptosis pathway, and up-regulation of the expression of some specific apoptotic genes.

We hypothesised that the chemopreventive effect of DBID on AOM-mediated carcinogenesis and oxidative stress in rat colon was associated with its effective activity against free radicals involved in the formation of colorogenic lesions. In conclusion, DBID as a novel synthetic compound showed potential chemopreventive properties.

6.2 Challenges and future studies

Limitations are inevitable in consideration of the therapeutic application of the synthetic compounds as anticancer agents due to the relatively high production cost. Hence, the design of new chemotherapeutic drugs involving the knowledge of bioinformatics and molecular docking studies which mimic the mode of antiproliferative action of the synthetised compounds could be a promising alternative.

Exploration of the *in vitro* and *in vivo* pharmacological properties of the new synthetic benzo indole derivative revealed that the compound may represent a new generation of potential drug candidates for the treatment of colon cancer. However, further *in vivo* studies and clinical trials are required to assess the bioavailability, pharmacokinetic and pharmacodynamics profiles in humans prior to application in the pharmaceutical industry as a therapeutic agent.

REFERENCES

Abd Ghafar, S. A., Ismail, M., Saiful Yazan, L., Fakurazi, S., Ismail, N., Chan, K. W., & Md Tahir, P. (2013). Cytotoxic activity of kenaf seed oils from supercritical carbon dioxide fluid extraction towards human colorectal cancer (ht29) cell lines. *Evidence-Based Complementary and Alternative Medicine, 2013*.

Adelstein, B.-A., Macaskill, P., Chan, S. F., Katelaris, P. H., & Irwig, L. (2011). Most bowel cancer symptoms do not indicate colorectal cancer and polyps: A systematic review. *BMC Gastroenterology, 11*(1), 65.

Alberts, B., Johnson, A., Lewis, J., Raff, M., Roberts, K., & Walter, P. (2002). The molecular basis of cancer-cell behavior. *Molecular biology of the cell* (4th ed.). New York: Garland Science.

Ali, M., Jesmin, M., Salahuddin, M., Habib, M., & Khanam, J. (2008). Antineoplastic activity of n–salicylideneglycinato–di–aquanickel (ii) complex against ehrlich ascites carcinoma (eac) cells in mice. *International Journal of Biological and Chemical Sciences, 2*(3), 292-298.

American Cancer Society. (2013). *Cancer facts & figures 2013. Atlanta: American Cancer Society.*

American Cancer Society. (2015a). *Cancer facts & figures 2015. Atlanta: American Cancer Society.*

American Cancer Society. (2015b). *Global cancer facts & figures* (3rd ed.). *Atlanta: American Cancer Society.*

American Cancer Society. (2016). *Cancer facts & figures 2016. Atlanta: American Cancer Society.*

American Cancer Society. (2017). *Cancer facts & figures 2017. Atlanta: American Cancer Society.*

André, T., Boni, C., Mounedji-Boudiaf, L., Navarro, M., Tabernero, J., Hickish, T., . . . Bridgewater, J. (2004). Oxaliplatin, fluorouracil, and leucovorin as adjuvant treatment for colon cancer. *New England Journal of Medicine, 350*(23), 2343-2351.

Andre, T., Louvet, C., Maindrault-Goebel, F., Couteau, C., Mabro, M., Lotz, J., . . . Izrael, V. (1999). Cpt-11 (irinotecan) addition to bimonthly, high-dose leucovorin and bolus and continuous-infusion 5-fluorouracil (folfiri) for pretreated metastatic colorectal cancer. *European Journal of Cancer, 35*(9), 1343-1347.

Arora, P., Arora, V., Lamba, H., & Wadhwa, D. (2012). Importance of heterocyclic chemistry: A review. *International Journal of Pharmaceutical Sciences and Research, 3*(9), 2947.

Ashe, P. C., & Berry, M. D. (2003). Apoptotic signaling cascades. *Progress in Neuro-Psychopharmacology and Biological Psychiatry, 27*(2), 199-214.

Ashwaq, A. S., AlQubaisi, M. S., Rasedee, A., Abdul, A. B., TaufiqYap, Y. H., & Yeap, S. K. (2016). Inducing g2/m cell cycle arrest and apoptosis through generation reactive oxygen species (ros)-mediated mitochondria pathway in ht-29 cells by dentatin (den) and dentatin incorporated in hydroxypropyl-β-cyclodextrin (den-hpβcd). *International Journal of Molecular Sciences, 17*(10), 1653.

Assayaghi, R. M., Alabsi, A. M., & Ali, A. M. (2016). Apoptosis induction of newcastle disease virus strains (af 2240 & v4-upm) on ht-29 human colorectal adenocarcinoma cells. *Journal of Cancer Research and Therapeutic Oncology, 4*, 101.

Asselin, E., Mills, G. B., & Tsang, B. K. (2001). Xiap regulates akt activity and caspase-3-dependent cleavage during cisplatin-induced apoptosis in human ovarian epithelial cancer cells. *Cancer Research, 61*(5), 1862-1868.

Astin, M., Griffin, T., Neal, R. D., Rose, P., & Hamilton, W. (2011). The diagnostic value of symptoms for colorectal cancer in primary care: A systematic review. *The British Journal of General Practice, 61*(586), e231.

Atterhög, J.-H., Duner, H., & Pernow, B. (1976). Experience with pindolol, a betareceptor blocker, in the treatment of hypertension. *The American Journal of Medicine, 60*(6), 872-876.

Ayala, A., Muñoz, M. F., & Argüelles, S. (2014). Lipid peroxidation: Production, metabolism, and signaling mechanisms of malondialdehyde and 4-hydroxy-2-nonenal. *Oxidative Medicine and Cellular Longevity, 2014*.

Baird-Lambert, J., Davis, P., & Taylor, K. (1982). Methylaplysinopsin: A natural product of marine origin with effects on serotonergic neurotransmission. *Clinical and Experimental Pharmacology and Physiology, 9*(2), 203-212.

Bardhan, K., & Liu, K. (2013). Epigenetics and colorectal cancer pathogenesis. *Cancers, 5*(2), 676-713.

Bardi, D. A., Halabi, M. F., Hassandarvish, P., Rouhollahi, E., Paydar, M., Moghadamtousi, S. Z., . . . Abdulla, M. A. (2014). Andrographis paniculata leaf extract prevents thioacetamide-induced liver cirrhosis in rats. *PloS ONE, 9*(10), e109424.

Beahrs, O. H., & Henson, D. E. (1992). Manual for staging of cancer. *Cancer, 69*(11), 2869-2869.

Beauparlant, P., & Shore, G. (2003). Therapeutic activation of caspases in cancer: A question of selectivity. *Current Opinion in Drug Discovery & Development, 6*(2), 179-187.

Benzie, I. F., & Strain, J. J. (1996). The ferric reducing ability of plasma (frap) as a measure of "antioxidant power": The frap assay. *Analytical Biochemistry, 239*(1), 70-76.

Bertram, J. S. (2000). The molecular biology of cancer. *Molecular Aspects of Medicine, 21*(6), 167-223.

Bhati, S. K., & Kumar, A. (2008). Synthesis of new substituted azetidinoyl and thiazolidinoyl-1, 3, 4-thiadiazino (6, 5-b) indoles as promising anti-inflammatory agents. *European Journal of Medicinal Chemistry, 43*(11), 2323-2330.

Bienz, M., & Clevers, H. (2000). Linking colorectal cancer to wnt signaling. *Cell, 103*(2), 311-320.

Bird, R. P. (1987). Observation and quantification of aberrant crypts in the murine colon treated with a colon carcinogen: Preliminary findings. *Cancer Letters, 37*(2), 147-151.

Bolt, M. W., & Mahoney, P. A. (1997). High-efficiency blotting of proteins of diverse sizes following sodium dodecyl sulfate-polyacrylamide gel electrophoresis. *Analytical Biochemistry, 247*(2), 185-192.

Borges, H. L., Linden, R., & Wang, J. Y. J. (2008). DNA damage-induced cell death: Lessons from the central nervous system. *Cell Research, 18*(1), 17-26.

Brancale, A., & Silvestri, R. (2007). Indole, a core nucleus for potent inhibitors of tubulin polymerization. *Medicinal Research Reviews, 27*(2), 209-238.

Bröker, L. E., Kruyt, F. A., & Giaccone, G. (2005). Cell death independent of caspases: A review. *Clinical Cancer Research, 11*(9), 3155-3162.

Bustin, S. A. (2000). Absolute quantification of mrna using real-time reverse transcription polymerase chain reaction assays. *Journal of Molecular Endocrinology, 25*(2), 169-193.

Cain, K., Bratton, S. B., & Cohen, G. M. (2002). The apaf-1 apoptosome: A large caspase-activating complex. *Biochimie, 84*(2), 203-214.

Cheeseman, S., Joel, S., Chester, J., Wilson, G., Dent, J., Richards, F., & Seymour, M. (2002). A 'modified de gramont'regimen of fluorouracil, alone and with oxaliplatin, for advanced colorectal cancer. *British Journal of Cancer, 87*(4), 393-399.

Chen, J., & Huang, X. F. (2009). The signal pathways in azoxymethane-induced colon cancer and preventive implications. *Cancer Biology & Therapy, 8*(14), 1313-1317.

Cheng, L., & Lai, M.-D. (2003). Aberrant crypt foci as microscopic precursors of colorectal cancer. *World Journal of Gastroenterology, 9*(12), 2642-2649.

Chernyshev, A., Fleischmann, T., & Kohen, A. (2007). Thymidyl biosynthesis enzymes as antibiotic targets. *Applied Microbiology and Biotechnology, 74*(2), 282-289.

Cholody, W. M., Kosakowska-Cholody, T., Hollingshead, M. G., Hariprakasha, H. K., & Michejda, C. J. (2005). A new synthetic agent with potent but selective cytotoxic activity against cancer. *Journal of Medicinal Chemistry, 48*(13), 4474-4481.

Chung, Y. M., Bae, Y. S., & Lee, S. Y. (2003). Molecular ordering of ros production, mitochondrial changes, and caspase activation during sodium salicylate-induced apoptosis. *Free Radical Biology and Medicine, 34*(4), 434-442.

Circu, M. L., & Aw, T. Y. (2010). Reactive oxygen species, cellular redox systems, and apoptosis. *Free Radical Biology and Medicine, 48*(6), 749-762.

Clark, D. (2010). *Guide for the care and use of laboratory animals* (8th ed.). Washington, DC: National Academy Press.

Corpet, D. E., & Taché, S. (2002). Most effective colon cancer chemopreventive agents in rats: A systematic review of aberrant crypt foci and tumor data, ranked by potency. *Nutrition and Cancer, 43*(1), 1-21.

Cory, S., Huang, D. C., & Adams, J. M. (2003). The bcl-2 family: Roles in cell survival and oncogenesis. *Oncogene, 22*(53), 8590-8607.

Cos, P., Rajan, P., Vedernikova, I., Calomme, M., Pieters, L., Vlietinck, A. J., . . . Berghe, D. V. (2002). *In vitro* antioxidant profile of phenolic acid derivatives. *Free Radical Research, 36*(6), 711-716.

Coussens, L. M., & Werb, Z. (2002). Inflammation and cancer. *Nature, 420*(6917), 860-867.

Cunningham, D., Pyrhönen, S., James, R. D., Punt, C. J., Hickish, T. F., Heikkila, R., . . . Awad, L. (1998). Randomised trial of irinotecan plus supportive care versus supportive care alone after fluorouracil failure for patients with metastatic colorectal cancer. *The Lancet, 352*(9138), 1413-1418.

Daghastanli, N. A., Itri, R., & Baptista, M. S. (2008). Singlet oxygen reacts with 2′, 7′-dichlorodihydrofluorescein and contributes to the formation of 2′, 7′-dichlorofluorescein. *Photochemistry and Photobiology, 84*(5), 1238-1243.

Danenberg, P. V. (1977). Thymidylate synthetase-a target enzyme in cancer chemotherapy. *Biochimica et Biophysica Acta, 473*(2), 73-92.

Davies, R. J., Miller, R., & Coleman, N. (2005). Colorectal cancer screening: Prospects for molecular stool analysis. *Nature Reviews Cancer, 5*(3), 199-209.

De Gramont, A. d., Figer, A., Seymour, M., Homerin, M., Hmissi, A., Cassidy, J., . . . Freyer, G. (2000). Leucovorin and fluorouracil with or without oxaliplatin as first-line treatment in advanced colorectal cancer. *Journal of Clinical Oncology, 18*(16), 2938-2947.

De Leon, M. P., & Di Gregorio, C. (2001). Pathology of colorectal cancer. *Digestive and Liver Disease, 33*(4), 372-388.

Diers, J. A., Ivey, K. D., El-Alfy, A., Shaikh, J., Wang, J., Kochanowska, A. J., . . . Matsumoto, R. R. (2008). Identification of antidepressant drug leads through the evaluation of marine natural products with neuropsychiatric pharmacophores. *Pharmacology Biochemistry and Behavior, 89*(1), 46-53.

Dikalov, S. I., & Harrison, D. G. (2014). Methods for detection of mitochondrial and cellular reactive oxygen species. *Antioxidants & Redox Signaling, 20*(2), 372-382.

Ding, H., Zhang, C., Wu, X., Yang, C., Zhang, X., Ding, J., & Xie, Y. (2005). Novel indole α-methylene-γ-lactones as potent inhibitors for akt-mtor signaling pathway kinases. *Bioorganic & Medicinal Chemistry Letters, 15*(21), 4799-4802.

Diss, L. B., Robinson, S. D., Wu, Y., Fidalgo, S., Yeoman, M. S., & Patel, B. A. (2013). Age-related changes in melatonin release in the murine distal colon. *ACS Chemical Neuroscience, 4*(5), 879-887.

Dreher, D., & Junod, A. F. (1996). Role of oxygen free radicals in cancer development. *European Journal of Cancer, 32*(1), 30-38.

Ebert, M. P., Mooney, S. H., Tonnes-Priddy, L., Lograsso, J., Hoffmann, J., Chent, J., . . . Lofton-Day, C. (2005). Hypermethylation of the tpef/hpp1 gene in primary, metastatic colorectal cancers. *Neoplasia, 7*(8), 771-778.

Edge, S. B., & Compton, C. C. (2010). The american joint committee on cancer: The 7th edition of the ajcc cancer staging manual and the future of tnm. *Annals of Surgical Oncology, 17*(6), 1471-1474.

Elmore, S. (2007). Apoptosis: A review of programmed cell death. *Toxicologic Pathology, 35*(4), 495-516.

Escribano, M., Molero, L., Lopez-Farre, A., Abarrategui, C., Carrasco, C., Garcia-Mendez, A., . . . Porres Cubero, J. C. (2004). Aspirin inhibits endothelial nitric oxide synthase (enos) and flk-1 (vascular endothelial growth factor receptor-2) prior to rat colon tumour development. *Clinical Science, 106*(1), 83-91.

Estevão, M. S., Carvalho, L. C., Ribeiro, D., Couto, D., Freitas, M., Gomes, A., . . . Marques, M. M. B. (2010). Antioxidant activity of unexplored indole derivatives: Synthesis and screening. *European Journal of Medicinal Chemistry, 45*(11), 4869-4878.

Fan, T.-J., Han, L.-H., Cong, R.-S., & Liang, J. (2005). Caspase family proteases and apoptosis. *Acta Biochimica et Biophysica Sinica, 37*(11), 719-727.

Faraj, F. L., Khaledi, H., Morimoto, Y., Itoh, S., Olmstead, M. M., & Ali, H. M. (2014a). A tetradentate β-diiminato ligand containing phenolate substituents: Flexivalent coordination to mniii, coiii, niii, and cuii. *European Journal of Inorganic Chemistry, 2014*(33), 5752-5759.

Faraj, F. L., Zahedifard, M., Paydar, M., Looi, C. Y., Abdul Majid, N., Ali, H. M., . . . Abdulla, M. A. (2014b). Synthesis, characterization, and anticancer activity of new quinazoline derivatives against mcf-7 cells. *The Scientific World Journal, 2014*.

Fearon, E. R., & Vogelstein, B. (1990). A genetic model for colorectal tumorigenesis. *Cell, 61*(5), 759-767.

Fedirko, V., Tramacere, I., Bagnardi, V., Rota, M., Scotti, L., Islami, F., . . . La Vecchia, C. (2011). Alcohol drinking and colorectal cancer risk: An overall and dose–response meta-analysis of published studies. *Annals of Oncology, 22*(9), 1958-1972.

Ferlay, J., Soerjomataram, I., Dikshit, R., Eser, S., Mathers, C., Rebelo, M., . . . Bray, F. (2015). Cancer incidence and mortality worldwide: Sources, methods and major patterns in globocan 2012. *International Journal of Cancer, 136*(5).

Fiala, E. S., Sohn, O. S., Puz, C., & Czerniak, R. (1987). Differential effects of 4-iodopyrazole and 3-methylpyrazole on the metabolic activation of methylazoxymethanol to a DNA methylating species by rat liver and rat colon mucosa in vivo. *Journal of Cancer Research and Clinical Oncology, 113*(2), 145-150.

Forstrom, J. W., Zakowski, J. J., & Tappel, A. L. (1978). Identification of the catalytic site of rat liver glutathione peroxidase as selenocysteine. *Biochemistry, 17*(13), 2639-2644.

Franzén, R. G. (2000). Recent advances in the preparation of heterocycles on solid support: A review of the literature. *Journal of Combinatorial Chemistry, 2*(3), 195-214.

Fridovich, I. (1997). Superoxide anion radical (o· 2), superoxide dismutases, and related matters. *Journal of Biological Chemistry, 272*(30), 18515-18517.

Fukai, T., & Ushio-Fukai, M. (2011). Superoxide dismutases: Role in redox signaling, vascular function, and diseases. *Antioxidants & Redox Signaling, 15*(6), 1583-1606.

Fulda, S., & Debatin, K. M. (2006). Extrinsic versus intrinsic apoptosis pathways in anticancer chemotherapy. *Oncogene, 25*(34), 4798-4811.

Gomes, A., Fernandes, E., & Lima, J. L. (2005). Fluorescence probes used for detection of reactive oxygen species. *Journal of Biochemical and Biophysical Methods, 65*(2), 45-80.

Goyal, M. M., & Basak, A. (2010). Human catalase: Looking for complete identity. *Protein & Cell, 1*(10), 888-897.

Grady, W. M., & Markowitz, S. D. (2015). The molecular pathogenesis of colorectal cancer and its potential application to colorectal cancer screening. *Digestive Diseases and Sciences, 60*(3), 762-772.

Grem, J. L. (2000). 5-fluorouracil: Forty-plus and still ticking. A review of its preclinical and clinical development. *Investigational New Drugs, 18*(4), 299-313.

Grivennikov, S., Karin, E., Terzic, J., Mucida, D., Yu, G.-Y., Vallabhapurapu, S., . . . Eckmann, L. (2009). Il-6 and stat3 are required for survival of intestinal epithelial cells and development of colitis-associated cancer. *Cancer Cell, 15*(2), 103-113.

Gross, A., McDonnell, J. M., & Korsmeyer, S. J. (1999). Bcl-2 family members and the mitochondria in apoptosis. *Genes & Development, 13*(15), 1899-1911.

Gupta, A. K., Varshney, K., Singh, N., Mishra, V., Saxena, M., Palit, G., & Saxena, A. K. (2012). Identification of novel amino acid derived cck-2r antagonists as potential anti-ulcer agent: Homology, modeling, design, synthesis, and pharmacology *Journal of Chemical Information and Modeling 53*(1), 176-187.

Hajiaghaalipour, F., Faraj, F. L., Bagheri, E., Ali, H. M., Abdulla, M. A., & Majid, N. A. (2017). Synthesis and characterization of a new benzoindole derivative with apoptotic activity against colon cancer cells. *Current Pharmaceutical Design, 23*(41), 6358-6365.

Hajiaghaalipour, F., Kanthimathi, M., Sanusi, J., & Rajarajeswaran, J. (2015). White tea (camellia sinensis) inhibits proliferation of the colon cancer cell line, ht-29, activates caspases and protects DNA of normal cells against oxidative damage. *Food Chemistry, 169*, 401-410.

Hajrezaie, M., Hassandarvish, P., Moghadamtousi, S. Z., Gwaram, N. S., Golbabapour, S., NajiHussien, A., . . . Karimian, H. (2014a). Chemopreventive evaluation of a schiff base derived copper (ii) complex against azoxymethane-induced colorectal cancer in rats. *PloS ONE, 9*(3), e91246.

Hajrezaie, M., Paydar, M., Looi, C. Y., Moghadamtousi, S. Z., Hassandarvish, P., Salga, M. S., . . . Majid, N. A. (2015). Apoptotic effect of novel schiff based cdcl2 (c14h21n3o2) complex is mediated via activation of the mitochondrial pathway in colon cancer cells. *Scientific Reports, 5*.

Hajrezaie, M., Paydar, M., Zorofchian Moghadamtousi, S., Hassandarvish, P., Gwaram, N. S., Zahedifard, M., . . . Ali, H. M. (2014b). A schiff base-derived copper (ii) complex is a potent inducer of apoptosis in colon cancer cells by activating the intrinsic pathway. *The Scientific World Journal, 2014*.

Hall, J. E. (2015). *Guyton and hall textbook of medical physiology* (13th ed.). Philadelphia: Elsevier Health Sciences.

Haller, D. G., Catalano, P. J., Macdonald, J. S., O'rourke, M. A., Frontiera, M. S., Jackson, D. V., & Mayer, R. J. (2005). Phase iii study of fluorouracil, leucovorin, and levamisole in high-risk stage ii and iii colon cancer: Final report of intergroup 0089. *Journal of Clinical Oncology, 23*(34), 8671-8678.

Hassan, M., Watari, H., AbuAlmaaty, A., Ohba, Y., & Sakuragi, N. (2014). Apoptosis and molecular targeting therapy in cancer. *BioMed Research International, 2014*, 150845.

He, Y. F., Wei, W., Zhang, X., Li, Y. H., Li, S., Wang, F. H., . . . Huang, H. Q. (2008). Analysis of the dpyd gene implicated in 5-fluorouracil catabolism in chinese cancer patients. *Journal of Clinical Pharmacy and Therapeutics, 33*(3), 307-314.

Hengartner, M. O. (2000). The biochemistry of apoptosis. *Nature, 407*(6805), 770.

Hensley, P., Mishra, M., & Kyprianou, N. (2013). Targeting caspases in cancer therapeutics. *Biological Chemistry, 394*(7), 831-843.

Hidalgo, I. J., Raub, T. J., & Borchardt, R. T. (1989). Characterization of the human colon carcinoma cell line (caco-2) as a model system for intestinal epithelial permeability. *Gastroenterology, 96*(3), 736-749.

Hirose, Y., Yoshimi, N., Makita, H., Kara, A., Tanaka, T., & Mori, H. (1996). Early alterations of apoptosis and cell proliferation in azoxymethane-initiated rat colonic epithelium. *Cancer Science, 87*(6), 575-582.

Hofmann, B., Hecht, H.-J., & Flohé, L. (2002). Peroxiredoxins. *Biological Chemistry, 383*(3-4), 347-364.

Huang, D., Ou, B., & Prior, R. L. (2005). The chemistry behind antioxidant capacity assays. *Journal of Agricultural and Food Chemistry, 53*(6), 1841-1856.

Huang, S. M., Hsu, P. C., Chen, M. Y., Li, W. S., More, S. V., Lu, K. T., & Wang, Y. C. (2012). The novel indole compound sk228 induces apoptosis and fak/paxillin disruption in tumor cell lines and inhibits growth of tumor graft in the nude mouse. *International Journal of Cancer, 131*(3), 722-732.

Hue, J. J., Miga, M., Kang, B. S., Kim, J. S., Nam, S. Y., Ahn, B., . . . Lee, B. J. (2009). Effect of phytic acid on the formation of colonic aberrant crypt foci induced by azoxymethane in fe-overloaded mice. *Laboratory Animal Research, 25*(1), 51-57.

Islam, K., Ali, S. M. M., Jesmin, M., & Khanam, J. A. (2012). In vivo anticancer activities of benzophenone semicarbazone against ehrlich ascites carcinoma cells in swiss albino mice. *Cancer Biology & Medicine, 9*(4), 242.

Jacquemard, U., Dias, N., Lansiaux, A., Bailly, C., Logé, C., Robert, J.-M., . . . Routier, S. (2008). Synthesis of 3,5-bis(2-indolyl)pyridine and 3-[(2-indolyl)-5-phenyl]pyridine derivatives as cdk inhibitors and cytotoxic agents. *Bioorganic & Medicinal Chemistry, 16*(9), 4932-4953.

Jäger, E., Heike, M., Bernhard, H. a., Klein, O., Bernhard, G., Lautz, D., . . . Knuth, A. (1996). Weekly high-dose leucovorin versus low-dose leucovorin combined with fluorouracil in advanced colorectal cancer: Results of a randomized multicenter trial. Study group for palliative treatment of metastatic colorectal cancer study protocol 1. *Journal of Clinical Oncology, 14*(8), 2274-2279.

Jass, J. R., & Sobin, L. H. (2012). *Histological typing of intestinal tumours* (2nd ed.). Washington: Springer Science & Business Media.

Jawad, N., Direkze, N., & Leedham, S. J. (2011). Inflammatory bowel disease and colon cancer. *Inflammation and Gastrointestinal Cancers*, 99-115.

Jesmin, M., Ali, M., & Khanam, J. (2010). Antitumour activities of some schiff bases derived from benzoin, salicylaldehyde, amino phenol and 2, 4 dinitrophenyl hydrazine. *Thai Journal of Pharmaceutical Sciences, 34*, 20-31.

Ji, Y. L., Li, R. Z., Xue, L. F., Li, P., Liang, X. H., Dong, L., . . . Pang, M. X. (2015). Therapeutic effects of 5-fluorouracil sustained-release particles in 81 malignant pericardial effusion patients. *Kaohsiung Journal of Medical Sciences 31*(2), 96-101.

Jiang, C., Wang, Z., Ganther, H., & Lu, J. (2001). Caspases as key executors of methyl selenium-induced apoptosis (anoikis) of du-145 prostate cancer cells. *Cancer Research, 61*(7), 3062-3070.

Jin, Z., & El-Deiry, W. S. (2005). Overview of cell death signaling pathways. *Cancer Biology & Therapy, 4*(2), 147-171.

Johansson, L. H., & Borg, L. H. (1988). A spectrophotometric method for determination of catalase activity in small tissue samples. *Analytical Biochemistry, 174*(1), 331-336.

Kamal, A., Srikanth, Y., Khan, M. N. A., Shaik, T. B., & Ashraf, M. (2010). Synthesis of 3, 3-diindolyl oxyindoles efficiently catalysed by fecl3 and their in vitro evaluation for anticancer activity. *Bioorganic & Medicinal Chemistry Letters, 20*(17), 5229-5231.

Kanamaru, R., & Wakui, A. (1988). Mechanism of action of anti-cancer drugs from the viewpoint of rna metabolism. *Gan To Kagaku Ryoho, 15*(4 Pt 2-1), 1011-1018.

Karadag, A., Ozcelik, B., & Saner, S. (2009). Review of methods to determine antioxidant capacities. *Food Analytical Methods, 2*(1), 41-60.

Karin, M., & Greten, F. R. (2005). Nf-κb: Linking inflammation and immunity to cancer development and progression. *Nature Reviews Immunology, 5*(10), 749-759.

Karnofsky, D. A. (1968). Mechanism of action of anticancer drugs at a cellular level. *CA: A Cancer Journal for Clinicians, 18*(4), 232-234.

Kaufmann, D., Pojarová, M., Vogel, S., Liebl, R., Gastpar, R., Gross, D., . . . von Angerer, E. (2007). Antimitotic activities of 2-phenylindole-3-carbaldehydes in human breast cancer cells. *Bioorganic & Medicinal Chemistry, 15*(15), 5122-5136. doi: https://doi.org/10.1016/j.bmc.2007.05.030

Kaushik, N. K., Kaushik, N., Attri, P., Kumar, N., Kim, C. H., Verma, A. K., & Choi, E. H. (2013). Biomedical importance of indoles. *Molecules, 18*(6), 6620-6662.

Kehrer, J. P., Robertson, J. D., & Smith, C. V. (2010). Free radicals and reactive oxygen species. In C. A. McQueen (Ed.), *Comprehensive toxicology* (2nd ed.). Oxford: Elsevier.

Kehrer, J. P., Tipple, T. E., Robertson, J. D., & Smith, C. V. (2015). Free radicals and reactive oxygen species. *Reference module in biomedical sciences*. Oxford: Elsevier.

Khan, M. A., Tania, M., Zhang, D.-z., & Chen, H.-c. (2010). Antioxidant enzymes and cancer. *Chinese Journal of Cancer Research, 22*(2), 87-92.

Kim, D., Park, G. B., & Hur, D. Y. (2014). Apoptotic signaling through reactive oxygen species in cancer cells. *World Journal of Immunology, 4*(3), 158-173.

Kim, E. R., & Chang, D. K. (2014). Colorectal cancer in inflammatory bowel disease: The risk, pathogenesis, prevention and diagnosis. *World Journal of Gastroenterology, 20*(29), 9872-9881.

Kim, R., Tanabe, K., Uchida, Y., Emi, M., Inoue, H., & Toge, T. (2002). Current status of the molecular mechanisms of anticancer drug-induced apoptosis. *Cancer Chemotherapy and Pharmacology, 50*(5), 343-352.

Kroemer, G., & Martin, S. J. (2005). Caspase-independent cell death. *Nature Medicine, 11*(7), 725.

Kubiak, K., Malinowska, K., Langer, E., Dziki, L., Dziki, A., & Majsterek, I. (2011). Effect of cu(ii) coordination compounds on the activity of antioxidant enzymes catalase and superoxide dismutase in patients with colorectal cancer. *Polski Przeglad Chirurgiczny, 83*(3), 155-160.

Labianca, R., Nordlinger, B., Beretta, G., Mosconi, S., Mandalà, M., Cervantes, A., & Arnold, D. (2013). Early colon cancer: Esmo clinical practice guidelines for diagnosis, treatment and follow-up. *Annals of oncology, 24*(suppl_6), vi64-vi72.

Lee, C., Sohn, J. H., Jang, J.-H., Ahn, J. S., Oh, H., Baltrusaitis, J., . . . Gloer, J. B. (2015). Cycloexpansamines a and b: Spiroindolinone alkaloids from a marine isolate of penicillium sp.(sf-5292). *Journal of Antibiotics, 68*(11), 715.

Lee, I. M., Shiroma, E. J., Lobelo, F., Puska, P., Blair, S. N., & Katzmarzyk, P. T. (2012). Effect of physical inactivity on major non-communicable diseases worldwide: An analysis of burden of disease and life expectancy. *The Lancet, 380*(9838), 219-229.

Leung, P. S. (2014). *The gastrointestinal system: Gastrointestinal, nutritional and hepatobiliary physiology*: Springer Science & Business.

Li, H., Zhu, H., Xu, C.-j., & Yuan, J. (1998). Cleavage of bid by caspase 8 mediates the mitochondrial damage in the fas pathway of apoptosis. *Cell, 94*(4), 491-501.

Li, Y.-Y., Wu, H.-S., Tang, L., Feng, C.-R., Yu, J.-H., Li, Y., . . . He, Q.-J. (2007). The potential insulin sensitizing and glucose lowering effects of a novel indole derivative in vitro and in vivo. *Pharmacological Research, 56*(4), 335-343.

Lijinsky, W. (1985). The metabolism and cellular interactions of some aliphatic nitrogenous carcinogens. *Cancer Letters, 26*(1), 33-42.

Liou, G.-Y., & Storz, P. (2010). Reactive oxygen species in cancer. *Free Radical Research, 44*(5), 479-496.

Lobo, V., Patil, A., Phatak, A., & Chandra, N. (2010). Free radicals, antioxidants and functional foods: Impact on human health. *Pharmacognosy Reviews, 4*(8), 118.

London, G. M., Asmar, R. G., O'Rourke, M. F., & Safar, M. E. (2004). Mechanism (s) of selective systolic blood pressure reduction after a low-dose combination of perindopril/indapamide in hypertensive subjects: Comparison with atenolol. *Journal of the American College of Cardiology, 43*(1), 92-99.

Longley, D. B., Harkin, D. P., & Johnston, P. G. (2003a). 5-fluorouracil: Mechanisms of action and clinical strategies. *Nature Reviews Cancer, 3*(5), 330.

Longley, D. B., Latif, T., Boyer, J., Allen, W. L., Maxwell, P. J., & Johnston, P. G. (2003b). The interaction of thymidylate synthase expression with p53-regulated signaling pathways in tumor cells. *Seminars in Oncology, 30*(3), 3-9.

Loupakis, F., Cremolini, C., Masi, G., Lonardi, S., Zagonel, V., Trenta, P., . . . Zaniboni, A. (2013). Folfoxiri plus bevacizumab (bev) versus folfiri plus bev as first-line treatment of metastatic colorectal cancer (mcrc): Results of the phase iii randomized tribe trial. *Journal of Clinical Oncology 31*(4), 336-336.

Lowe, S. W., Ruley, H. E., Jacks, T., & Housman, D. E. (1993). P53-dependent apoptosis modulates the cytotoxicity of anticancer agents. *Cell, 74*(6), 957-967.

Luo, J., Manning, B. D., & Cantley, L. C. (2003). Targeting the pi3k-akt pathway in human cancer: Rationale and promise. *Cancer Cell, 4*(4), 257-262.

Mahmood, N. A. (2010). Oxidative stress and antioxidant status in colorectal cancer and healthy subject. *Cancer and Medical Genetics, 3*, 1-6.

Malaysia National Cancer Registry. (2015). *Malaysian national cancer registry report 2007-2011*.

Malstrom, B., Andreasson, L., Reinhammer, B., & Boyer, P. (1975). The enzymes, xiib. *PMid, 1218088*.

Markowitz, S. D., & Bertagnolli, M. M. (2009). Molecular origins of cancer: Molecular basis of colorectal cancer. *The New England Journal of Medicine, 361*(25), 2449-2460.

Mates, J. (2000). Effects of antioxidant enzymes in the molecular control of reactive oxygen species toxicology. *Toxicology, 153*(1), 83-104.

MatÉs, J. M., Pérez-Gómez, C., & De Castro, I. N. (1999). Antioxidant enzymes and human diseases. *Clinical Biochemistry, 32*(8), 595-603.

Matés, J. M., & Sánchez-Jiménez, F. M. (2000). Role of reactive oxygen species in apoptosis: Implications for cancer therapy. *The International Journal of Biochemistry & Cell Biology, 32*(2), 157-170.

McKinnell, R. G., Parchment, R. E., Perantoni, A. O., & Pierce, B. G. (1998). *The biological basis of cancer*. Cambridge, UK: Cambridge University Press.

McMahon, B. T., Sievert Jr, C. E., Wilson, S. R., Zimmermann, R. R., Palme, R. A., Yager, J. G., & Walsh, D. R. (2001). Optical biopsy system and methods for tissue diagnosis: Google Patents.

Meir, S., Kanner, J., Akiri, B., & Philosoph-Hadas, S. (1995). Determination and involvement of aqueous reducing compounds in oxidative defense systems of various senescing leaves. *Journal of Agricultural and Food Chemistry, 43*(7), 1813-1819.

Mescher, A. L. (2013). *Junqueira's basic histology: Text and atlas* (13th ed.). USA: McGraw Hill Professional.

Messersmith, W., Oppenheimer, D., Peralba, J., Sebastiani, V., Amador, M., Jimeno, A., . . . Iacobuzio-Donahue, C. A. (2005). Assessment of epidermal growth factor receptor (egfr) signaling in paired colorectal cancer and normal colon tissue samples using computer-aided immunohistochemical analysis. *Cancer Biology & Therapy, 4*(12), 1381-1386.

Mgomha, S., Hatem, A., & Abdel, A. (2012). Synthesis of new heterocycles derived from 3-(3-methyl-1h-indol-2-yl)-3-oxopropanenitrile as potent antifungal agents. *Bulletin of the Korean Chemical Society, 33*(9), 2985.

Milardović, S., Iveković, D., & Grabarić, B. S. (2006). A novel amperometric method for antioxidant activity determination using dpph free radical. *Bioelectrochemistry, 68*(2), 175-180.

Mironova, E. V., Evstratova, A. A., & Antonov, S. M. (2007). A fluorescence vital assay for the recognition and quantification of excitotoxic cell death by necrosis and apoptosis using confocal microscopy on neurons in culture. *Journal of Neuroscience Methods, 163*(1), 1-8.

Misra, U., Hitkari, A., Saxena, A., Gurtu, S., & Shanker, K. (1996). Biologically active indolylmethyl-1, 3, 4-oxadiazoles, 1, 3, 4-thiadiazoles, 4h--1, 3, 4-triazoles and 1, 2, 4-triazines. *European Journal of Medicinal Chemistry, 31*(7-8), 629-634.

Mohamed, M. S., Youns, M. M., & Ahmed, N. M. (2014). Novel indolyl-pyrimidine derivatives: Synthesis, antimicrobial, and antioxidant evaluations. *Medicinal Chemistry Research, 23*(7), 3374-3388.

Mohler, M. L., He, Y., Wu, Z., Hwang, D. J., & Miller, D. D. (2009). Recent and emerging anti-diabetes targets. *Medicinal Research Reviews, 29*(1), 125-195.

Molyneux, P. (2004). The use of the stable free radical diphenylpicrylhydrazyl (dpph) for estimating antioxidant activity. *Songklanakarin Journal of Science and Technology, 26*(2), 211-219.

Mosmann, T. (1983). Rapid colorimetric assay for cellular growth and survival: Application to proliferation and cytotoxicity assays. *Journal of Immunological Methods, 65*, 55-63.

Nagasawa, H. T., Shirota, F. N., & Matsumoto, H. (1972). Decomposition of methylazoxymethanol, the aglycone of cycasin, in d2o. *Nature, 236*(5344), 234-235.

Nassar, E. (2010). Synthesis,(in vitro) antitumor and antimicrobial activity of some pyrazoline, pyridine, and pyrimidine derivatives linked to indole moiety. *Journal of American Science, 6*(8), 463-471.

National Cancer Patient Registry-Colorectal Cancer. (2014). *The second report of the ncpr-colorectal cancer 2008 - 2013*

National Cancer Registry. (2006). *Malaysia cancer statistics – data and figure.*

National Cancer Registry. (2007). *Malaysia cancer statistics – data and figure.*

Newby, Z., Lee, T. T., Morse, R. J., Liu, Y., Liu, L., Venkatraman, P., . . . Stroud, R. M. (2006). The role of protein dynamics in thymidylate synthase catalysis: Variants of conserved 2'-deoxyuridine 5'-monophosphate (dump)-binding tyr-261. *Biochemistry, 45*(24), 7415-7428.

Ng, K., Bustamam, A., Sukari, M. A., Abdelwahab, S. I., Mohan, S., Buckle, M. J. C., . . . Hadi, A. H. A. (2013). Induction of selective cytotoxicity and apoptosis in human t4-lymphoblastoid cell line (cemss) by boesenbergin a isolated from boesenbergia rotunda rhizomes involves mitochondrial pathway, activation of caspase 3 and g2/m phase cell cycle arrest. *BMC Complementary and Alternative Medicine, 13*(1), 1.

Ngan, N. K., Lo, K. M., & Wong, C. S. R. (2011). Synthesis, structure studies and electrochemistry of molybdenum (vi) schiff base complexes in the presence of different donor solvent molecules. *Polyhedron, 30*(17), 2922-2932.

Noordhuis, P., Holwerda, U., Van der Wilt, C., Van Groeningen, C., Smid, K., Meijer, S., . . . Peters, G. (2004). 5-fluorouracil incorporation into rna and DNA in relation to thymidylate synthase inhibition of human colorectal cancers. *Annals of Oncology, 15*(7), 1025-1032.

Norberg, E., Orrenius, S., & Zhivotovsky, B. (2010). Mitochondrial regulation of cell death: Processing of apoptosis-inducing factor (aif). *Biochemical and Biophysical Research Communications, 396*(1), 95-100.

OECD Guideline. (2001). 423: Acute oral toxicity-acute toxic class method. *OECD guidelines for the testing of chemicals. OECD Publishing*, 1-14.

OECD Guideline. (2008). Test no. 407: Repeated dose 28-day oral toxicity study in rodents. *OECD guidelines for the testing of chemicals. OECD Publishing*, 1-13.

Olsson, M., & Zhivotovsky, B. (2011). Caspases and cancer. *Cell Death & Differentiation, 18*(9), 1441-1449.

Ondroušková, E., Souček, K., Horváth, V., & Šmarda, J. (2008). Alternative pathways of programmed cell death are activated in cells with defective caspase-dependent apoptosis. *Leukemia Research, 32*(4), 599-609.

Overbergh, L., Giulietti, A., Valckx, D., & Mathieu, C. (2010). Real time polymerase chain reaction. *Molecular Diagnostics*, 87-105.

Pahari, N., Saha, D., Jain, V. K., Jain, B., & Mridha, D. (2010). Synthesis and evaluation of acute toxicity studies and analgesic characters of some novel indole derivatives. *International Journal of Pharmaceutical Sciences and Research, 1*, 399-408.

Panda, S., Tripathy, J. K., & Panda, J. R. (2012). A comparative study of antioxidant properties of 2-[substituted arylideamino]-1, 3, 4-thiadiazino [6, 5b] indoles and their inclusion complexes with β-cyclodextrin. *International Journal of Pharmaceutical Sciences and Drug Research, 4*(3), 191-194.

Panda, S., & Tripathy, K. (2010). Studies on inclusion complexes of substituted indole derivatives with activating and deactivating group *Journal of Chemical and Pharmaceutical Research, 2*(3), 722-732.

Parasuraman, S. (2011). Toxicological screening. *Journal of Pharmacology & Pharmacotherapeutics, 2*(2), 74-79.

Parrish, A. B., Freel, C. D., & Kornbluth, S. (2013). Cellular mechanisms controlling caspase activation and function. *Cold Spring Harbor Perspectives in Biology, 5*(6), 1-24.

Patel, H., Darji, N., Pillai, J., & Patel, B. (2017). Recent advance in anti-cancer activity of indole derivatives. *International Journal of Drug Research and Technology, 2*(3), 5.

Pelicano, H., Carney, D., & Huang, P. (2004). Ros stress in cancer cells and therapeutic implications. *Drug Resistance Updates, 7*(2), 97-110.

Pettegrew, C. J., Jayini, R., & Islam, M. R. (2009). Transfer buffer containing methanol can be reused multiple times in protein electrotransfer. *Journal of Biomolecular Techniques, 20*(2), 93-95.

Pham-Huy, L. A., He, H., & Pham-Huy, C. (2008). Free radicals, antioxidants in disease and health. *International Journal of Biomedical Science, 4*(2), 89-96.

Philchenkov, A., Zavelevich, M., Kroczak, T. J., & Los, M. J. (2004). Caspases and cancer: Mechanisms of inactivation and new treatment modalities. *Experimental Oncology, 26*(2), 82-97.

Pignone, M., Saha, S., Hoerger, T., & Mandelblatt, J. (2002). Cost-effectiveness analyses of colorectal cancer screening: A systematic review for the us preventive services task force. *Annals of Internal Medicine, 137*(2), 96-104.

Pljesaercegovac, M., Mimicoka, J., Dragicevic, D., Savicradojevic, A., Opacic, M., Pljesa, S., . . . Simic, T. (2008). Altered antioxidant capacity in human renal cell carcinoma: Role of glutathione associated enzymes. *Urologic Oncology: Seminars and Original Investigations, 26*(2), 175-181.

Ponzdeleon, M., & Percesepe, A. (2000). Pathogenesis of colorectal cancer. *Digestive and Liver Disease, 32*(9), 807-821.

Power, E., Miles, A., von Wagner, C., Robb, K., & Wardle, J. (2009). Uptake of colorectal cancer screening: System, provider and individual factors and strategies to improve participation. *Future Oncology, 5*(9), 1371-1388.

Prasad, A. V., Venkateswara, R. P., & Prasad, P. S. (2014). Synthesis, characterization, antifungal, antibacterial studies of heterocyclic schiff base metal complexes *3*, 1-1.

Rani, P., Srivastava, V. K., & Kumar, A. (2004). Synthesis and antiinflammatory activity of heterocyclic indole derivatives. *European Journal of Medicinal Chemistry, 39*(5), 449-452.

Rapolu, M., Kumanan, R., Duganath, N., Srinivasa, M., Ahmed, N., & Subramanyam, S. (2011). Synthesis, characterization and pharmacological screening of 2-methyl-1h-indole-3-carboxylic acid [2-(2-1 substituted-phenyl)-4-oxo-thiazolidin-3-yl]-amides derivatives. *International Journal of Chemical Sciences and Applications 12*(1), 91-99.

Reeves, P. G., Nielsen, F. H., & Fahey, G. C. (1993). Ain-93 purified diets for laboratory rodents: Final report of the american institute of nutrition ad hoc writing committee on the reformulation of the ain-76a rodent diet. *The Journal of Nutrition, 123*(11), 1939–1951.

Ricci, J.-E., Gottlieb, R. A., & Green, D. R. (2003). Caspase-mediated loss of mitochondrial function and generation of reactive oxygen species during apoptosis. *The Journal of Cell Biology, 160*(1), 65-75.

Rizzo, D. C. (2015). *Fundamentals of anatomy and physiology* (4th Ed.). USA: Cengage Learning.

Roberts, S. A., Hyatt, D. C., Honts, J. E., Changchien, L., Maley, G. F., Maley, F., & Montfort, W. R. (2006). Structure of the y94f mutant of escherichia coli thymidylate synthase. *Acta Crystallographica Section F: Structural Biology and Crystallization Communications, 62*(9), 840-843.

Rosen, E. M. (2013). Brca1 in the DNA damage response and at telomeres. *Frontiers in Genetics, 4*, 85.

Rutman, R. J., Cantarow, A., & Paschkis, K. E. (1954). Studies in 2-acetylaminofluorene carcinogenesis iii. The utilization of uracil-2-c14 by preneoplastic rat liver and rat hepatoma. *Cancer Research, 14*(2), 119-123.

Salman, A. S., Mahmoud, N. A., Abdel-Aziem, A., Mohamed, M. A., & Elsisi, D. M. (2015). Synthesis, reactions and antimicrobial activity of some new 3-substituted indole derivatives. *International Journal of Organic Chemistry, 5*(02), 81.

Sashidhara, K. V., Kumar, A., Kumar, M., Sarkar, J., & Sinha, S. (2010). Synthesis and in vitro evaluation of novel coumarin–chalcone hybrids as potential anticancer agents. *Bioorganic & Medicinal Chemistry Letters, 20*(24), 7205-7211.

Schultz, D. R., & Harringto, W. J. (2003). Apoptosis: Programmed cell death at a molecular level. *Seminars in Arthritis and Rheumatism, 32*(6), 345-369.

Sherwood, L. (2015). *Human physiology: From cells to systems* (9th Ed.). Belmont, USA: Cengage learning.

Shih, I., Wang, T., Traverso, G., Romans, K., Hamilton, S. R., Ben-Sasson, S., . . . Vogelstein, B. (2001). Top-down morphogenesis of colorectal tumors. *Proceedings of the National Academy of Sciences, 98*(5), 2640-2645.

Shivarama Holla, B., Veerendra, B., Shivananda, M. K., & Poojary, B. (2003). Synthesis characterization and anticancer activity studies on some mannich bases derived from 1,2,4-triazoles. *European Journal of Medicinal Chemistry, 38*(7–8), 759-767.

Sidotide Fraisse, C., Rincheval, V., Risler, Y., Mignotte, B., & Vayssiere, J. (1998). Tnf-activates at least two apoptotic signaling cascades. *Oncogene, 17*, 1639-1651.

Sillarshardebol, A. H., Carvalho, B., De Wit, M., Postma, C., Delisvan Diemen, P. M., Mongera, S., . . . Fijneman, R. A. (2010). Identification of key genes for carcinogenic pathways associated with colorectal adenoma-to-carcinoma progression. *Tumor Biology, 31*(2), 89-96.

Simon, H. U., Hajyehia, A., & Levschaffer, F. (2000). Role of reactive oxygen species (ros) in apoptosis induction. *Apoptosis, 5*(5), 415-418.

Singh, P., Prasher, P., Dhillon, P., & Bhatti, R. (2015). Indole based peptidomimetics as anti-inflammatory and anti-hyperalgesic agents: Dual inhibition of 5-lox and cox-2 enzymes. *European Journal of Medicinal Chemistry, 97*, 104-123.

Singhal, P. C. (2015). *Application of liquid chromatography tandem mass spectrometry lc ms ms for the quantitation of anti cancer drugs in biological fluids for bioequivalence studies*. Kadi Sarva Vishwavidyalaya, Gandhinagar, India.

Sinha, A. K. (1972). Colorimetric assay of catalase. *Analytical Biochemistry, 47*(2), 389-394.

Siu, I. M., Robinson, D. R., Schwartz, S., Kung, H. J., Pretlow, T. G., Petersen, R. B., & Pretlow, T. P. (1999). The identification of monoclonality in human aberrant crypt foci. *Cancer Research, 59*(1), 63-66.

Sivaprasad, G., Perumal, P. T., Prabavathy, V. R., & Mathivanan, N. (2006). Synthesis and anti-microbial activity of pyrazolylbisindoles—promising anti-fungal compounds. *Bioorganic & Medicinal Chemistry Letters, 16*(24), 6302-6305.

Sotelomundo, R. R., Changchien, L., Maley, F., & Montfort, W. R. (2006). Crystal structures of thymidylate synthase mutant r166q: Structural basis for the nearly complete loss of catalytic activity. *Journal of Biochemical and Molecular Toxicology, 20*(2), 88-92.

Strzelczyk, J. K., Wielkoszyński, T., Krakowczyk, Ł., Adamek, B., Zalewska-Ziob, M., Gawron, K., . . . Wiczkowski, A. (2012). The activity of antioxidant enzymes in colorectal adenocarcinoma and corresponding normal mucosa. *Acta Biochimica Polonica, 59*(4), 549-556.

Sung, J. Y., Lau, J. W., Young, G. P., Sano, Y., Chiu, H. M., Byeon, J. S., . . . Rerknimitr, R. (2008). Asia pacific consensus recommendations for colorectal cancer screening. *Gut, 57*(8), 1166-1176.

Takayama, T., Katsuki, S., Takahashi, Y., Ohi, M., Nojiri, S., Sakamaki, S., . . . Niitsu, Y. (1998). Aberrant crypt foci of the colon as precursors of adenoma and cancer. *New England Journal of Medicine, 339*(18), 1277-1284.

Torre, L. A., Bray, F., Siegel, R. L., Ferlay, J., Lortet-Tieulent, J., & Jemal, A. (2015). Global cancer statistics, 2012. *A Cancer Journal for Clinicians, 65*(2), 87-108.

Trachootham, D., Alexandre, J., & Huang, P. (2009). Targeting cancer cells by ros-mediated mechanisms: A radical therapeutic approach? *Nature Reviews Drug Discovery, 8*(7), 579-591.

Treanor, D., & Quirke, P. (2007). Pathology of colorectal cancer. *Clinical Oncology, 19*(10), 769-776.

Twelves, C., Wong, A., Nowacki, M. P., Abt, M., Burris III, H., Carrato, A., . . . Georgoulias, V. (2005). Capecitabine as adjuvant treatment for stage iii colon cancer. *New England Journal of Medicine, 352*(26), 2696-2704.

Ursini, F., Maiorino, M., & Gregolin, C. (1985). The selenoenzyme phospholipid hydroperoxide glutathione peroxidase. *Biochimica et Biophysica Acta (BBA)-General Subjects, 839*(1), 62-70.

Vainio, H., & Miller, A. B. (2003). Primary and secondary prevention in colorectal cancer. *Acta Oncologica, 42*(8), 809-815.

Valasek, M. A., & Repa, J. J. (2005). The power of real-time pcr. *Advances in Physiology Education, 29*(3), 151-159.

Valko, M., Leibfritz, D., Moncol, J., Cronin, M. T. D., Mazur, M., & Telser, J. (2007). Free radicals and antioxidants in normal physiological functions and human disease. *The International Journal of Biochemistry & Cell Biology, 39*(1), 44-84.

Van Cutsem, E., Twelves, C., Cassidy, J., Allman, D., Bajetta, E., Boyer, M., . . . Jahn, M. (2001). Oral capecitabine compared with intravenous fluorouracil plus leucovorin in patients with metastatic colorectal cancer: Results of a large phase iii study. *Journal of Clinical Oncology, 19*(21), 4097-4106.

Vazquez, A., Bond, E. E., Levine, A. J., & Bond, G. L. (2008). The genetics of the p53 pathway, apoptosis and cancer therapy. *Nature Reviews Drug Discovery, 7*(12), 979-987.

Villalain, J. (2010). Membranotropic effects of arbidol, a broad anti-viral molecule, on phospholipid model membranes. *The Journal of Physical Chemistry B, 114*(25), 8544-8554.

Vogelstein, B., Fearon, E. R., Hamilton, S. R., Kern, S. E., Preisinger, A. C., Leppert, M., . . . Bos, J. (1988a). Genetic alterations during colorectal-tumor development. *The New England Journal of Medicine, 319*(9), 525-532.

Vogelstein, B., Fearon, E. R., Hamilton, S. R., Kern, S. E., Preisinger, A. C., Leppert, M., . . . Bos, J. L. (1988b). Genetic alterations during colorectal-tumor development. *New England Journal of Medicine, 319*(9), 525-532.

Vogelstein, B., & Kinzler, K. W. (2004). Cancer genes and the pathways they control. *Nature Medicine, 10*(8), 789-799.

Von Bertalanffy, L. (1963). Acridine orange fluorescence in cell physiology, cytochemistry and medicine. *Protoplasma, 57*(1-4), 51-83.

Wajant, H., Gerspach, J., & Pfizenmaier, K. (2005). Tumor therapeutics by design: Targeting and activation of death receptors. *Cytokine & Growth Factor Reviews, 16*(1), 55-76.

Walker, J. M. (1996). *The protein protocols handbook* (Vol. 1996): Springer.

Walsh, J. M. E., & Terdiman, J. P. (2003). Colorectal cancer screening. *Journal of the American Medical Association, 289*(10), 1288-1296.

Wargovich, M. J., Brown, V. R., & Morris, J. (2010). Aberrant crypt foci: The case for inclusion as a biomarker for colon cancer. *Cancers, 2*(3), 1705-1716.

Watson, A. J. M., & Collins, P. D. (2011). Colon cancer: A civilization disorder. *Digestive Diseases, 29*(2), 222-228.

Weinberg, R. (2013). *The biology of cancer* (2nd ed.). New York: Garland science.

Weinberg, R. A. (1989). Oncogenes, antioncogenes, and the molecular bases of multistep carcinogenesis. *Cancer Research, 49*(14), 3713-3721.

Weinstein, J. N., Myers, T. G., O'Connor, P. M., Friend, S. H., Fornace, A. J., Kohn, K. W., . . . Anderson, N. L. (1997). An information-intensive approach to the molecular pharmacology of cancer. *Science, 275*(5298), 343-349.

Williams, A., Balasooriya, B., & Day, D. (1982). Polyps and cancer of the large bowel: A necropsy study in liverpool. *Gut, 23*(10), 835-842.

Won, C., Shen, X., Mashiguchi, K., Zheng, Z., Dai, X., Cheng, Y., . . . Zhao, Y. (2011). Conversion of tryptophan to indole-3-acetic acid by tryptophan aminotransferases of arabidopsis and yuccas in arabidopsis. *Proceedings of the National Academy of Sciences, 108*(45), 18518-18523.

Wong, M. L., & Medrano, J. F. (2005). Real-time pcr for mrna quantitation. *Biotechniques, 39*(1), 75-88.

Wu, Y. S., Coumar, M. S., Chang, J. Y., Sun, H. Y., Kuo, F. M., Kuo, C. C., . . . Liou, J. P. (2009). Synthesis and evaluation of 3-aroylindoles as anticancer agents: Metabolite approach. *Journal of Medicinal Chemistry, 52*(15), 4941-4945.

Xiong, S., Mu, T., Wang, G., & Jiang, X. (2014). Mitochondria-mediated apoptosis in mammals. *Protein & Cell, 5*(10), 737-749.

Xu, H., & Lv, M. (2009). Developments of indoles as anti-hiv-1 inhibitors. *Current Pharmaceutical Design, 15*(18), 2120-2148.

Yamagishi, H., Kuroda, H., Imai, Y., & Hiraishi, H. (2016). Molecular pathogenesis of sporadic colorectal cancers. *Chinese Journal of Cancer, 35*, 4.

Yeung, T. M., Gandhi, S. C., Wilding, J. L., Muschel, R., & Bodmer, W. F. (2010). Cancer stem cells from colorectal cancer-derived cell lines. *Proceedings of the National Academy of Sciences of the United States of America, 107*(8), 3722-3727.

Yoshida, H., & Nappi, J. (2001). Three-dimensional computer-aided diagnosis scheme for detection of colonic polyps. *IEEE Transactions on Medical Imaging, 20*(12), 1261-1274.

Youle, R. J., & Strasser, A. (2008). The bcl-2 protein family: Opposing activities that mediate cell death. *Nature Reviews Molecular Cell Biology, 9*(1), 47.

Young, S. N. (2007). How to increase serotonin in the human brain without drugs. *Journal of Psychiatry and Neuroscience, 32*(6), 394.

Zahedifard, M., Faraj, F. L., Paydar, M., Looi, C. Y., Hajrezaei, M., Hasanpourghadi, M., . . . Abdulla, M. A. (2015a). Synthesis, characterization and apoptotic activity of quinazolinone schiff base derivatives toward mcf-7 cells via intrinsic and extrinsic apoptosis pathways. *Scientific Reports, 5*.

Zahedifard, M., Lafta Faraj, F., Paydar, M., Yeng Looi, C., Hasandarvish, P., Hajrezaie, M., . . . Mohd Ali, H. (2015b). Synthesis of apoptotic new quinazolinone-based compound and identification of its underlying mitochondrial signalling pathway in breast cancer cells. *Current Pharmaceutical Design, 21*(23), 3417-3426.

Zahran, M. A., Salama, H. F., Abdin, Y. G., & Gamal-Eldeen, A. M. (2010). Efficient microwave irradiation enhanced stereoselective synthesis and antitumor activity of indolylchalcones and their pyrazoline analogs. *Journal of Chemical Sciences, 122*(4), 587-595.

Zhang, F., Zhao, Y., Sun, L., Ding, L., Gu, Y., & Gong, P. (2011). Synthesis and anti-tumor activity of 2-amino-3-cyano-6-(1h-indol-3-yl)-4-phenylpyridine derivatives in vitro. *European Journal of Medicinal Chemistry, 46*(7), 3149-3157.

Zhang, M.-Z., Chen, Q., & Yang, G.-F. (2015). A review on recent developments of indole-containing antiviral agents. *European Journal of Medicinal Chemistry, 89*, 421-441.

Zhang, M.-Z., Mulholland, N., Beattie, D., Irwin, D., Gu, Y.-C., Chen, Q., . . . Clough, J. (2013). Synthesis and antifungal activity of 3-(1, 3, 4-oxadiazol-5-yl)-indoles and 3-(1, 3, 4-oxadiazol-5-yl) methyl-indoles. *European Journal of Medicinal Chemistry, 63*, 22-32.

LIST OF PUBLICATIONS AND PROCEEDINGS

Publications

Hajiaghaalipour, F., Faraj, F. L., Bagheri, E., Ali, H. M., Majid, N. A., & Abdulla, M. A. (2017). Synthesis and characterization of a new benzo indole derivative with apoptotic activity against colon cancer cells. *Current Pharmaceutical Design*, *23*, 1-8.

Hajiaghaalipour, F., Bagheri, E., Faraj, F. L., Abdulla, M. A., & Majid, N. A. (2017). Underlying mechanism for the modulation of apoptosis induced by a new benzoindole derivative on HT-29 colon cancer cells. *RSC Advances, 7*(61), 38257-38263.

Proceedings

Hajiaghaalipour, F., Bagheri, E., Salehin, N. A., Abdulla, M. A., & Majid, N. A. (2017). Inhibition of azoxymethane-induced colonic aberrant crypt foci formation by a new synthetic compound. *5th International Postgraduate Conference on Pharmaceutical Sciences (IPoPS)*, UiTM Puncak Alam Campus, Malaysia.

Hajiaghaalipour, F., Bagheri, E., Salehin, N. A., Abdulla, M. A., & Majid, N. A. (2016). The antioxidants and anticancer properties of a new synthetic compound against colorectal cancer cell line, HT-29. *International Conference on Science and Technology 2016 (ICSNR)*, Kota Kinabalu, Sabah, Malaysia.